LA-UR-13-26944
Approved for public release; distribution is unlimited.

Title: Validation and Verification of MCNP6 Against High-Energy Experimental Data and Calculations by Other Codes. III. The MPI Testing Primer

Author(s): Mashnik, Stepan G

Intended for: The MCNP6 Code Package

Issued: 2013-10-01 (rev.1)

Validation and Verification of MCNP6 Against High-Energy Experimental Data and Calculations by Other Codes. III. The MPI Testing Primer

Stepan G. Mashnik

XCP-3, Los Alamos National Laboratory, Los Alamos, NM 87545, USA

Abstract

This primer presents a set of Validation and Verification (V&V) MCNP6 results calculated in parallel, with MPI, obtained mostly using its event generators at intermediate and high-energies, but also several examples of results using data libraries at energies below 150 MeV, against various recent experimental data. It is the third part of a set of MCNP6 Testing Primers, after its first, LA-UR-11-05129, and second, LA-UR-11-05627, publications. The MCNP6 test-problems discussed here are presented in the **/VALIDATION_CEM/**, **/VALIDATION_LAQGSM/**, and **/DELAYED_PARTICLES/** subdirectories in the MCNP6 **/Testing/** directory. README files that contain short descriptions of every input file, the experiment, the quantity of interest that the experiment measures and its description in the MCNP6 output files, and the publication reference of that experiment are presented for every test-problem. Templates for plotting the corresponding results with **xmgrace** as well as pdf files with figures representing the final results of our V&V efforts are presented. Several technical "bugs" in MCNP6 while running it in parallel with MPI using its event generators were discovered during our current V&V of MCNP6 and were fixed mostly by Dr. Jeffrey S. Bull. Our results show that MCNP6 using its CEM03.03, LAQGSM03.03, Bertini, INCL+ABLA, and ISABEL event generators describes, as a rule, reasonably well different intermediate- and high-energy measured data and agrees very well with calculations by other codes. Just as expected, the MCNP6 results obtained with MPI are practically the same as the ones calculated with MCNP6 in a sequential mode. This primer isn't meant to be read from cover to cover. Readers may skip some sections and go directly to a test-problem they are interested in.

September 2013

Contents

1. Introduction

During the past several years, a major effort has been undertaken at the Los Alamos National Laboratory (LANL) to develop the transport code MCNP6 [1]-[6], the latest and most advanced LANL Monte Carlo transport code produced by the XCP-3 and NEN-5 LANL Groups representing a merger of MCNP5 [7] and MCNPX [8], but containing also many new useful features not considered either by MCNP5 or by MCNPX. After our initial, "internal" development versions of MCNP6 [1, 2], several preliminary versions of MCNP6, namely, Beta 1 [3], Beta 2 [4], and Beta 3 [5], were delivered to the Radiation Safety Information Computational Center (RSICC) for distribution to users during 2011 and 2012, until the first "production" version of MCNP6 was made available to users via RSICC in July 2013 [6, 9].

As multilateral Validation and Verification (V&V) of all our codes is very important and necessary, 23 test suits containing several hundred specific problems testing that MCNP6 is running as expected and provides reliable predictions were created [6]. Among them, the **/VALIDATION_CEM/** and **/VALIDATION_LAQGSM/** subdirectories in the **/MCNP6/Testing/** directory were created to V&V the event generators used by MCNP6 at high energies, above the regions covered by data libraries, as well as to describe interactions not covered at present at all by any data libraries, like nuclear reactions induced by heavy ions.

Various results on V&V of the Cascade-Exciton Model (CEM) as implemented in the code CEM03.03 (see [10, 11, 12] and references therein) and used at present as the default option of MCNP6 to simulate reactions induced by nucleons, pions, and photons at energies up to several GeV were published in Refs. [13, 14]. Refs. [14, 15] present an extended V&V of the Los Alamos version of the Quark-Gluon String Model (LAQGSM) as implemented in the code LAQGSM03.03 (see [12, 16, 17] and references therein) and used in MCNP6 as the default event generators to calculate relativistic reactions at energies above 3.5 GeV (for incident nucleons and pions, or above 1.2 GeV, for incident photons) and all nuclear interactions of heavy ions. Besides, Refs. [13, 14, 15] present about two dozen examples of reactions simulated in MCNP6 with the Bertini intranuclear cascade (INC) [18], followed by the multistage preequilibrium model (MPM) [19], followed by the evaporation model as described with the EVAP code by Dresner [20], followed by or in competition with the RAL fission model [21], referred to herein simply as "Bertini" option of MCNP6. Refs. [13, 14, 15] present also about two dozen examples of reactions simulated in MCNP6 using the intranuclear cascade developed at Liege (INCL) University by Cugnon with his coauthors from CEA, Saclay, France [22] merged with the evaporation-fission model as implemented in the code ABLA developed at GSI, Darmstadt, Germany [23], referred to herein simply as "INCL+ABLA" option of MCNP6. Refs. [13, 14, 15] present also several examples of reactions simulated with the intranuclear cascade model ISABEL [24], used in MCNP6 as a default option to simulate reactions induced by complex particles (d, t, ^{4}He, ^{4}He), antinucleons, and kaons, at energies below several GeV, as well as several examples of comparisons with results by several other modern models of nuclear reactions, not included in MCNP6.

The numerous and various examples presented in Refs. [13, 14, 15] have been simulated with different versions of MCNP6, on different computers, but all the calculations have been done in a sequential mode. Because of this, it was not known how MCNP6 with its high-energy event generators runs in parallel, with MPI. The current Primer is intended to address this problem:

First, we recalculated all the examples discussed in Refs. [13, 14, 15] running MCNP6 in parallel, with MPI. Part of these results are presented below in sub-sections 3.1 and 4.1.

Then, we study more than a dozen other, new, test-problems, running MCNP6 with MPI. This extends our confidence in MCNP6 predictions for such reactions, but also helped us to find and to fix several bugs observed while using the event generators and running the early beta versions of MCNP6 with MPI. Such results on our study using different event-generators are presented below in sub-sections 3.2 to 3.6 and 4.2 to 4.4, and 5.4

In addition, in sub-sections 5.1 to 5.3 we test MCNP6 on several reactions at lower energies, using data libraries, to see how MCNP6 predicts delayed neutron production from ^{235}U, ^{233}U, and ^{239}Pu while using ACE (ENDF/B-VII.0) [25] data libraries and the CINDER model [26]

Last, we tested about two dozen new test-problems running the latest, "production version 1" of MCNP6 [6] in parallel, with MPI. These very recent results obtained with the production version of MCNP6 are presented in Section 6.

2. Running MCNP6 with MPI

To run MCNP6 in parallel with MPI, we need first to compile it with MPI on our computers. At different times, we have tested the MPI version of MCNP6 on several different LANL supercomputers, like Flash, Yellowrail, Turing, and Moonlight.

To compile ("build") MCNP6 with MPI on a supercomputer we intend to use, we first need to ssh to log-on to a front-end node from our workstation, and to check that we have there all the modules we need to compile MCNP6. So, if we plan to use the Intel compiler, and may need to use also the debugger **Totalview**, if we encounter any problems while running MCNP6, we may need to have loaded only the following three modules:
1) intel/11.1.072
2) openmpi/1.4.5 and
3) totalview/8.11.0-2.

We check which modules we have already loaded with the command **module list**. If our modules are not loaded, we check which modules are available with the command **module avail**, and assuming we find available the needed modules, we load them with the command **module load**. After loading the needed modules, we check again with **module list** that all needed modules are loaded and compile ("build") MCNP6 from the subdirectory /Source/ of the MCNP6 directory, typing:

```
make build CONFIF=''openmpi intel plot'' GNUJ=6
```

After a successful compilation, in subdirectory */Source/src/, we get the executable file named **mcnp6.mpi**. We can compile MCNP6 either on front-end or on the back-end of our supercomputer, but to perform real calculations, we need to log-in to the back-end nodes. If, for example, we like to use 8 nodes, 64 processors of the Moonlight, ml-fey, machine, we can log-in to the back-end nodes by typing:

```
llogin -l nodes=8 -A acces
```

This would provide us 63 (plus one "master") processors to perform MCNP6 calculations, but only for one hour. If we need a longer time, we can log-in with the command

```
llogin -l nodes=8 -A acces -l walltime=10:00
```

that would allow us to run MCNP6 with MPI up to 10 hours.

To run interactively MCNP6 with MPI, for example on Moonlight, ml-fey, supercomputer using 64 (more exactly, 63, plus one "master") processors, using an MCNP6 input file with a name, e.g., **C600Be**, which is located, e.g., in our own subdirectory */Testing/My-test/, we type from our subdirectory:

```
mpirun --mca mpi_paffinity_alone 0 --bynode -np 64 ../../Sou*/src/mcnp6.mpi
i=C600Be n=C600Be.mpi.
```

In this particular case, after the calculation is completed, we get the output file **C600Be.mpi.o** and the runtype file **C600Be.mpi.r** in the same subdirectory.

If the statistics of our calculation is not enough, we can continue the calculation of this problem using the runtype file **C600Be.mpi.r** we already have and an auxiliary two-line file named, e.g., **1e7** using the command:

```
mpirun --mca mpi_paffinity_alone 0 --bynode -np 64 ../../Sou*/src/mcnp6.mpi c
i=1e7 o=C600Be.mpi.1.o r=C600Be.mpi.r
```

The auxiliary file, **1e7**, looks like

```
continue
1e7
```

and the output file from this continue run has the name **C600Be.mpi.1.o**. If even now the statistics is not enough, we can continue further our calculations, using the same runtype file **C600Be.mpi.r**, but specifying a new name for the output file, e.g., **C600Be.mpi.2.o**, and so on.

3. Testing CEM, Bertini, and INCL+ABLA

All the test-problems discussed in this Section are presented in the **VALIDATION_CEM** subdirectory in the basic **/MCNP6/Testing/** directory.

3.1. Old test-problems using CEM, Bertini, and INCL+ABLA

Initially, we have recalculated all the examples discussed in Ref. [13] running different parallel versions of MCNP6 [3]-[6]. As a rule, all versions of MCNP6 yielded the same results for all those test-problems run either with MPI, as described in the previous Section, or in a sequential mode, as done for Ref. [13], with only some very little differences in the last digits of some of the calculated values. We used above the words "as a rule," because during a particular period of time, in the very early days of the "Beta 3" version of MCNP6 [5], when Dr. Grady Hughes changed the default option of event generators to be used in MCNP6 to simulate reactions induced by nucleons and pions below 3.5 GeV from "Bertini" to "CEM" without notifying us at once about those changes, we got some very unusual and unexpected results with MPI for all test-problems discussed in Ref. [13] where the "Bertini" model was used. It took us some time to understand that in spite the fact that in our MCNP6 input files it was specified the "Bertini" model (more exactly, we did not specify anything for the 9th parameter of the **LCA** card, as it was assumed that we use the Bertini, model, that corresponds

to **LCA 8j 0**, by default), and in our output files was printed explicitly that **LCA(9) = 0**, that indicated to us that the Bertini model was used, actually, MCNP6 did performed such calculations with CEM03.03, providing, naturally, completely different results from the ones we got previously using the Bertini model in a sequential run. Later on, Grady informed us about that his modifications in MCNP6 and those changes were described explicitly in the MCNP6 Manual [27], but before that, the "different results" obtained with MPI and in a sequential mode was an unexpected "puzzle". Several other little "bugs" were also observed, while running MCNP6 with MPI. These were fixed later most often by Dr. Jeffrey S. Bull, but in some cases also by Drs. Richard E. Prael and H. Grady Hughes, and will be outlined bellow in the corresponding sub-sections.

However, even after the description of the default option changes in the MCNP6 Manual [27], some uncertainties about the models actually used in a particular simulation by MCNP6 still remained, especially in complex problems with reactions on different materials, initiated by different projectiles, of different energies, when MCNP6 would use a given model for one particular energy/projectile/material region and some another model(s) in other energy/projectile/material regions.

To avoid possible confusions in the future about what models have been actually used in a particular MCNP6 simulation, Grady Hughes made one more change in MCNP6 concerning this point: Now, all versions of MCNP6 produced after August 8 2013 do print explicitly in their MCNP6 output files the number of attempts (and the number of successes) to process a model interaction by any of the seven models available currently in MCNP6. These are BERTINI, CEM, INCL, ISABEL, LAQGSM, LAQGSM_H1, and HYD. The code's internal choice of model is important information both for the developers and the users.

In this sub-section, we discuss only the 18 MCNP6 test-problems described in Ref. [13]. Because all the input and output files for these problems were described in detail in Ref. [13], as was done with all the experimental data used, and because the results obtained here with MPI are practically the same as the old results calculated in Ref. [13] in a sequential mode, we do not provide explicitly our new output files and all the new figures with results from our MPI runs for all these 18 test-problems: Readers can find them in Ref. [13]. Instead, Figs. 1 to 4 below show only a few examples of comparisons of our old MCNP6 results from Ref. [13] obtained in sequential runs with our current results obtained with MPI, namely, for the test-problems # 1, 3, 6, and 11 of Ref. [13]. As we can see, because the differences between the current MPI results and the ones obtained in Ref. [13] in sequential runs are only in the last digits on only some of calculated values, these tiny differences can not be distinguished almost at all in the scale we use for our figures. This is a good result, just as expected. Let us recall again that all details about all the test-problems from this sub-section can be found in Ref. [13].

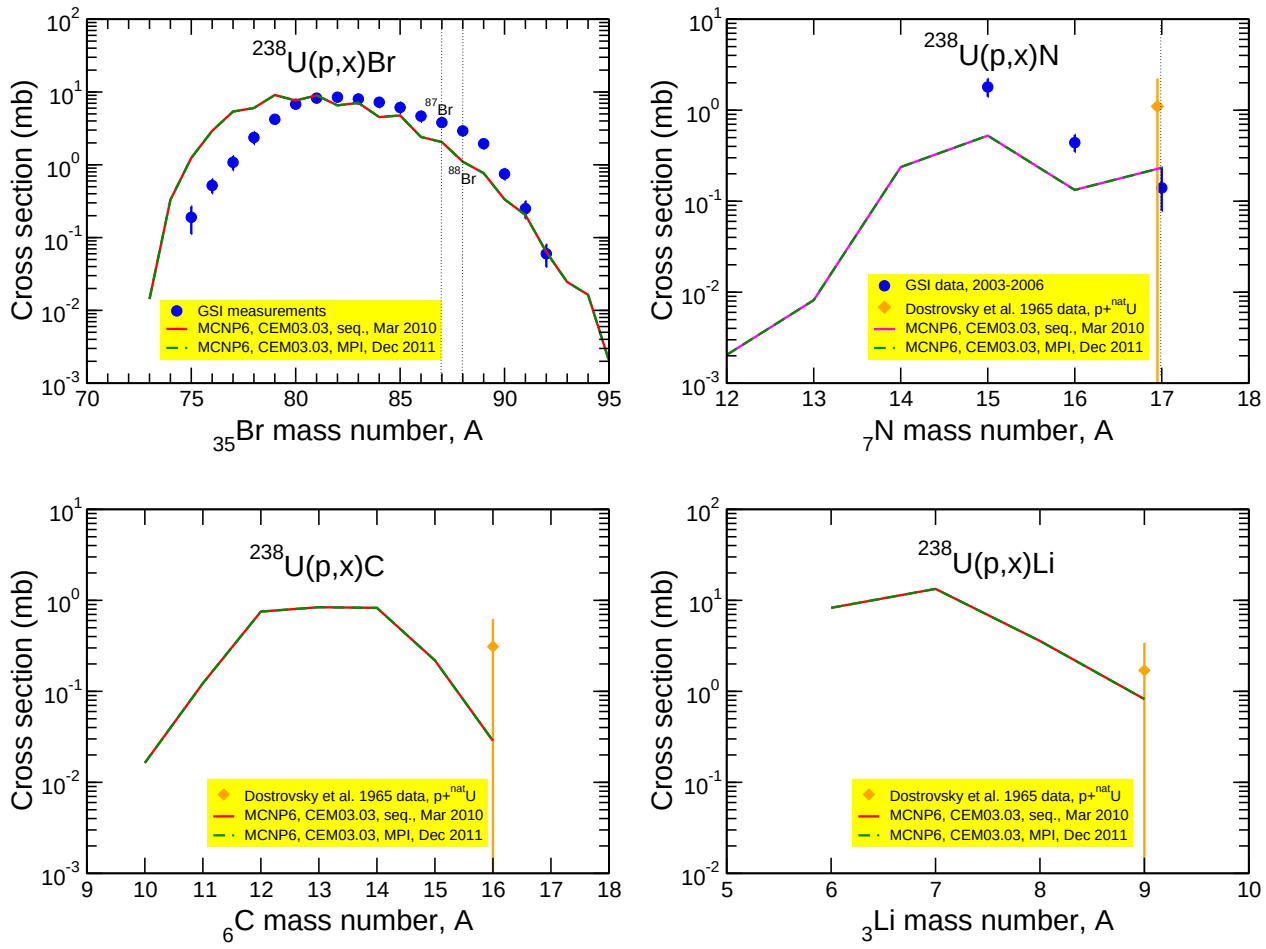

Figure 1: Experimental (symbols) mass distributions [28]-[32] for the yields of Br, N, C, and Li isotopes from ^{238}U thin targets bombarded with a 1 GeV proton beam compared with MCNP6 results using the CEM03.03 event-generator [12] obtained in a sequential run (red lines), as presented in Fig. 2 of Ref. [13] as well as calculated later in parallel, with MPI (dashed green lines). For comparison, results by CEM03.03 [12] used as a stand alone code, by INCL4.5+ABLA07 [33]-[35], by ISABEL+ABLA07 [24, 34], and by the transport code MCNPX 2.6.0 [36] with default options, i.e., using the Bertini INC [18], Multistage Preequilibrium Model (MPM) [19], Dresner evaporation model [20], and the RAL fission model [21], as presented at the International Benchmark of Spallation Models organized by IAEA during 2008-2009 [37] can be found in Fig. 2 of Ref. [13].

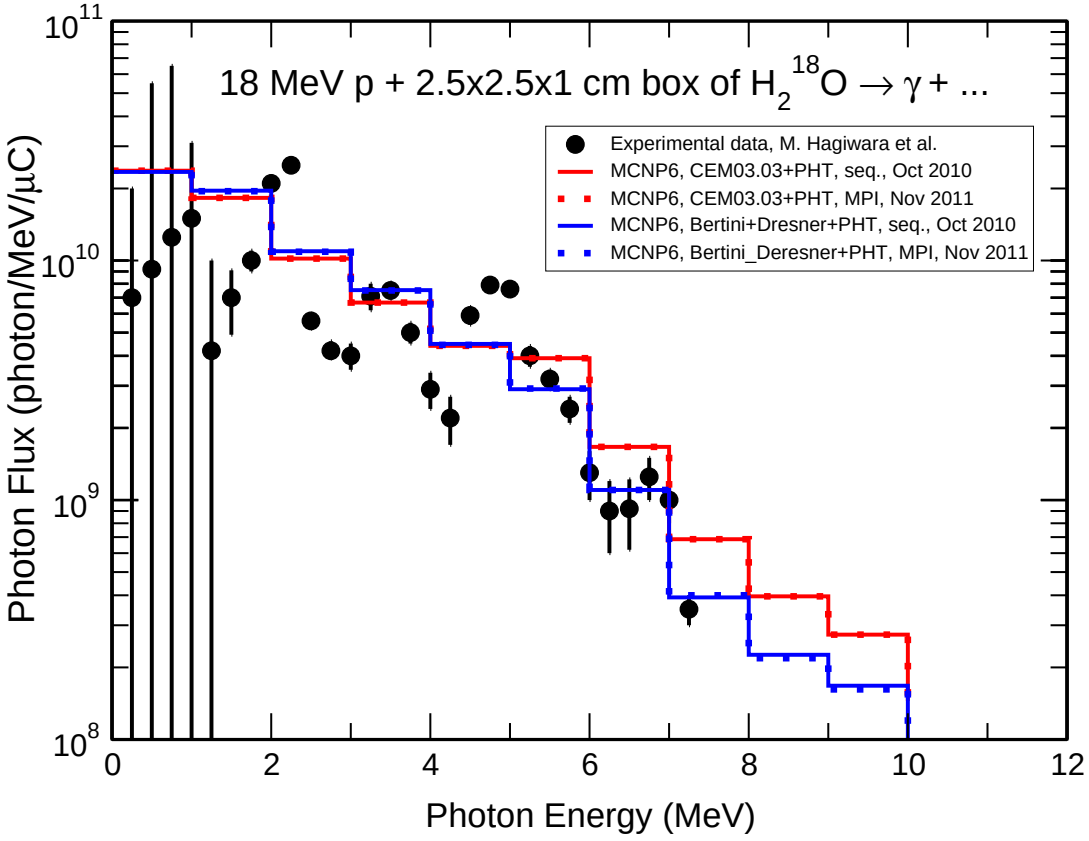

Figure 2: Comparison of the measured [38] energy spectrum of prompt γ-rays from a thick $H_2^{18}O$ target bombarded with 18 MeV protons with old MCNP6 results calculated in a sequential mode using the CEM03.03 [12] and the Bertini+MPM+Dresner [18, 19, 20] event generators (solid lines), as presented in Fig. 5 of Ref. [13] as well as calculated later in parallel, with MPI (dotted lines). Note that neither CEM03.03, nor Bertini+MPM+Dresner, nor any other high-energy event generators incorporated presently in MCNP6 describe direct emission of any photons: γ-rays from reactions simulated by MCNP6 with its event generators are estimated as deexcitation of residual nuclei produced after all stages on nuclear reactions using the PHT semi-phenomenological model as implemented in the LAHET code by Prael and Lichtenstein [39].

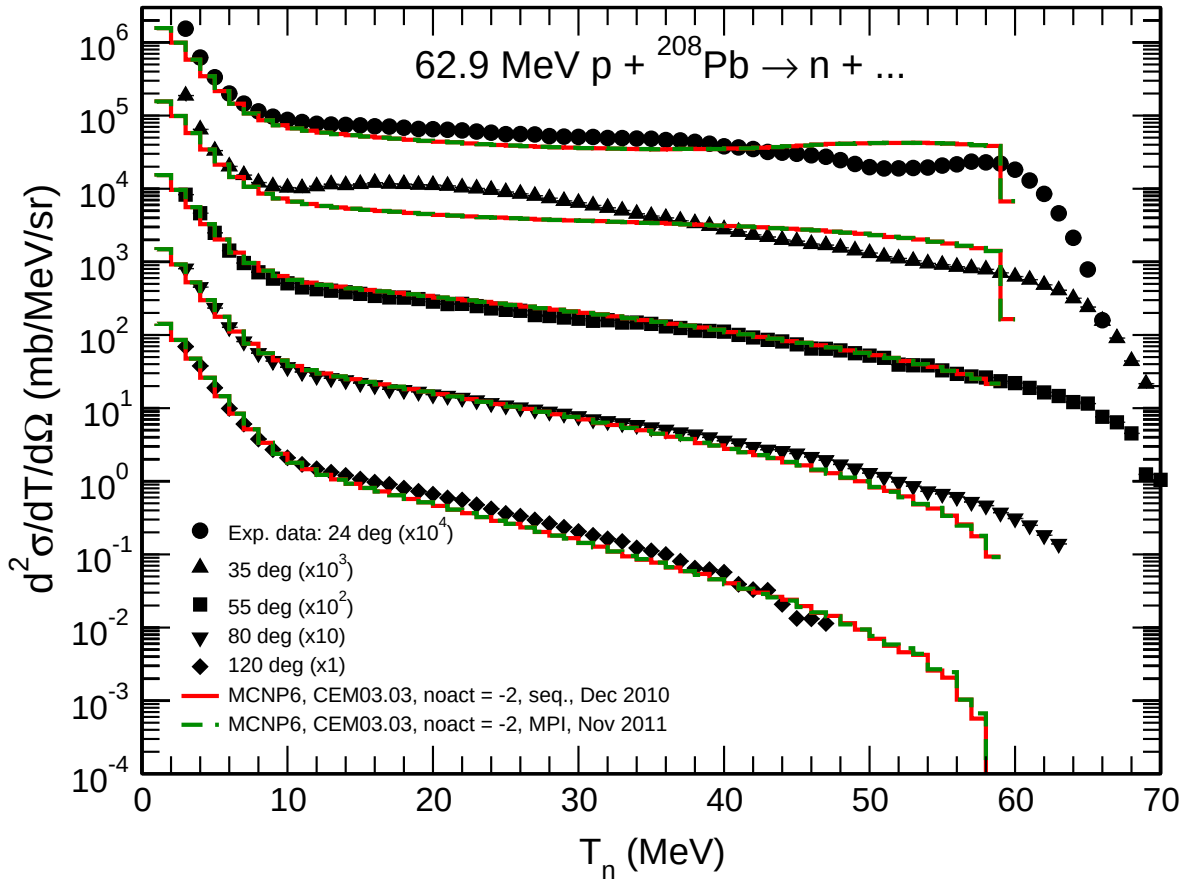

Figure 3: Experimental [40] double-differential spectra of neutrons at 24, 35, 55, 80, and 120 degrees from interactions of 62.9 MeV protons with a thin ^{208}Pb target compared with old MCNP6 calculations in a sequential mode using the CEM03.03 event generators (red solid lines), as presented in Fig. 8 of Ref. [13], as well as calculated later in parallel, with MPI (green dashed lines). For comparison, results by CEM03.03 [12] used as a stand alone code, by INCL4.5+ABLA07 [33]-[35] and results by MCNPX 2.6.0 calculated by Franz Gallmeier with default options (i.e., Bertini INC [18] + Multistage Preequilibrium Model [19] + Dresner evaporation [20] + RAL fission model [21]) as presented at the recent International Benchmark of Spallation Models [37], can be found in Fig. 8 of Ref. [13].

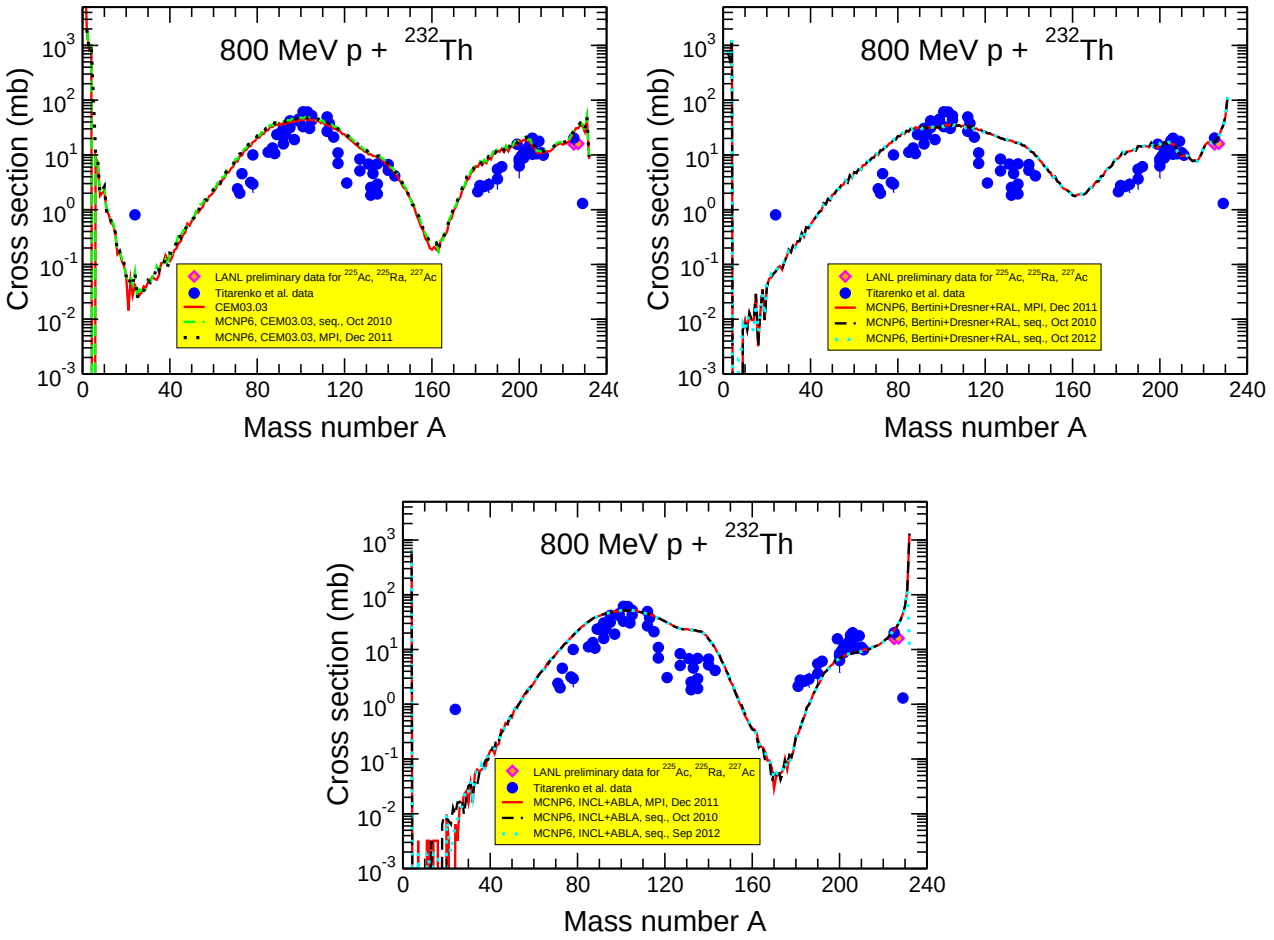

Figure 4: Comparison of the measured [41, 42] mass distribution of products from the reaction 800 MeV p + ^{232}Th with results by CEM03.03 used as a stand alone code and with old results by MCNP6 obtained in a sequential mode with the GENXS option using the CEM03.03 [12], Bertini+MPM+Dresner+RAL [18, 19, 20, 21], and INCL+ABLA [22, 23] event-generators, as presented in Fig. 14 of Ref. [13] as well as calculated later in parallel, with MPI, as indicated. Note that before the end of 2011 the default option of MCNP6 to calculate proton-induced reactions at energies up to 3.5 GeV was Bertini+MPM+Dresner+RAL [18, 19, 20, 21] while later the default was changed to the CEM03.03 [12] event generator. This change of the default options of models used by MCNP6 caused some confusion and misunderstanding of some results obtained at that time with MCNP6. For this reason, we show here MCNP6 results calculated in a sequential mode before changing the default (labeled as "Oct. 2010") and after that change (labeled as "Oct. 2012"), to prove that everything is self-consistent and the old results coincide with the new ones.

3.2. A) 35MeVLi7CEM; B) 35MeVLi7Bert; C) 35MeVLi7lib4

This test problem is to study the applicability of MCNP6 to simulate quasi-monoenergetic neutron sources from interaction of proton beams (incident energies below 150 MeV) with thick ^{7}Li targets. Such problems are of interest in applications where quasi-monoenergetic neutrons of different energies are needed to measure activation cross sections for the estimation of induced radioactivity and for other applications.

A real monoenergetic neutron source in the MeV energy region is not feasible, therefore "quasi-monoenergetic" neutron sources are used in different applications. Among such sources, the ones based on the ^{7}Li(p,n) reaction are widespread. Although this reaction was measured many times by different authors at several laboratories (see reviews on available data in Refs. [43, 44, 45]), the measured data do not cover continuously the whole incident proton energy region and the whole kinematics region of secondary neutrons. Therefore evaluated nuclear data libraries are needed for the ^{7}Li(p,n) reaction, to be used in simulations with transport codes of the "quasi-monoenergetic" neutron production from thick lithium targets in every particular application.

In Refs.[43, 44], an ENDF-formated data library for incident protons with energies up to 150 MeV was developed. In those papers, the important ^{7}Li(p,n_0) and ^{7}Li(p,n_1) reactions were evaluated from the experimental data, with their angular distributions represented using Legendre polynomial expansions. The decay of the remaining reaction flux was estimated from GNASH nuclear model calculations. This leads to the emission of lower-energy neutrons and other charged particles and gamma-rays from preequilibrium and compound nucleus decay processes. Examples of the use of these data in representative applications by a radiation transport simulation with the code MCNPX [8] are also presented in Refs. [43, 44].

More recently, our data library was used successfully by Simakov et al. in MCNPX simulations to study the activation cross sections on Bi, Au, Co, and Nb targets bombarded with quasi-monoenergetic neutrons produced from the p+^{7}Li reaction at the NPI/Řež cyclotron facility [46]. However, we never tested the p+^{7}Li data library with the latest Los Alamos Monte Carlo transport code MCNP6 [3]-[6]. To fill this gap, we test [47] the applicability of MCNP6 to simulate quasi-monoenergetic neutron sources from interactions of proton beams with energies below 150 MeV on thick ^{7}Li targets. We used in our study the neutron spectra measured recently by Uwamino et al. from a 2 mm thick ^{7}Li target bombarded with protons of 20, 25, 30, 35, and 40 MeV [48] and took advantage of an MCNPX input file kindly sent to us by Dr. Simakov to simulate the geometry of the problem (see Fig. 1 in Ref. [47]), that we modified later for our MCNP6 needs.

Here, we test this problem using the LANL 3007.00h, li7mod data library [43, 44], as well as the Bertini+Dresner and CEM03.03 event-generators and compare the calculation results with available measured data only at one proton-incident energy of 35 MeV.

Tabulated values of these experimental data were posted recently in the EXFOR data base, ENTRY E1826, and the 35 MeV measured neutron spectra is presented here in the file */VALIDATION_CEM/Experimental_data/pLi7_n/35MeV.exp.dat.

The input file for this problem while using CEM03.03 is **p35MeVLi7CEM**. It is provided in subdirectory **/VALIDATION_CEM/Inputs/** and is shown also below.

```
Uwamino'Exp: Ep=35MeV+Li+C,LA150+MODEL
c  ----------------------
C    CELL CARDS
```

```
c  ----------------------
C      Li Volume
1    1 -0.534   -960  950 -951                    imp:h=1 imp:n=1 imp:e=0
C      Graphite beam stop
2    2  -2.0    -960  951 -952                    imp:h=1 imp:n=1 imp:e=0 $
c      Al Flange
3    3 -2.7 (-960  952 -953):(960 -961 950 -953)  imp:h=0 imp:n=1 imp:e=0
c  d-beam vacuum tube
4    0       -960  940 -950                      imp:h=1 imp:n=1 imp:e=0
C    Rest of World
90   9 -1.293E-3 -980  #1 #2 #3 #4               imp:h=0 imp:n=1 imp:e=0
991  0  980 -990                                 imp:h=0 imp:n=0 imp:e=0

c  ----------------------
C    SURFACE CARDS
c  ----------------------
C    TARGET - Neutron Source
c 900  pz    0.
950  pz    0.0    $ Li7 target left  plane
951  pz    0.2    $ Li7 target right plane
952  pz    1.4    $ C  backup right plane
953  pz    1.5    $ Al flange right plane
960  cz    1.25   $ Li+C inner Cylinder
961  cz   10.0    $ Al   outer Cylinder
c
980  so   50.     $ Sphere for NE-detector
999  pz  -25.
910  cz    0.5    $ Beam cookie-cutter cylinder
C
C    UNIVERSE/SYSTEM boundary
940  pz -15.0      $ proton start surface
990  so  2000
c
C    Segmenting surfaces
110    cz 1.0         $ 0  deg  $ Teta = 1.1 deg
10     cz 2.5         $ 0  deg  $ Teta = 2.9 deg
21  21 cz 2.5         $ 10 deg
22  22 cz 2.5         $ 20 deg
23  23 cz 2.5         $ 30 deg
24  24 cz 2.5         $ 40 deg
26  26 cz 2.5         $ 60 deg
30     cy 2.5         $ 90  deg
31  21 cy 2.5         $ 90+15=105 deg
32  22 cy 2.5         $ 90+20=110 deg
33  23 cy 2.5         $ 90+40=130 deg
34  24 cy 2.5         $ 90+60=150 deg
35  25 cy 2.5         $ 90+80=170 deg
```

```
C       DATA CARDS
c
c --- 10 deg
TR21  0 0 0 1 0 0 0 0.984808 0.1736482
c --- 15deg
c TR21  0 0 0 1 0 0 0 0.9659258 0.2588190
c --- 20 deg
TR22  0 0 0 1 0 0 0 0.9396926 0.3420201
c --- 30 deg
TR23  0 0 0 1 0 0 0 0.8660254 0.5
c --- 40 deg
TR24  0 0 0 1 0 0 0 0.7660444 0.6427876
c 45 deg
c TR45  0 0 0 1 0 0 0 0.70710678 0.70710678
c --- 60 deg
TR26  0 0 0 1 0 0 0 0.5      0.866025
c  75 deg
c TR25  0 0 0 1 0 0 0 0.2588190 0.9659258
c 80 deg
TR25  0 0 0 1 0 0 0 0.1736482 0.9848078
c
C     --- Li-7         24 - LANL-150
M1     3007 1.0      nlib=24c hlib=24h
MX1:h  MODEL
MX1:n  MODEL
c         Li-7 + p      LA evaluation
c M1     3007 1.0      nlib=24c hlib=00h
c MX1:n  MODEL
c
C      --- Graphite (available in LA150: 6012.24h 6000.24c)
c M2    6012.24h 1.0  6000.24c 1.0   nlib=24c hlib=24h
M2     6012 0.989  6013 0.011   nlib=24c hlib=24h
MX2:h     j        MODEL
MX2:n  6000        MODEL
C      --- Aliminium
M3    13027 1.0     nlib=24c hlib=24h
C      --- Cupper
c M5   29063.24c 0.6917  29065.24c 0.3083
c      ---  Luft
M9    8016.24c 0.2      7014.24c 0.8
c     Eurofer
MODE h n
lca 8j 1   $ use CEM03.03
c
c void 1  $ no Lithium target
c void 2  $ no Carbon stopper
```

```
c void 9  $ no Air
c
C  -------  Cutoff Cards -------
CUT:h   1j 3.5     $ cut to remove error sampling from La150.24h
c CUT:n   1j 0.1
c CUT:n 1j  14.6                $ Low   Energy = 14.6 MeV
C  ------- Physics Cards ---------
c n:  Emax Ean iunr dnb   Tbl Fism recl
C PHYS:n 100 0  j j  -1 j j $ n: upper Energy = 100MeV, Tabl data = Mix&Match
PHYS:n 100   0    j   j  j  j $ n: upper Energy = 100MeV, Tabl data = Mix&Match
c h:  Emax Ean  Tbl   j istrg    j recl
PHYS:h 100   0 -1 j  j j j $ h: Upper Energy = 100MeV, Tabl data = Mix&Match
c
c SPABI:n h 50 1
C  ========================================
C             Source Specification
c  ========================================
c        E = 40 (Li) = 38.7 (only C)
SDEF PAR=h ERG=35.0 SUR=940 DIR=1 VEC=0 0 1 x=0 y=0 z=-1.0
c   Gauss(FWHM,Mean)
c SP1  -41   0.3   0
c  ----------------------------------
C    Neutron Tally Cards
c  ----------------------------------
c Normalization (n/mkC/sr): [1/p] = 6.2415E12 muC^-1
c Omega = (S_ring/S)sphere)*4pi = 2*pi*h(h=(R-R*cos(Theta)))/R =
C         = 7.8589E-3 [sr]
FC32 Neutron Flux Detector (F2, n/sr/mkC) at 0,10,20,30,40,60
F32:N   980
FS32   -999 -10 -21 -22 -23 -24 -26
FM32  6.2415E12    $ This convert [1/proton]  muC^-1
SD32  1.E+24 7.8589E-3 5r 1.E+24 $ This provides us [1/sr]; not for 1st & 8th
E0  1.0 48i 50 $ This provides us [1/MeV] automatically, as the E-step = 1 MeV
C E0    0.2 0.4 0.6 0.8 1.0 1.2 1.4 1.6 1.8 2.0
C      2.5 3.0 3.5 4 5 6 8 10 4i 20 4i 30 19i 50
FC132 Neutron Flux Detector (F2, n/sr/mkC) at 0 (dTeta=2*1.1deg)
F132:N   980
FS132   -999 -110
FM132   15.6035E+15
SD132   1.E+24 3.141592  1.E+24   $ pi*r**2
c
FC12   Threshold Neutron Flux:(E > 4MeV) (n/sr/mkC) (0,10,20,30,40,60deg)
FM12    15.6035E+15
F12:n   980
FS12   -999 -10 -21 -22 -23 -24 -26
sD12      1.E+24 19.6472 5r 1.E+24
E12    4.0   50
```

```
C
PRDMP   -300 -300 1 10 0
PRINT
c
NPS   1.E+8
c nps 1E5
dbcn 28j 1
```

The input files for this problem using the Bertini event-generator is **p35MeVLi7Bert**, while for the case using our LANL 3007.00h, li7mod data library, the input file is **p35MeVLi7lib4**; both of them are presented in subdirectory **/VALIDATION_CEM/Inputs/**. These are the real input files we used in our MCNP6 calculations with MPI in March 2012, using the Beta 2 version of MCNP6 [4]. However, later, in the Beta 3 [5] and 1st production [6] versions of MCNP6, many changes have been done, some of them affecting slightly these inputs files. So, as we already mentioned above in Sec. 3.1, starting with the Beta 3 version of MCNP6, the default option of models for reactions induced by nucleons and pions at energies below 3.5 GeV was set to CEM03.03 instead of Bertini. To the current test-problem, this means that in the input file **p35MeVLi7CEM** we do not need any more the card

```
lca 8j 1   $ use CEM03.03
```

as **lca(9) = 1** is set in MCNP6 as default. This card does not do any harm and can be left in the input file for the CEM03.03 model, but it is not needed any more. Just the same is true about the very last card of the input file

```
dbcn 28j 1
```

In the production version of MCNP6 [6] this card is not needed any more [49], though we can leave it there: MCNP6 will simply ignore and not use it. On the other had, if in the later versions of MCNP6, starting with Beta 3, we like to invoke the Bertini model with **lca(9) = 0**, then we need to add the card

```
lca 8j 0   $ use Bertini
```

in the input file **p35MeVLi7Bert**, otherwise MCNP6 would perform the calculation using CEM03.03, as we had in the "puzzle" described in Sec. 3.1.

Neutron spectra at 0 ($\pm$2.9) degrees calculated using the MPI (4 nodes, 64 processors) version of MCNP6 with CEM03.03 using the input file **p35MeVLi7CEM** is tabulated in units of [neutrons/MeV/sr/muC] in the output file **p35MeVLi7CEM.mpi.o** as tally 32 for "segment": segment: 999 -10, as well as in the MCTAL file **p35MeVLi7CEM.mpi.m**, both presented in subdirectory */VALIDATION_CEM/Templates/LINUX/. Similar results calculated using the Bertini INC + Dresner evaporation options of MCNP6 (input file **p35MeVLi7Bert**) are presented in the same units, the same "segment" of the same tally 32 in the output file **p35MeVLi7Bert.mpi.o**, as well as in the MCTAL file **p35MeVLi7Bert.mpi.m**. Results calculated with the recent LANL 3007.00h, li7mod data library (input file **p35MeVLi7lib4**) are presented in the same units, the same "segment" of the same tally 32 in the output file **p35MeVLi7lib4.mpi.o**, as well as in the MCTAL file **p35MeVLi7lib4.mpi.m**.

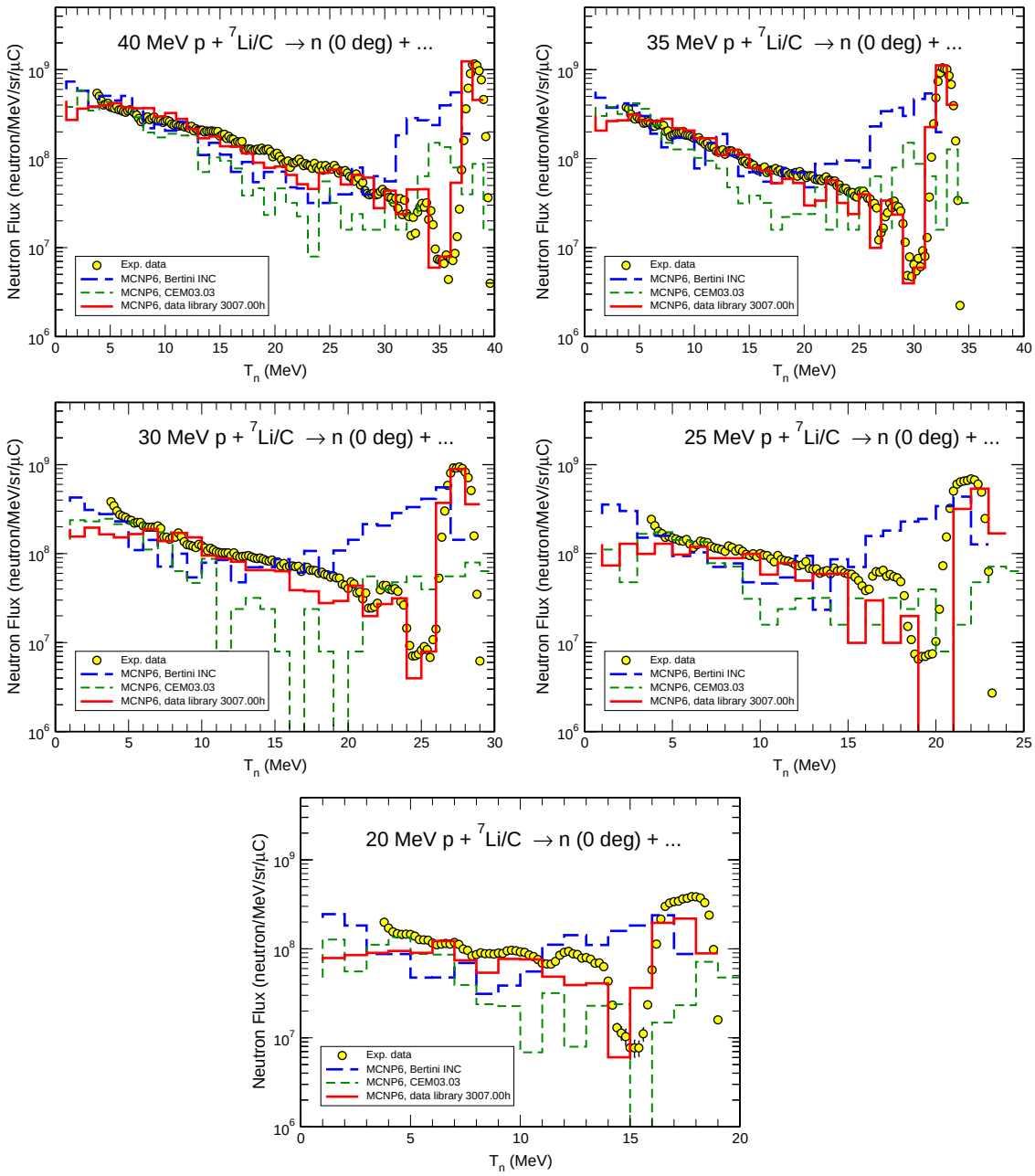

Figure 5: Comparison of the MCNP6 results (histograms) for neutron spectra from a thick ^{7}Li target bombarded with proton beams of 40, 35, 30, 25, and 20 MeV with the experimental data by Uwamino et al. [48] (solid circles). MCNP6 spectra calculated in parallel, with MPI, using the p+^{7}Li data library [43] and, for comparison, with the Bertini+Dresner [18, 20] and CEM03.03 [12] event generators are shown with solid red, blue dashed, and green dashed histograms, as indicated in legends.

Note that as is often adopted in the literature, the measured neutron spectra for this test-problem have been published not normalized with the units of [per proton], but with the normalization [per microcurie (muC)]. To convert [1/proton] to [1/muC] we use in our input files the **FM32** card. Also, to normalize the calculated neutron spectra to the solid angle, i.e., to get [1/sr], as in the published experimental spectra, we use in our input files the **SD32** card. We get the units of [1/MeV] in the MCNP6 neutron spectra automatically, without a division to the energy steps of the spectra, as we have chosen in the **E0** card of our input files all the energy steps to be equal to 1 MeV.

To help plot the neutron spectra with xmgrace, the MCNP6 results with Bertini+Dresner, CEM03.03, and LANL 3007.00h, li7mod data library options and the experimental spectrum are copied to separate files 35MeV.Bert.dat, 35MeV.CEM.dat, 35MeV.lib.dat, and 35MeV.exp.dat, respectively.

An xmgrace template for the figure with these four neutron spectra is presented in the file p35MeVLi7_n.fig. The final pdf file for the figure is p35MeVLi7_n.pdf, shown in the upper left corner of Fig. 5.

Although in this test problem we address only the 35 MeV incident energy of the proton beam, for comparison, Fig. 5 shows also similar results for the proton beams of 40, 30, 25, and 20 MeV published in Ref. [47]. Readers can easily get such results with MCNP6 modifying only one card in the input files presented here, namely changing the value of the **ERG** parameter on the **SDEF** card from 35.0 to the needed proton incident energy (in MeV). The experimental values of spectra at 40, 30, 25, and 20 MeV are available already in EXFOR.

From Fig. 5, we can see that, just as expected for such low energies of incident protons, neither the Bertini+Dresner [18, 20] nor the newer CEM03.03 [12] event generators can reproduce satisfactorily the measured neutron spectra from our ^{7}Li target: The higher the incident energy the better the agreement, but the quasi-monoenergetic neutron peak is not reproduced well by the models even at 40 MeV. At the same time, all the MCNP6 neutron spectra calculated using the p+^{7}Li data library agree well with the measured data, including in the region of the quasi-monoenergetic neutron peak of interest to our study, for all tested bombarding energies of the proton beam.

3.3. A) p800Tb_CEMo; B) p800Tb_Berto; C) p800Tb_INCLo

This problem is to test the applicability of MCNP6 using the CEM03.03, Bertini, and INCL+ABLA event-generators to calculate cross sections for the production of isotopes of interest in medical, astrophysical, and basic science research from a thin terbium target bombarded with a 800 MeV proton beam.

The proton-induced fission cross section of Tb is very low, therefore some models like the RAL fission model used as the default option in MCNP6 (before its Beta 3 version) for such reactions together with the Bertini INC, the Multistage Preequilibrium Model (MPM) and the Dresner evaporation model, does not account for fission of Tb at all. In addition, predictions by CEM03.03 and INCL+ABLA event generators for such processes differ significantly, therefore the MCNPS's ability to simulate proton-induced reactions on Tb must be carefully investigated.

Experimental cross sections of nuclide production from terbium were very scarce until recently: We are aware of only one study overlapping slightly with our current problem that have measured the ^{83}Rb cumulative cross section for proton reaction with terbium at 600 MeV performed at CERN by M. Lagarde-Siminoff and G. N. Simonoff [50]. We show that old cross sec-

tion in the file */VALIDATION_CEM/Experimental_data/p800Tb/p600Tb_Rb83cum.dat and compare it with our calculations and the very recent LANL measurements [51]. In addition, related to our test problem are the measured proton-induced fission cross section of Tb of 1.9 ± 0.2 mb at 600 MeV [52] and of 9.0 ± 1.5 mb at 1 GeV [53].

New measurements for this reaction at 800 MeV have just been completed at LANSCE, LANL. The new LANL data are tabulated in the paper [51]. Experimental values of the A-distribution of product yield measured at LANL are presented here in the file */VALIDATION_CEM/Experimental_data/p800Tb/p800Tb_A-cum.exp.dat. Values of 35 cross sections (cumulative and/or individual) for separately measured isotopes are presented in the files iso1.exp.dat and iso2.exp.dat, respectively, of the same subdirectory.

The main MCNP6 input file for the CEM03.03 event generator is **p800Tb_CEMo**. The GENXS option of MCNP6 requires a second auxiliary input file, **inxc95**, both provided in the subdirectory **/VALIDATION_CEM/Inputs/** and also shown below.

p800Tb_CEMo:

```
MCNP6 test: p + Tb159 by CEM03.03 at 800 MeV, nevtype=66
C Medical Ac-225 production for alpha cancer therapy
  1  1  1.0   -1 2 -3
  2  0        -4 (1:-2:3)
  3  0         4

c -------------------------------------------------------------
  1  cz  4.0
  2  pz  -1.0
  3  pz  1.0
  4  so  50.0

c -------------------------------------------------------------
  m1   65159 1.0
  sdef erg = 800 par = H dir = 1 pos = 0 0 0 vec 0 0 1
  imp:h 1 1 0
  phys:h 1000
  mode   h
LCA  8j 1    $ use CEM03.03, nevtype = 66                  !!!
  tropt genxs inxc95  nreact on  nescat off
c -------------------------------------------------------------
  print 40 110 95
  nps 10000000
c  prdmp 2j -1
```

inxc95:

```
MCNP6 test: p + Th232 by CEM03.03 at 800 MeV, nevtype=66
1 0 1 /
Cross Section Edit
50 0 9 /
```

```
5. 10. 15. 20. 25. 30. 35. 40. 45. 50. 55. 60. 65. 70. 75. 80.
85. 90. 95. 100. 120. /
1 5 6 7 8 21 22 23 24 /
```

The main MCNP6 input files for the Bertini and INCL+ABLA models are **p800Tb_Berto** and **p800Tb_INCLo**. Both of them use the same auxiliary input file, **inxc95**, shown above, and both are provided in the subdirectory **/VALIDATION_CEM/Inputs/**.

The only difference of **p800Tb_INCLo** from the **p800Tb_CEMo** and **p800Tb_Berto** input files is in the **LCA** and **LEA** cards. In the case of INCL+ABLA, these cards in the input file look like:

```
LCA  2 1 0 4j -1 2    $ use INCL+ABLA                    !!!
lea 2j 0
```

while for the Bertini option, we did not need those card at all, with the Beta 2 version of MCNP6 [4] we performed our calculations in April of 2012. However, as mentioned above in Sections 3.1 and 3.2, starting from the Beta 3 version of MCNP6 [5], CEM03.03 was set as the default option in MCNP6 to describe reactions induced by nucleons and pions with energies below 3.5 GeV. This means that in the latest versions of MCNP6, **LCA(9) = 1** by default, and we do not need to use any more the LCA card in our input files in order to invoke the CEM03.03 model. On the contrary, if we like to use Bertini, now we have to specify in our input file explicitly that **LCA(9) = 0**, i.e., in the input file **p800Tb_Berto**, we need to add now the card:

```
LCA 8j 0    $ use Bertini                    !!!
```

otherwise MCNP6 will perform calculations using CEM03.03.

The MCNP6 mass-distribution of products from the reaction 800 MeV p + ^{159}Tb calculated with the CEM03.03 event generator with MPI as described in Sec. 2, using 4 nodes, 64 processors of the LANL supercomputer **Turing** is presented in the table entitled "Summary by mass number:" of the MCNP6 output file **p800Tb_CEMo.mpi.o**. It is also copied here in a separate auxiliary file, p800Tb_M6CEMo.dat, to help plot this A-distribution with xmgrace. Cross sections for the production of all isotopes from this reaction are printed in table entitled "Distribution of residual nuclei" of the MCNP6 output file.

MCNP6 results using the Bertini+Dresner+RAL event-generator are presented in the output file p800Tb_Berto.mpi.o, with the mass-distribution of all products copied here in the auxiliary file p800Tb_M6Bert.dat (to help plot this A-distribution with xmgrace).

Similarly, results by MCNP6 using the INCL+ABLA event-generator are presented in the output file p800Tb_INCLo.mpi.o, with the mass-distribution of all products copied here in the auxiliary file p800Tb_M6INCL.dat (to help plot this A-distribution with xmgrace).

The file p800Tb_A-cum.fig is a template for plotting the mass distributions of all products from our p + ^{159}Tb reaction with with xmgrace, as calculated by all three event-generators tested here. The pdf file for the figure is p800Tb_A-cum.pdf; it is shown as Fig. 3 in Ref. [51] as well as in subdirectory */VALIDATION_CEM/Experimental_data/p800Tb/ and in the lower plot of the Fig. 6 below.

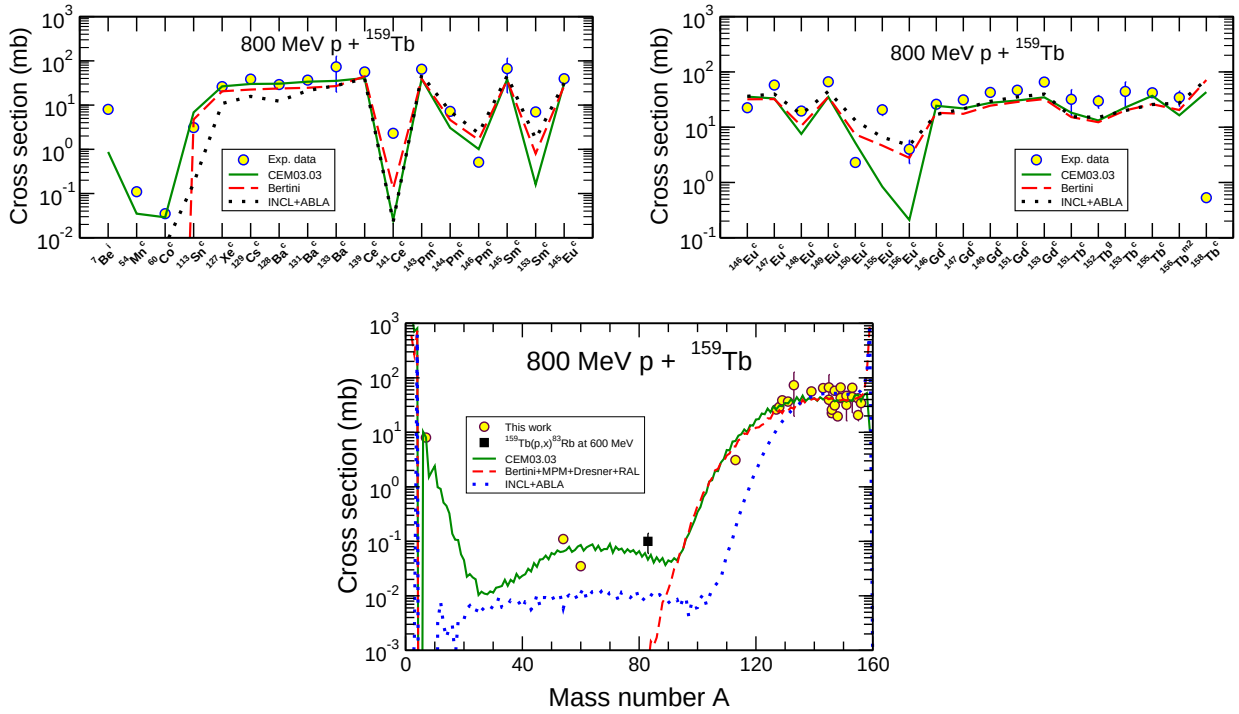

Figure 6: Detailed comparison between all cross sections measured in Ref. [51] and those predicted by MCNP6 using CEM03.03, Bertini+MPM+Dresner+RAL, and INCL+ABLA event generators (upper plots), as indicated in legends. All calculations were done in parallel, with MPI. The cumulative cross sections are labeled with a "c" and the independent cross sections, with an "i". Though in the upper plots we see some very good agreements of different calculation results with each other and with the measured data for some products, and some big discrepancies for several other isotopes, the reason of the observed disagreement is not completely clear. No unambiguous conclusions about possible ways to improve the models can be done from such comparisons. The lower plot, comparing the mass distributions of product yields, is actually more informative about possible ways of further model improvements.

Note that all the event generators of MCNP6 compute only independent cross sections; cumulative cross sections were calculated using these independent values summed thereafter separately according to the decay behavior of calculated products, using the Table of Isotopes by R. B. Firestone [54].

Measured cumulative and/or independent cross sections for the production of isotopes from ^{7}Be to ^{145}Eu are presented in the file iso1.exp.dat. The corresponding MCNP6 cross sections calculated with CEM03.03, Bertini, and INCL+ABLA are presented in the files iso1.cem.dat, iso1.bert.dat, and iso1.incl.dat, respectively. Similar, measured and calculated cross sections for products from ^{146}Eu to ^{158}Tb are listed in the files iso2.exp.dat, iso2.cem.dat, iso2.bert.dat, and iso2.incl.dat, respectively, all presented in the subdirectory /VALIDATION_CEM/Experimental_data/p800Tb/.

Templates to plot these two group of cross sections with xmgrace are presented in the files p800Tb-iso1.fig and p800Tb-iso2.fig, respectively. Postscript and pdf files for plots with these two group of cross sections are presented in the files p800Tb-iso1.ps, p800Tb-iso1.pdf, p800Tb-iso2.ps, and p800Tb-iso2.pdf. The two postscript files were incorporated in a single

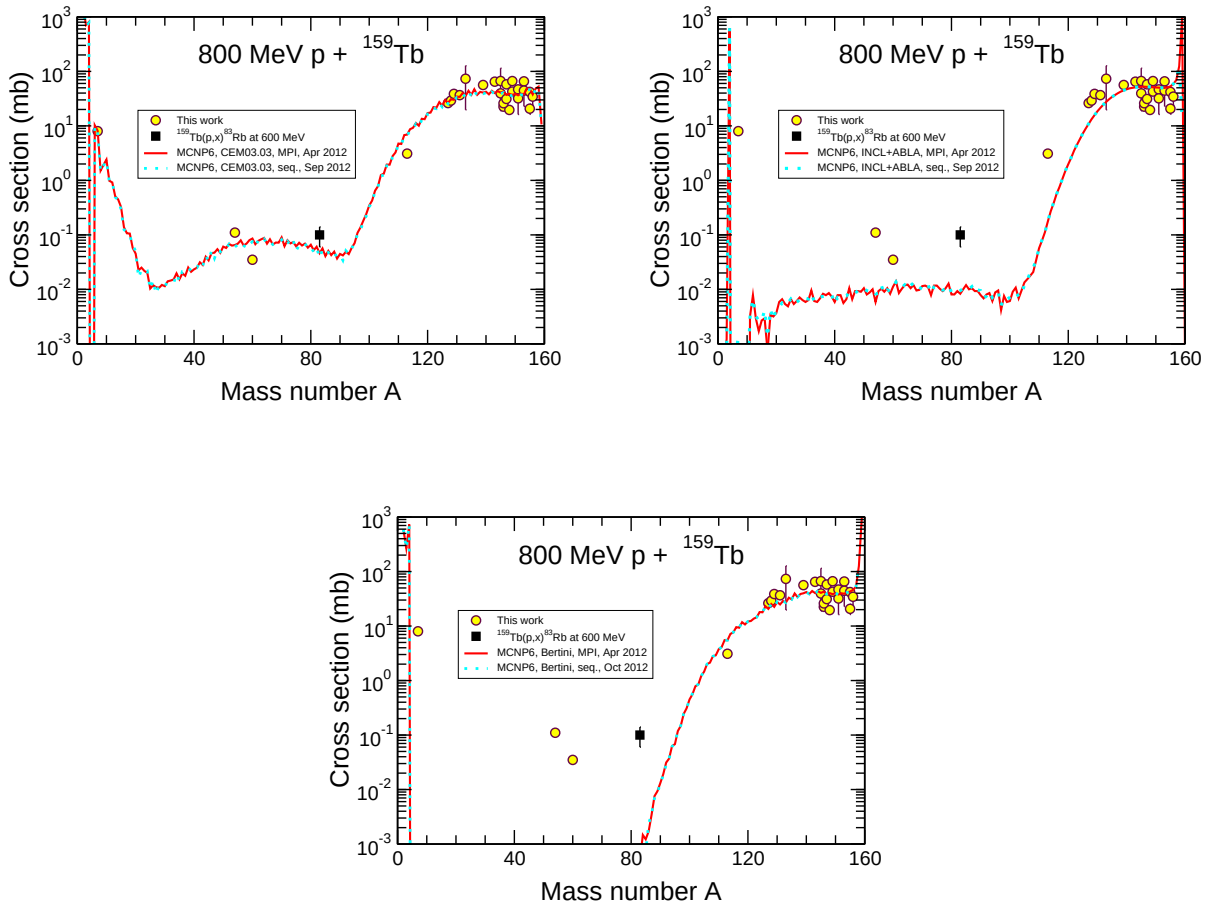

Figure 7: Comparison of mass distributions of product yields calculated in parallel with MPI and in a sequential mode by MCNP6 using CEM03.03, Bertini+MPM+Dresner+RAL, and INCL+ABLA from 800 MeV p + ^{159}Tb with cumulative cross sections measured in Ref. [51], as indicated in legends. The only product yield in the fragmentation region measured in Ref. [51], the independent cross section of ^{7}Be, and the independent cross section of ^{54}Mn produced via fission, are shown as well, for comparison. The ^{159}Tb(p, x)^{83}Rb data point at 600 MeV was measured by Lagarde-Simonoff and Simonoff and was published in Ref. [50].

figure with LaTeX using the file p800Tb-iso.tex. The final pdf file with all 35 measured cumulative and/or independent cross sections produced with LaTeX is p800Tb-iso.pdf, presented in the same subdirectory, as Fig. 4 in Ref. [51], and here, in the upper part of Fig. 6.

For comparison, we performed also calculations for this test-problem in a sequential mode. Fig. 7 presents a comparison of the mass distributions of all products from our reaction calculated with the three event-generators tested here while running MCNP6 in a sequential mode with similar results obtained with MPI, shown above in Fig. 6. We can see, that just as expected, the results obtained with MPI are practically the same as the ones calculated in a sequential mode (with only some tiny differences in the last digits of some values, not seen at all in the scale of our figures).

From the presented results we can see that calculations by all event generators agree with the measured data in the mass region near $A = 159$ where spallation reactions dominate. CEM03.03

and INCL+ABLA predictions differ from one another in the region of fission fragments by an order of magnitude, with the CEM03.03 results much closer to the measured values. The RAL fission model used with the Bertini option of MCNP6 does not calculate at all fission of nuclei with atomic number $Z < 70$. Only one product, ^{7}Be, could be measured in the fragmentation region in Ref. [51]. CEM03.03 predicts a cross section for ^{7}Be about nine times lower than the measured value, while INCL + ABLA predicts a still lower yield, and Bertini does not predict the formation of ^{7}Be products from 800 MeV protons incident on terbium. In the region of fission fragments, CEM03.03 predicts the yield of ^{54}Mn within a factor of three of the measured value and a yield of ^{60}Co which is within experimental measurement [51] uncertainty. The computational models studied here are expected to benefit from modifications to improve their predictive accuracy in light of this test-problem and comparison with the experimental data from Ref. [51].

3.4. A) cu800b-cor; B) cu800c-cor; C) cu800i-cor

This MCNP6 problem is to test the applicability of MCNP6 using the CEM03.03 event generator to describe backward emission of particles from thick targets bombarded by intermediate-energy (800-1200 MeV) protons. To be specific, this test problem is to study neutron emission at 175 degrees from a 800 MeV proton beam hitting a face plane of a cylindrical copper target of 20 cm in diameter and 25 cm thick.

First, we need such information for shielding consideration, to be able to prevent cases when personnel may receive radiation from backward fluxes.

Second, it is much more difficult for all models to describe particle production at very backward angles than at intermediate or forward angles; that is, this problem is a good test to see how the CEM03.03 event generator does work in such a "difficult" kinematics region.

Third, spectra of secondary particles at very backward angles are of great academic interest, to understand the mechanisms of cumulative particle production, under investigation for almost four decades, but still with many open questions.

From a formal point of view, this test-problem is somehow similar to the test-problem #2 (Fe1200) of the /VALIDATION_CEM/ Test Suite (see Ref. [13]). However, it is for another incident energy and another target. Most important, we run this test problem both in parallel, with MPI, and in a sequential mode, using the CEM03.03, as well as the Bertini+Dresner and the INCL+ABLA event generators. We needed such problems to find and fix a bug observed in the Beta 3 version of MCNP6 while using INCL+ABLA to calculate such reactions.

The experimental data for this problem were measured at the Institute of High Energy Physics in Protvino, Russia using the calorimetric-time-of-flight (CTOF) technique and are published in Ref. [55].

Though the current problem is to test the energy of the bombarding protons of only 800 MeV, the measurements were performed also at 1.0 and 1.2 GeV, therefore we present the experimental data and our MCNP6 calculations using CEM03.03, Bertini+Dresner, and INCL+ABLA event generators, from both MPI and sequential runs, for all three energies.

Experimental spectra in units of [neutron/MeV/sr/projectile] as functions of the neutron energy at incident proton energies of 800, 1000, and 1200 MeV are shown in files Cu-800-exp.dat, Cu-1000-exp.dat, and Cu-1200-exp.dat, respectively (the experimental errors are of the order of 8.5-9%, depending on the neutron energy).

The input file for this problem while using CEM03.03 is **cu800c-cor**. It is provided in

subdirectory **/VALIDATION_CEM/Inputs/** and is shown also below.

cu800c-cor:

```
MCNP6 test: 175 deg. n-spec. by CEM03.03 to compare with exp. data
c
c     **cellcards **
c
c    1  1 -11.35  -1 2 -3    $ m1 is Lead
     1  1 -8.96  -1 2 -3    $ m1 is Copper
     2  2 -0.001168  #1 -5
     3  0        5  -6
     6  0        6
   999  0       -999

c
c  *****surface card
c
     1  cz    10      $ diameter = 20 cm
     2  pz    0.0
     3  pz    25.0    $ 25 cm thick
     5  so    600
     6  so    800
     7  pz    -597.8168189
     8  pz    -597.6168189
   999  cz    10.000001

c  *
c  * Data Cards
c  *
c
c         Material cards
c
m1       29063.70h 69.17
         29065.70h 30.83
m2       7014.70h 1.555901784
         7015.60c 0.005778216
         8016.70h 0.448606754
         8017.60c 0.001079246
         1001.70h 0.06
         18000.35c 0.00934
         6000.60c 0.000383
c
c  importances
imp:n 1 1 1 0 0
imp:h 1 1 1 0 0
imp:p 1 1 1 0 0
```

```
imp:d 1 1 1 0 0
imp:t 1 1 1 0 0
imp:s 1 1 1 0 0
imp:a 1 1 1 0 0
imp:/ 1 1 1 0 0
imp:z 1 1 1 0 0
c *
c * source definition
c *
sdef erg=800 par=h dir=1 vec= 0 0 1 x=d1 y=d2 z=0 ccc=999
sp1  -41 2.4 0
sp2  -41 2.4 0
 nps   1e7
c nps   1000
print   10 110   40
prdmp 2.e7 1.e6 1 10 1e6
LCA  8j 1               $  use CEM03.03
c
c  tally
c
F11:n   5
SD11    1 753.9822369 1
FS11    -7 -8
FQ11    e u
TF11    6j 21
E11   1.059254E-03 1.188502E-03 1.333521E-03 1.496236E-03 1.678804E-03
      1.883649E-03 2.113489E-03 2.371374E-03 2.660725E-03 2.985383E-03
      3.349654E-03 3.758374E-03 4.216965E-03 4.731513E-03 5.308844E-03
      5.956621E-03 6.683439E-03 7.498942E-03 8.413951E-03 9.440609E-03
      1.059254E-02 1.188502E-02 1.333521E-02 1.496236E-02 1.678804E-02
      1.883649E-02 2.113489E-02 2.371374E-02 2.660725E-02 2.985383E-02
      3.349654E-02 3.758374E-02 4.216965E-02 4.731513E-02 5.308844E-02
      5.956621E-02 6.683439E-02 7.498942E-02 8.413951E-02 9.440609E-02
      1.059254E-01 1.188502E-01 1.333521E-01 1.496236E-01 1.678804E-01
      1.883649E-01 2.113489E-01 2.371374E-01 2.660725E-01 2.985383E-01
      3.349654E-01 3.758374E-01 4.216965E-01 4.731513E-01 5.308844E-01
      5.956621E-01 6.683439E-01 7.498942E-01 8.413951E-01 9.440609E-01
      1.059254E+00 1.188502E+00 1.333521E+00 1.496236E+00 1.678804E+00
      1.883649E+00 2.113489E+00 2.371374E+00 2.660725E+00 2.985383E+00
      3.349654E+00 3.758374E+00 4.216965E+00 4.731513E+00 5.308844E+00
      5.956621E+00 6.683439E+00 7.498942E+00 8.413951E+00 9.440609E+00
      1.059254E+01 1.188502E+01 1.333521E+01 1.496236E+01 1.678804E+01
      1.883649E+01 2.113489E+01 2.371374E+01 2.660725E+01 2.985383E+01
      3.349654E+01 3.758374E+01 4.216965E+01 4.731513E+01 5.308844E+01
      5.956621E+01 6.683439E+01 7.498942E+01 8.413951E+01 9.440609E+01
      1.059254E+02 1.188502E+02 1.333521E+02 1.496236E+02 1.678804E+02
      1.883649E+02 2.113489E+02 2.371374E+02 2.660725E+02 2.985383E+02
```

```
      3.349654E+02 3.758374E+02 4.216965E+02 4.731513E+02 5.308844E+02
      5.956621E+02 6.683439E+02 7.498942E+02 8.413951E+02 9.440609E+02
      1000
EM11  360000 120r  $ unit: n/sr/p
c
mode n h p d t s a / z
phys:h   1500.
phys:n   1500.
phys:p   1500
phys:/   1500
phys:z   1500
DBCN 28j 1
```

The input files for the Bertini and INCL+ABLA models are **cu800b-cor** and **cu800i-cor**. Both of them are provided in the subdirectory **/VALIDATION_CEM/Inputs/**.

The only difference in these three input files is with the **LCA** card. In the case of INCL+ABLA, the **LCA** card looks like:

```
LCA  8j 2                $  use INCL+ABLA
```

while for Bertini, it is:

```
LCA  8j 0                $  use Bertini + MPM + Dresner.
```

Note that as already mentioned above, starting from the Beta 3 version of MCNP6 [5], CEM03.03 was set as the default option in MCNP6 to describe reactions induced by nucleons and pions with energies below 3.5 GeV, therefore the **LCA** card for CEM03.03 is not needed any more, though it can be left in the input file as shown in our example: It will not change the results. Also, as mentioned above, starting from the Beta 3 version of MCNP6, the very last card of all these three input files

```
DBCN 28j 1
```

is not needed any more: It can be left in the input files, but MCNP6 will simply ignore it.

Our MCNP6 results obtained with MPI and sequential runs are practically the same, at all incident energies and for all tested event generators, therefore we present here only the output files from MPI runs. The output files obtained with MPI using CEM03.03, Bertini+Dresner, and INCL+ABLA are presented in subdirectory */VALIDATION_CEM/Templates/LINUX/ under the names: cu800c-cor.mpi.o, cu800b-cor.mpi.o, and cu800i-cor.mpi.o, respectively (the corresponding input files are cu800c-cor, cu800b-cor, and cu800i-cor, presented in the Input subdirectory /VALIDATION_CEM/Inputs/). To ease plotting with xmgrace the calculated neutron spectra printed in units of [neutron/sr/projectile] in the tables labeled as **segment: 7 -8** of the listed above output files, the same results, but already divided by the value of the energy bins (to get the final theoretical spectra in units of [neutron/MeV/sr/projectile]), are copied here in separate files Cu800C-cor.dat, Cu800B-cor.dat, and Cu800I-cor.dat, respectively.

As MCNP6 results at 1.0 and 1.2 GeV can be calculated changing only one number, the value for **erg** parameter on the **sdef** card, in the input files listed above, we do not present here either input or output files for incident energies of 1.0 and 1.2 GeV. However, to get the final plot with xmgrace with spectra at all three incident energies, our MCNP6 results from MPI

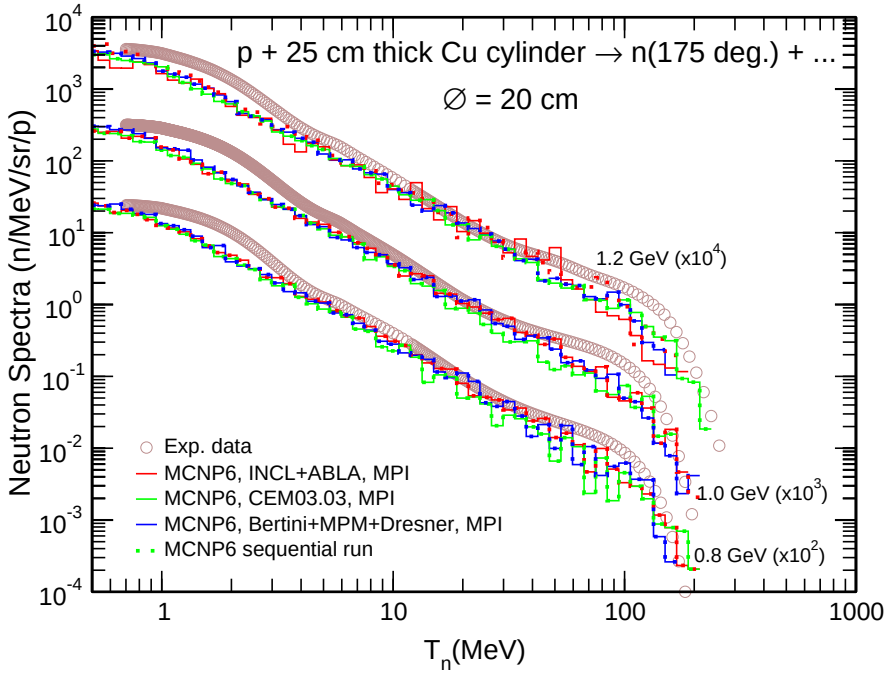

Figure 8: Experimental [55] neutron spectra at 175 degrees (symbols) from a thick Cu cylinder bombarded with 800, 1000, and 1200 MeV protons compared with results by MCNP6 calculated in parallel with MPI (solid histograms) and in a sequential mode (dotted histograms) using the CEM03.03 [12], Bertini INC [18] followed by the Multistage Preequilibrium Model (MPM) [19] and the evaporation model described with the Dresner code EVAP [20], and by the INCL+ABLA [22, 23] event-generators, as indicated in legend.

runs using CEM03.03, Bertini+Dresner, and INCL+ABLA at 1.0 and 1.2 GeV, divided by the value of the energy bins, i.e., in units of [neutron/MeV/sr/projectile], are shown in separate files Cu1000C-cor.dat, Cu1000B-cor.dat, Cu1000I-cor.dat, Cu1200C-cor.dat, Cu1200B-cor.at, and Cu1200I-cor.dat, respectively.

For comparison, in our plot, we show also MCNP6 results obtained from sequential runs. Such results are presented here in files with similar names (in the same units) as from MPI runs, but with an extra-extension, "seq", in their names. A template for plotting all spectra with xmgrace is presented in the file pCu_n.mpi-seq-cor.fig. The final pdf file with our results plotted with xmgrace is: pCu_n.mpi-seq-cor.pdf and is shown here in Fig. 8.

Note that for this particular reaction, MCNP6 using the INCL+ABLA did crash after a number of simulations at all three energies we tested, whether we ran MCNP6 with MPI or in a sequential mode. A detailed analysis had shown that this happened when in some very rare cases INCL+ABLA would produce an unphysical, unstable nuclide from such reactions as a "fission fragment". Dr. Grady Hughes fixed this problem so that MCNP6 does not crash anymore while simulating such reactions with INCL+ABLA. The reason why INCL+ABLA did produce in some rare cases such unphysical products from these reactions remains unclear to us. We plan to replace the relatively old versions of INCL+ABLA [22, 23] we have at present in MCNP6 with newer and better versions, so that this question would disappear at that time.

3.5. A) p1000Ho_CEM; B) p1000Yb_CEM (both with inxs96)

This problem is to test how MCNP6 using the CEM03.03 event-generator predicts proton-induced fission cross section of preactinide nuclei.

To be exact, this test-problem is to calculate with MCNP6 using CEM03.03 proton-induced fission cross section of ^{165}Ho and ^{173}Yb at energies from $\sim$ 100 MeV to $\sim$ 5 GeV and to compare the results with predictions by CEM03.03 used as a stand alone code and with available experimental data. All MCNP6 calculations were done in parallel, with MPI as described in Sec. 2. Such reactions are of interest for different applications. For example, at Accelerator Driven Systems (ADS), during a high-energy nuclear reaction on a heavier nucleus, like ^{209}Bi, used in spallation targets, after emitting several nucleons and pions, the initial heavier nucleus can be transformed into a much lighter ^{173}Yb or ^{165}Ho nucleus, still able to fission after interactions with secondary or primary protons in the thick spallation target.

For us, this test-problem was also needed to calculate and analyze fission cross sections of preactinides nuclei with MCNP6 using CEM03.03 in order to understand and fix a problem of predicting fission cross section of ^{181}Ta by CEM03.03 (see details in Ref. [56]).

For this problem, instead of using only a few available experimental data on proton-induced fission cross sections of ^{165}Ho and ^{173}Yb, we prefer to use the systematics by Prokofiev [57] that provide the best current estimations of the experimental fission cross sections for these nuclei in the energy region of interest to our problem. Files p_Ho165_Baznat.dat and p_Yb173_Baznat.dat in subdirectory */VALIDATION_CEM/Experimental_data/pHo-Yb_fiss/ provide the fission cross sections as predicted by the Prokofiev systematics for ^{165}He and ^{173}Yb, respectively. Files with final results of our calculations and the figures, described below, are presented in the same subdirectory.

The easiest way to calculate fission cross sections with MCNP6 is to use the GENXS option for a single incident energy of protons; then, to perform as many calculations as needed changing only the proton energy on the SDEF card of the MCNP6 input file. As all inputs at different proton energies are exactly the same, with the only difference in the proton energy on the SDEF card, we present here only one example of MCNP6 input at output, at $T_p = 1$ GeV. The input files for ^{165}Ho and ^{173}Yb at this energy are p1000Ho_CEM and p1000Yb_CEM, respectively. Let us recall here that the GENXS option of MCNP6 requires a second, auxiliary, input file. For both our examples, it is the same, namely: inxs96. All these three input files are presented in the subdirectory /VALIDATION_CEM/Inputs/. Below, we show only the example for ^{165}Ho, namely the **p1000Ho_CEM** and **inxs96** input files:

p1000Ho_CEM:

```
MCNP6 test: p + Ho165 -> fission xsec by CEM03.03 at 1000 MeV, nevtype=66
C To evaluate how MCNP6 with CEM describes preactinide fission cross sections
  1  1  1.0   -1 2 -3
  2  0        -4 (1:-2:3)
  3  0         4

c -------------------------------------------------------------
  1  cz  4.0
  2  pz  -1.0
  3  pz  1.0
```

```
  4  so  50.0

c ------------------------------------------------------------
  m1 67165 1.0
  sdef erg = 1000 par = h dir = 1 pos = 0 0 0 vec 0 0 1
  imp:h 1 1 0
  phys:h 5010
  mode   h
LCA  8j 1    $ use CEM03.03, nevtype = 66                  !!!
  tropt genxs inxs96  nreact on  nescat off
c ------------------------------------------------------------
  print 40 110 95
c  nps 10000
  nps 1000000
c  prdmp 2j -1
```

inxs96:

```
MCNP6 test: n + Bi -> fission cross section by CEM03.03 at 800 MeV, nevtype=66
0 0 1 /
Cross Section Edit
0 0 0 /
5. 10. 15. 20. 25. 30. 35. 40. 45. 50. 55. 60. 65. 70. 75. 80.
85. 90. 95. 100. 120. /
1 5 6 7 8 21 22 23 24 /
```

The main input file for ^{173}Yb is very similar, with a difference in only the material card, which for ^{173}Yb looks like:

```
  m1 70173 1.0
```

Let us recall here again that starting from the Beta 3 version of MCNP6 [5], CEM03.03 was set as the default option in MCNP6 to describe reactions induced by nucleons and pions with energies below 3.5 GeV, therefore the **LCA** card for CEM03.03 is not needed any more, though it can be left in the input file as shown in our example: It will not change any results.

The output files for ^{165}Ho and ^{173}Yb are p1000Ho_CEM.mpi.o and p1000Yb_CEM.mpi.o, respectively, both presented in the subdirectory */VALIDATION_CEM/Templates/LINUX/. The fission cross section is printed in the output files in barns, two lines before the tables with residual nuclei yields. Files p_Ho165_M6.dat and p_Yb173_M6.dat present fission cross sections at all energies calculated with MCNP6 for ^{165}Ho and ^{173}Yb extracted from the corresponding output files, respectively; we use these files to plot with xmgrace these fission cross sections. For comparison, we present in subdirectory */VALIDATION_CEM/Experimental_data/pHo-Yb_fiss/ also the files pHo165CEM.dat and pYb173CEM.dat with results by CEM03.03 used as a stand alone code for ^{165}Ho and ^{173}Yb, respectively.

The files p_Ho165_CEM.fig and p_Yb173_CEM.fig are templates for plotting with xmgrace the fission cross section for ^{165}Ho and ^{173}Yb at all incident energies of protons we calculated. The final pdf files with figures for ^{165}Ho and ^{173}Yb are p_Ho165_CEM.pdf and p_Yb173_CEM.pdf, respectively, both shown here in Fig. 9.

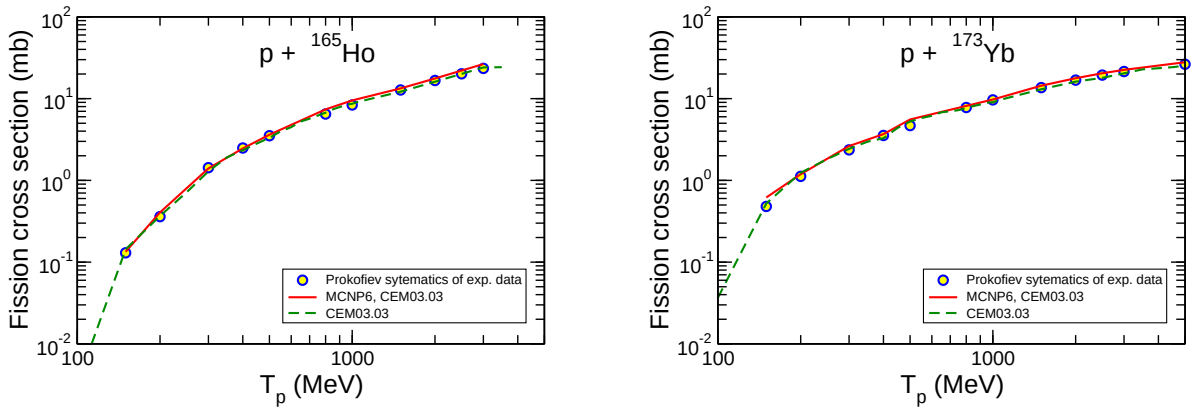

Figure 9: Prokofiev systematics [57] (open circles) of the experimental proton-induced fission cross sections of ^{165}Ho and ^{173}Yb compared with MCNP6 calculations in parallel, with MPI, using the CEM03.03 event generator with the GENXS option (red solid lines) and with calculations by CEM03.03 used as a stand alone code (green dashed lines), as indicated.

3.6. p500Xe136 (with inxc96)

This MCNP6 problem is to test the applicability of MCNP6 using the CEM03.03 event generator to describe nuclear reactions at intermediate energies on medium-sized nuclei with mass numbers A around and above $\sim$ 100, which are usually very difficult to calculate with any models. The production of residual nuclei in such reactions is of great interest for a number of applied and academic problems related to transmutation of nuclear wastes, radioactive beam facilities, propagation of cosmic radiation, understanding the reaction mechanisms leading to the production of highly-excited nuclei and to dissipation of kinetic energy in internal excitation energy of the nucleus and in the de-excitation process of such hot nuclei, to name just a few.

Namely, in this test problem, we calculate with MCNP6 using CEM03.03 with the GENXS option the yields of products from the 500 MeV p + ^{136}Xe interactions measured recently at GSI in inverse kinematics. Numerical values of measured data are published in the recent paper [58].

The MCNP6 main input file for this problem is **p500Xe136.CEM**, presented in subdirectory /VALIDATION_CEM/Inputs/. Let us recall that the GENXS option of MCNP6 requires a second, auxiliary, input file; for this problem, we use the auxiliary MCNP6 input file **inxc96**, presented in the same subdirectory and also shown here below.

p500Xe136.CEM:

```
MCNP6 test: p + Xe136 by CEM03.03 at 500 MeV, nevtype=66
  1   1   1.0    -1 2 -3
  2   0          -4 (1:-2:3)
  3   0           4
```

```
c ------------------------------------------------------------
  1  cz  4.0
  2  pz  -1.0
  3  pz  1.0
  4  so  50.0

c ------------------------------------------------------------
  m1   54136 1.0
  sdef erg = 500 par = H dir = 1 pos = 0 0 0 vec 0 0 1
  imp:h 1 1 0
  phys:h 1000
  mode   h
LCA  8j 1    $ use CEM03.03, nevtype = 66                  !!!
  tropt genxs inxc96  nreact on  nescat off
c ------------------------------------------------------------
  print 40 110 95
  nps 10000000
c  prdmp 2j -1
```

inxc96:

```
MCNP6 test: p + Xe136 by CEM03.03 at 500 MeV, nevtype=66
0 0 1 /
Cross Section Edit
0 0 9 /
1 5 6 7 8 21 22 23 24 /
```

We calculated this test problem with MPI using 8 nodes, 64 processors, on the **Moonlight** supercomputer of LANL. The output file, p500Xe136.CEM.mpi.o, is presented in subdirectory: /VALIDATION_CEM/Templates/LINUX/.

The MCNP6 cross sections for the production of different isotopes are printed (in barns) in the corresponding portion of the table entitled "Distribution of residual nuclei" of the output files. To help plotting these results with xmgrace, we copy the MCNP6 results for all measured (only) products in separate files. The cross sections for the production of isotopes with Z=41, 42, 43, 44, 45, 46, 47, 48, 49, 50, 51, 52, 53, 54, 55, and 56 are presented in files 41.m6c.dat, 42.m6c.dat, 43.m6c.dat, 44.m6c.dat, 45.m6c.dat, 46.m6c.dat, 47.m6c.dat, 48.m6c.dat, 49.m6c.dat, 50.m6c.dat, 51.m6c.dat, 52.m6c.dat, 53.m6c.dat, 54.m6c.dat, 55.m6c.dat, and 56.m6c.dat, respectively, in subdirectory:
/VALIDATION_CEM/Experimental_data/p500Xe136/.

Experimental data for all these products are presented in the same subdirectory in files with similar names, simply using in their names "exp" instead of "m6c".

Templates for plotting all these results compared with the measured data using xmgrace are presented there in files 41.fig, 42.fig, 43.fig, 44.fig, 45.fig, 46.fig, 47.fig, 48.fig, 49.fig, 50.fig, 51.fig, 52.fig, 53.fig, 54.fig, 55.fig, and 56.fig, respectively.

Postscript files generated by xmgrace for all the plots are presented in files with similar names, simply using in their names extensions "ps" instead of "fig".

In an overview of all these numerous and quite different product yields, we provide also a summary file p500Xe136_M6.pdf which shows cross sections for all products with Z from 41 to 56. This summary pdf file was produced with the LaTeX file p500Xe136_M6.tex using the above postscript files as input; It is also shown below in Fig. 10.

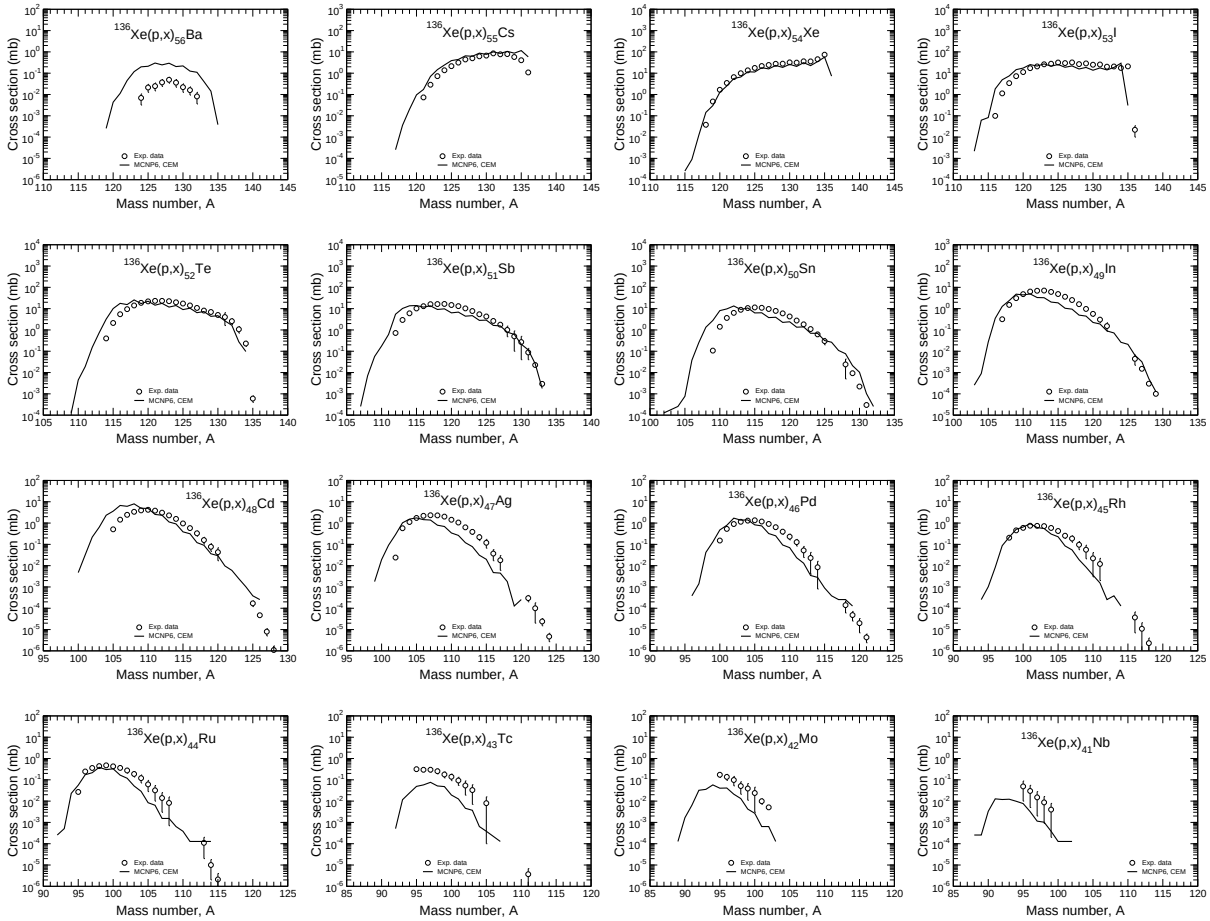

Figure 10: Isotopic cross sections of all measured at GSI by Giot at al. [58] products from the reaction 500 MeV p + ^{136}Xe (circles) compared with results by MCNP6 using the CEM03.03 event generator obtained with the GENXS option, running in parallel, with MPI.

We can see that MCNP6 reproduces reasonably well most of the measured cross sections. However, for the production of isotopes with a charge number greater than the charge number on the target by two units, we see an overestimation of almost an order of magnitude. This is a known problem of practically all models based on INC (see, e.g. Ref. [59]).

We found also quite big underestimation for the production of lighter isotopes, far from the target-nucleus, starting from Tc. Further investigations and further improvement of our event generators with a possible consideration of multifragmentation [60] and fission-like binary decays [61] are needed in order to predict well products from intermediate- and high-energy nuclear reactions far from the target-nuclei, in the deep spallation and fragmentation regions (see more details in [62]).

4. Testing LAQGSM

All the test-problems discussed in this Section are presented in the **VALIDATION_LAQGSM** subdirectory in the basic **/MCNP6/Testing/** directory.

4.1. Old test-problems using LAQGSM

We have recalculated all the examples discussed in Ref. [15] running different versions of MCNP6 [3]-[6] in parallel, with MPI, as described in Sec. 2. As a rule, results from all versions of MCNP6 for all those test-problems either run with MPI, as described in Sec. 2, or in a sequential mode, as done for Ref. [15] were the same, with only some very little differences in the last digits of some of the calculated values. We used above the words "as a rule," because in the "Beta 3" version of MCNP6 [5], Dr. Richard E. Prael changed the absolute normalization of the nucleus-nucleus reactions calculated with the GENXS option [63], to match the approximation adopted by MCNPX [8]. Before the "Beta 3" version of MCNP6 [5], the total reaction cross sections for nucleus-nucleus reactions calculated by MCNP6 using the GENXS option was taken to be the same as calculated by LAQGSM03.03 [16]. As a result of these changes, the absolute values of all characteristics of nucleus-nucleus reactions calculated with MCNP6 using the GENXS option changed, becoming a little lower, in comparison to similar results calculated with versions of MCNP6 earlier than Beta 3 and in comparison with similar calculations by LAQGSM03.03 used as a stand alone code. We will discuss briefly such differences in examples shown in Fig. 13 and 14 of this section as well as in Sec. 6 below: They are not too big, are self-consistent, and do not make the agreement of the calculated values with the available experimental data worse.

In this sub-section, we discuss only the 18 MCNP6 test-problems described already in Ref. [15]. Because all the input and output files for these problems were described in detail in Ref. [15], as was done with all the experimental data used, and because the results obtained here with MPI are practically the same as the old results calculated in Ref. [15] in a sequential mode, we do not provide here explicitly our new output files and all the new figures with results from our MPI runs for all these 18 test-problems: Readers can find them in Ref. [15]. Instead, Figs. 11 to 14 below show only a few examples of comparisons of our old MCNP6 results from Ref. [15] obtained in sequential runs with our current results obtained with MPI, namely, for the test-problems # 11, 12, 13, and 16 of Ref. [15]. As we can see from Figs. 11 and 12 for reactions induced by protons, because the differences between the current MPI results and the ones obtained in Ref. [15] in sequential runs are in only the last digits on only some of calculated values, these tiny differences can not be distinguished almost at all in the scale we use for our figures. This is a good result, just as expected. Let us recall again that all details about all the test-problems from this sub-section can be found in Ref. [15].

Figs. 13 and 14 show examples of several nucleus-nucleus reactions. Here, we can clearly see the mentioned above differences in the absolute normalization of the results. So, we can see a very good agreement of cross sections calculated in 2010 with MCNP6 using LAQGSM03.03 with the GENXS option with the results calculated with LAQGSM03.03 used as a stand alone code (compare the dashed green lines (MCNP6, 2010) with the black lines (LAQGSM03.03). The apparent "disagreement" between the 2010 results by MCNP6 and by LAQGSM used as a stand alone for products with $Z < 29$ in Fig. 13, and for products with $Z < 5$ in the right plot of Fig. 14 is actually a correct and good result but not a "disagreement".

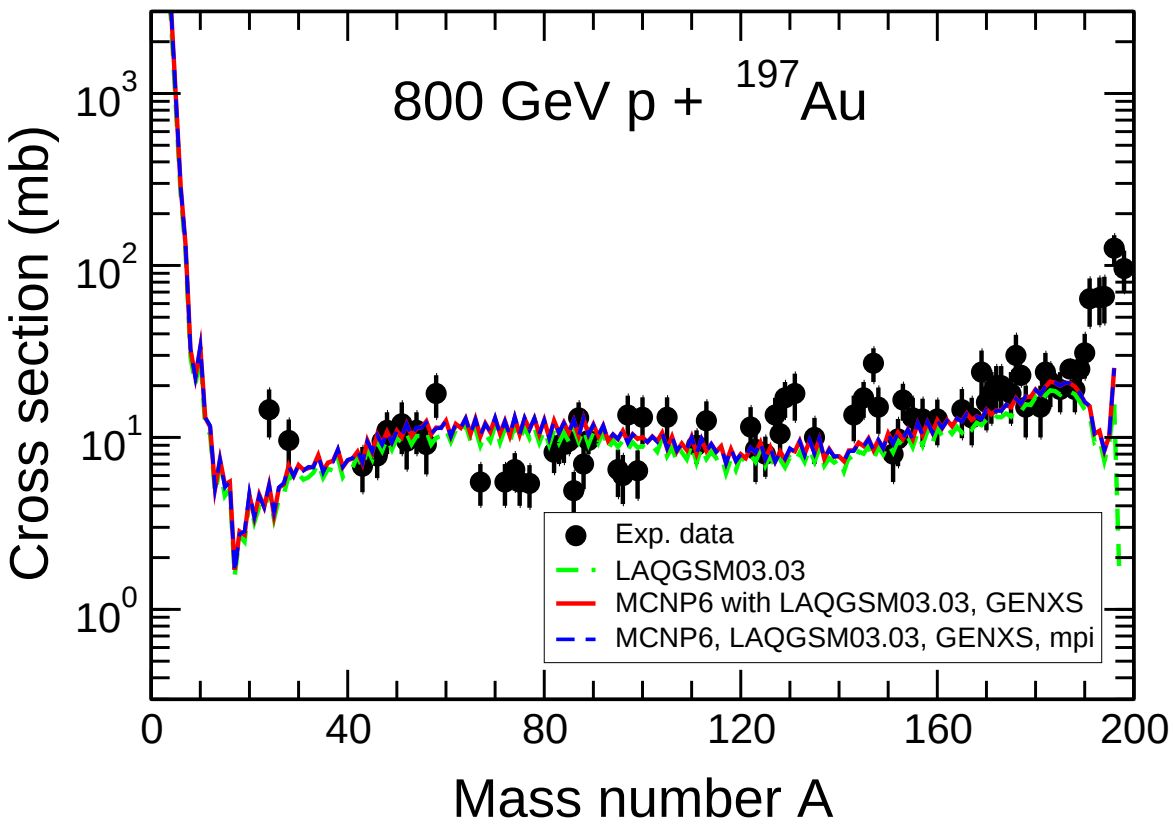

Figure 11: Experimental mass number distribution of product yields [64] (filled circles) from the 800 GeV p + Au reaction compared with results by LAQGSM03.03 [16] used as a stand alone code (dashed green line) and by MCNP6 using the LAQGSM03.03 event-generator; results from a run in a sequential mode are shown with a solid red line, while from a calculation in parallel, with MPI, by a dashed blue line, as indicated in legend.

The explanation for these "fictive disagreements" is that MCNP6 does calculate products from both the projectile and target nuclei, while the corresponding calculations with LAQGSM03.03 used as a stand alone code accounted only for products from the bombarding nuclei and do not contain contributions from the target-nuclei.

But in Figs. 13 and 14 we can see also some real differences: The results calculated in 2010 by MCNP6 in a sequential mode (dashed green lines) differ in the absolute values from the results calculated in parallel, with MPI, in 2012 (red lines). True, these differences are not related with the mode we did the calculations, in a sequential mode or with MPI, as we were "scared" initially when we got such results, before Dick Prael informed us that he had changed the absolute normalization of the MCNP6 nucleus-nucleus reactions calculated with his GENXS option [63] in the Beta 3 version of MCNP6, as mentioned above. These differences are related only with the absolute normalization of the nucleus-nucleus reactions calculated by MCNP6 with the GENXS option.

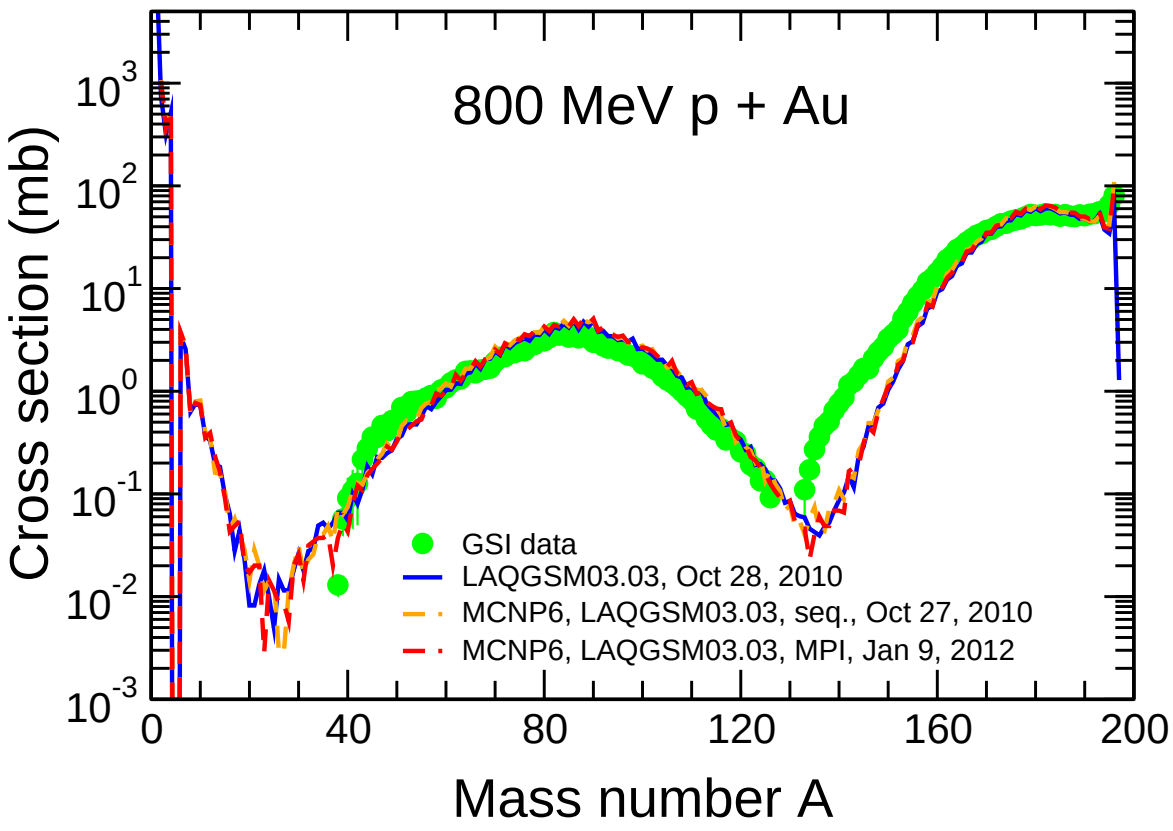

Figure 12: Experimental mass number distribution of product yields [65, 66] (filled circles) from the 800 MeV p + Au reaction compared with results by LAQGSM03.03 [16] used as a stand alone code and by MCNP6 using the LAQGSM03.03 event-generator, from a run in a sequential mode and other in parallel, with MPI, as indicated in legend.

If we compare the results calculated in 2012 with the Beta 3 version of MCNP6 [5] in a sequential mode (dotted green lines) with similar results calculated with MPI (red lines), we see a perfect agreement, just as must be.

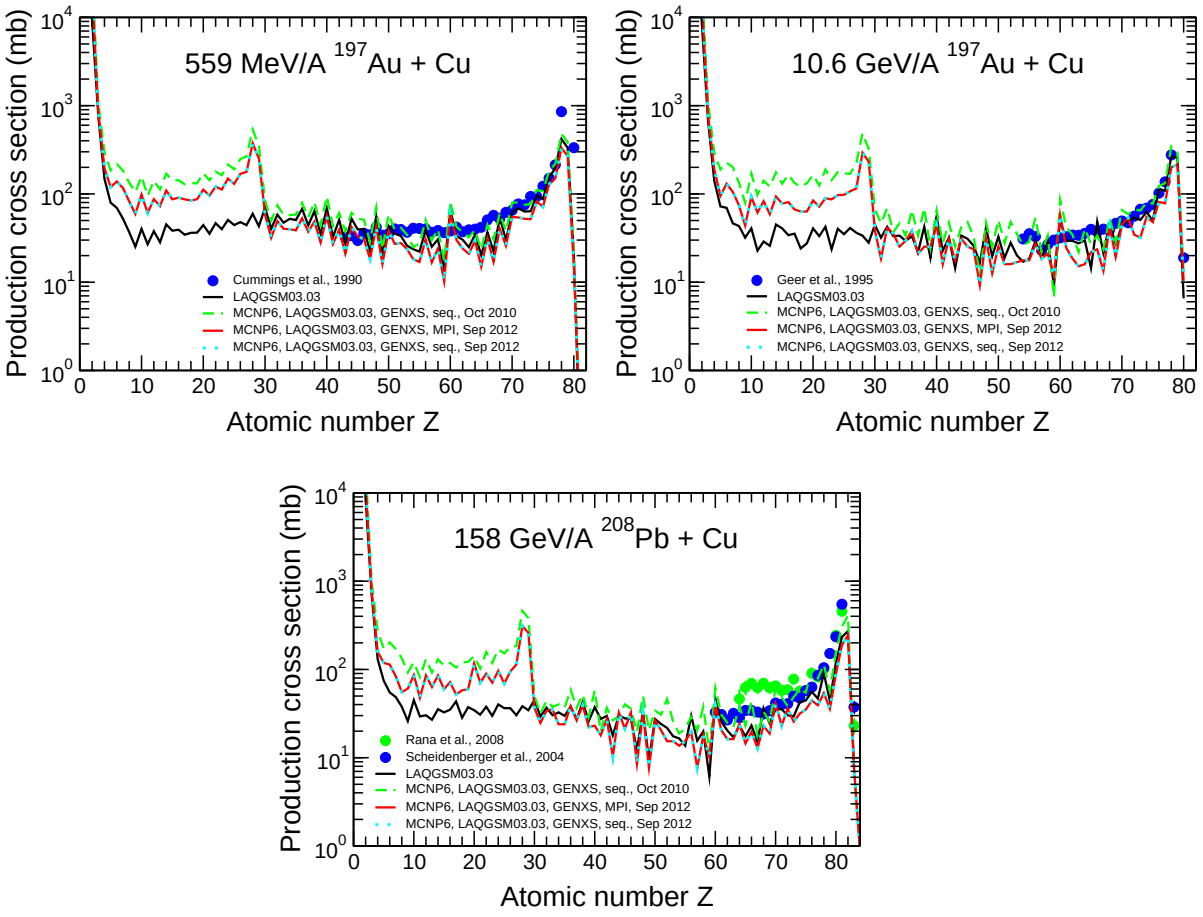

Figure 13: Experimental charge distributions of product yields [67]-[70] (color filled circles) from 559 MeV/A ^{197}Au + Cu, 10.6 GeV/A ^{197}Au + Cu, and 158 GeV/A ^{208}Pb + Cu reactions compared with results by LAQGSM03.03 [16] used as a stand alone code and with calculations by MCNP6 using the LAQGSM03.03 event-generator performed in a sequential mode and in parallel, with MPI, as indicated in legends.

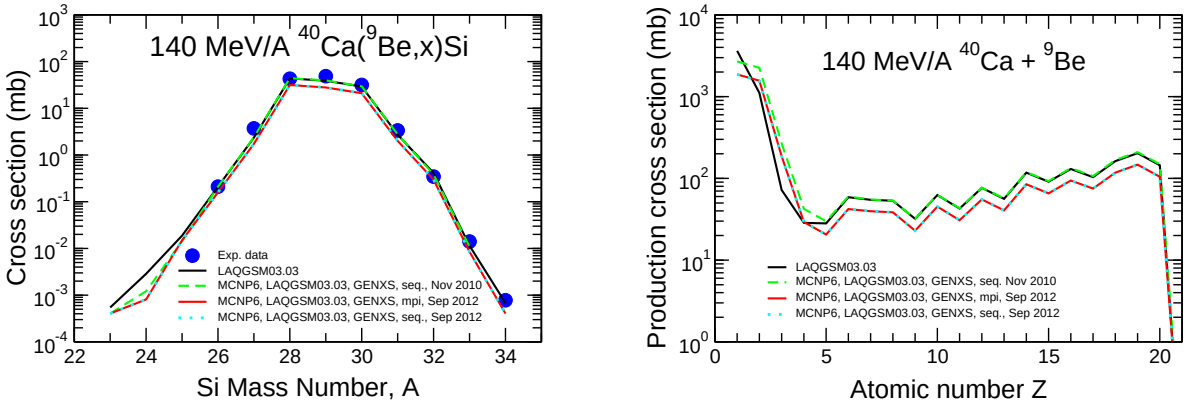

Figure 14: **Left plot**: Experimental mass number distribution of the Si ions yields [71] (green filled circles) from the 140 MeV/A ^{40}Ca + ^{9}Be reaction compared with results by LAQGSM03.03 [16] used as a stand alone code and with calculations by MCNP6 using the LAQGSM03.03 event-generator performed in a sequential mode and in parallel, with MPI, as indicated in legend. **Right plot**: Mass number distribution of all product yields from the same reaction calculated with LAQGSM03.03 [16] used as a stand alone code and with MCNP6 using the LAQGSM03.03 event-generator, performed in a sequential mode and in parallel, with MPI, as indicated in legend. The little differences as shown by different lines are explained in the text and do not indicate any disagreements between different calculations but actually prove a complete agreement and self-consistency between different results. A comparison with several similar results by EPAX [72], ABRABLA [73], HIPSE [74], and AMD [75] from [71] can be found in Fig. 7 of Ref. [14] and in Fig. 19 of Ref. [15].

4.2. Sn112_1AGeV_Sn112 and Sn124_1AGeV_Sn124, both with inxc69

This MCNP6 problem is to test the applicability of MCNP6 using the LAQGSM03.03 event generator to describe the influence of the isotopic composition of the projectile on the kinematical properties of projectile residues in peripheral and midperipheral relativistic heavy-ion collisions.

Besides a great academic interest in studying such processes, such reactions are of interest for different applications, including the Facility for Rare Isotope Beams (FRIB), an update and continuation of the initial U.S. DOE project known as "Rare Isotope Production" (RIA).

For us, this test-problem has also an additional aim to test the capability of MCNP6 to describe reactions where multifragmentation decay may play an important role. Multifragmentation reactions have been extensively studied to search for the signals of the liquid-gas phase transition in finite nuclear systems.

Namely, in this test problem, we calculate with MCNP6 using LAQGSM03.03 with the GENXS option the yields of products from two symmetric heavy-ion reactions, ^{112}Sn + ^{112}Sn and ^{124}Sn + ^{124}Sn, at the projectile energy of 1 GeV/nucleon. The N/Z ratio of ^{112}Sn is 1.24, and the one of ^{124}Sn is 1.48, resulting, for a given Z, in the largest span in N/Z values for stable nuclei in this mass range. Because in both reactions the target and projectile are

the same nuclei, the N/Z stays homogeneous for all possible impact parameters, despite the small effects coming from the neutron skin. This N/Z value is determined entirely by the corresponding tin nuclei in the system.

The experimental data for this study were measured recently at GSI, Darmstadt, Germany using the heavy-ion accelerator SIS18 and the Fragment Separator (FRS). The incident energy is chosen in such way to have the best conditions for the transmission of the reaction products through the FRS. Numerical values of measured data are published in the recent paper [76].

The MCNP6 main input files for the ^{112}Sn and ^{124}Sn cases are **Sn112_1AGeV_Sn112** and **Sn124_1AGeV_Sn124**, both presented in subdirectory /VALIDATION_LAQGSM/Inputs/. Let us recall that the GENXS option of MCNP6 requires a second, auxiliary, input file; for this problem, we use the same auxiliary MCNP6 input file **inxc69**, shown in the same subdirectory. For completeness sake, we show all these three input files below:

Sn112_1AGeV_Sn112:

```
MCNP6 test: 1 GeV/A Sn112 + Sn112 by LAQGSM03.03, nevtype=66
  1  1  1.0   -1 2 -3
  2  0        -4 (1:-2:3)
  3  0         4

c -------------------------------------------------------------
  1  cz  4.0
  2  pz  -1.0
  3  pz  1.0
  4  so  50.0

c -------------------------------------------------------------
dbcn 28j 1
  m1 50112  1.0
  sdef erg=112000 par=50112 dir=1 pos=0 0 0 vec 0 0 1
  imp:n 1 1 0
  imp:h 1 1 0
  phys:g 200
  phys:d 200
  phys:h 200
  phys:# 112100
  mode  # n a t d s h
LCA  2 1 5j -1 1j 1    $ use LAQGSM, nevtype = 66                    !!!
lcb  0 0 0 0 0 0
lea  2j 0
  tropt genxs inxc69  nreact on  nescat off
c  tropt genxs inxc69
c -------------------------------------------------------------
  print 40 110 95
c  nps 100
  nps 1000000
  prdmp 500000 200000 1
```

Sn124_1AGeV_Sn124:

```
MCNP6 test: 1 GeV/A Sn124 + Sn124 by LAQGSM03.03, nevtype=66
  1  1  1.0   -1 2 -3
  2  0        -4 (1:-2:3)
  3  0         4

c -------------------------------------------------------------
  1  cz  4.0
  2  pz  -1.0
  3  pz  1.0
  4  so  50.0

c -------------------------------------------------------------
dbcn 28j 1
  m1 50124  1.0
  sdef erg=124000 par=50124 dir=1 pos=0 0 0 vec 0 0 1
  imp:n 1 1 0
  imp:h 1 1 0
  phys:g 200
  phys:d 200
  phys:h 200
  phys:# 124100
  mode  # n a t d s h
LCA  2 1 5j -1 1j 1    $ use LAQGSM, nevtype = 66                    !!!
lcb  0 0 0 0 0 0
lea  2j 0
  tropt genxs inxc69  nreact on  nescat off
c  tropt genxs inxc69
c -------------------------------------------------------------
  print 40 110 95
c  nps 1000
  nps 1000000
  prdmp 500000 200000 1
```

inxc69:

```
MCNP6 test: 10.6 GeV/A Au197 + Cu64 by LASQGSM03.0, nevtype=66
1 0 1 /
Cross Section Edit
50 0 9 /
5. 10. 15. 20. 25. 30. 35. 40. 45. 50. 55. 60. 65. 70. 75. 80.
85. 90. 95. 100. 150. /
1 5 6 7 8 21 22 23 24 /
```

We calculated this test problem with MPI using 4 nodes, 64 processors, on the **Turing** supercomputer of LANL using the "continue" option. For comparison, we perform our

MCNP6 calculations also in a sequential mode. Because the results obtained this way are practically the same as the ones obtained with MPI, we present in subdirectory */VALIDATION_LAQGSM/Templates/LINUX/ only MPI results. The initial output files for the ^{112}Sn and ^{124}Sn cases are Sn112_1AGeV_Sn112.mpi.o and Sn124_1AGeV_Sn124.mpi.o presented in the subdirectory listed above. The final outputs for the ^{112}Sn and ^{124}Sn cases are Sn112_1AGeV_Sn112.mpi_c.o and Sn124_1AGeV_Sn124.mpi_c.o presented in the same subdirectory. Let us note that in our MCNP6 output files are listed the cross sections for the production of all possible isotopes from both projectile and target heavy ions, while at GSI the measurements were done only for products from projectile nuclei. As in this particular case the projectile and target nuclei are the same, we need simply to divide the MCNP6 results by two in order to compare with the measured data.

The MCNP6 cross sections for the production of different isotopes are printed (in barns) in the corresponding portion of the table entitled "Distribution of residual nuclei" of the output files. To help plot these results with xmgrace, we copy here the MCNP6 results for all measured (only) products in separate files. The cross sections for the production of isotopes with Z = 10, 11, 12, 13, 14, 15, 16, 17, 18, 19, 20, 21, 22, 23, 24, 25, 26, 27, 28, 29, 30, 31, 32, 33, 34, 35, 36, 37, 38, 39, 40, 41, 42, 43, 44, 45, 46, 47, 48, 49, and 50 from ^{112}Sn are presented in subdirectory */VALIDATION_LAQGSM/Experimental_data/SnSn_1GeVperA/ in the files 10_112M6.dat, 11_112M6.dat, 12_112M6.dat, 13_112M6.dat, 14_112M6.dat, 15_112M6.dat, 16_112M6.dat, 17_112M6.dat, 18_112M6.dat, 19_112M6.dat, 20_112M6.dat, 21_112M6.dat, 22_112M6.dat, 23_112M6.dat, 24_112M6.dat, 25_112M6.dat, 26_112M6.dat, 27_112M6.dat, 28_112M6.dat, 29_112M6.dat, 30_112M6.dat, 31_112M6.dat, 32_112M6.dat, 33_112M6.dat, 34_112M6.dat, 35_112M6.dat, 36_112M6.dat, 37_112M6.dat, 38_112M6.dat, 39_112M6.dat, 40_112M6.dat, 41_112M6.dat, 42_112M6.dat, 43_112M6.dat, 44_112M6.dat, 45_112M6.dat, 46_112M6.dat, 47_112M6.dat, 48_112M6.dat, 49_112M6.dat, and 50_112M6.dat, respectively. Similar results from ^{124}Sn are presented in files with similar names, simply substitute in their names "124" for "112".

Experimental data for all these products from ^{112}Sn and ^{124}Sn are presented in the same subdirectory in files with similar names, simply substitute in their names "GSI" for "M6".

Templates for plotting all these results compared with the measured data using xmgrace are presented in the same subdirectory for ^{112}Sn in the files 10_112Sn.fig, 11_112Sn.fig, 12_112Sn.fig, 13_112Sn.fig, 14_112Sn.fig, 15_112Sn.fig, 16_112Sn.fig, 17_112Sn.fig, 18_112Sn.fig, 19_112Sn.fig, 20_112Sn.fig, 21_112Sn.fig, 22_112Sn.fig, 23_112Sn.fig, 24_112Sn.fig, 25_112Sn.fig, 26_112Sn.fig, 27_112Sn.fig, 28_112Sn.fig, 29_112Sn.fig, 30_112Sn.fig, 31_112Sn.fig, 32_112Sn.fig, 33_112Sn.fig, 34_112Sn.fig, 35_112Sn.fig, 36_112Sn.fig, 37_112Sn.fig, 38_112Sn.fig, 39_112Sn.fig, 40_112Sn.fig, 41_112Sn.fig, 42_112Sn.fig, 43_112Sn.fig, 44_112Sn.fig, 45_112Sn.fig, 46_112Sn.fig, 47_112Sn.fig, 48_112Sn.fig, 49_112Sn.fig, and 50_112Sn.fig, respectively, and for ^{124}Sn, are presented in files with similar names, simply substitute in their names "124" for "112".

Postscript files generated by xmgrace for all the plots are presented in files with similar names, simply substitute in their names extensions "ps" for "fig".

To present an overview of all these numerous and quite different product yields, we provide also summary files 10to33_112.pdf, 34to50_112.pdf, 10to33_124.pdf, and 34to50_124.pdf which show cross sections for all products with Z from 10 to 33 and from 34 to 50 on summary figures for ^{112}Sn and ^{124}Sn, respectively. These summary pdf files were produced with the LaTeX files 10to33_112.tex, 34to50_112.tex, 10to33_124.tex, and 34to50_124.tex using the listed above postscript files as input. These results are shown below in Figs. 15 to 18.

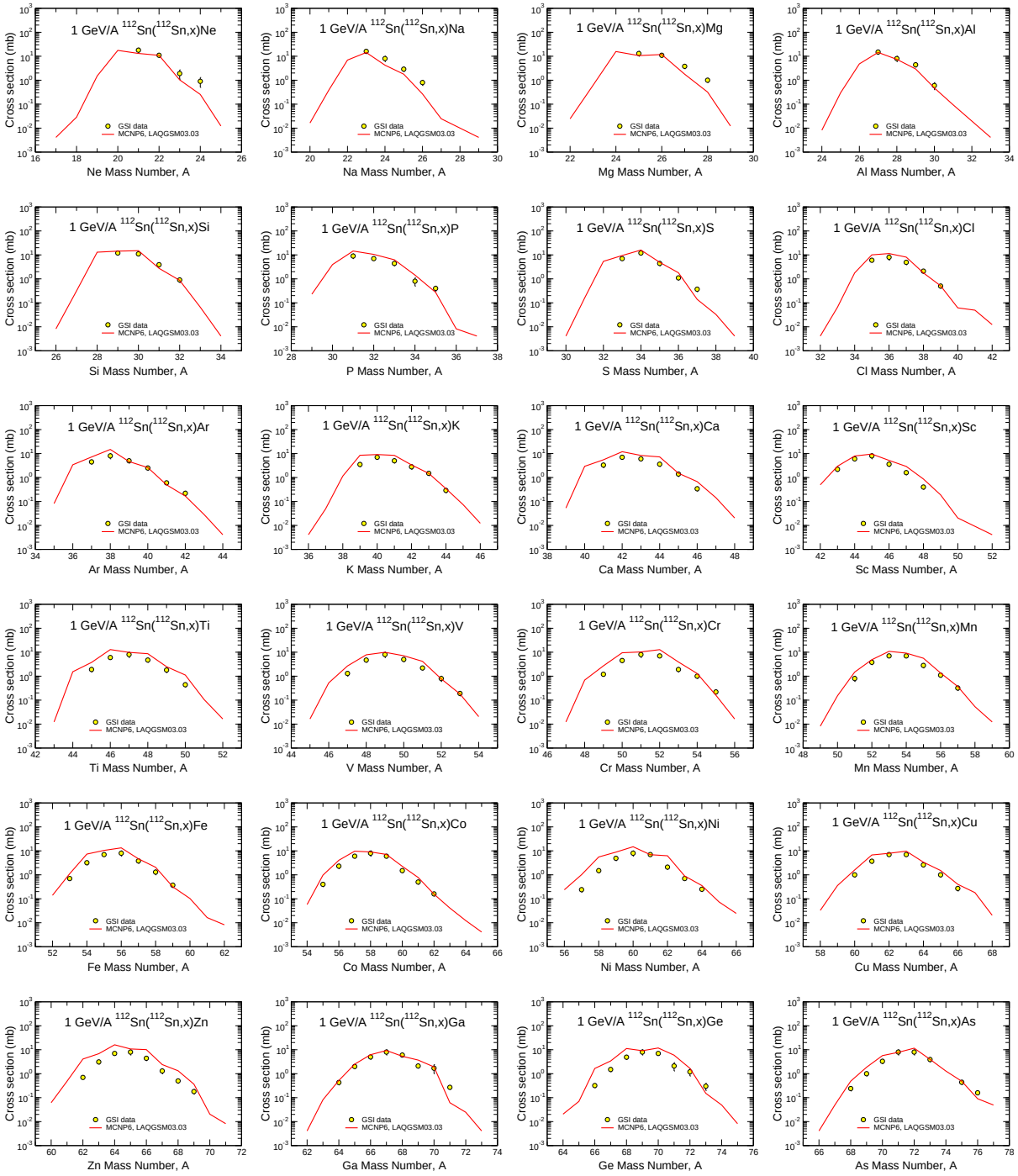

Figure 15: Isotopic cross sections of fragments with Z from 10 to 33 measured at GSI [76] in the reaction 1 GeV/A ^{112}Sn+^{112}Sn (circles) compared with MCNP6 calculations in parallel (MPI, red solid lines), as indicated in legends.

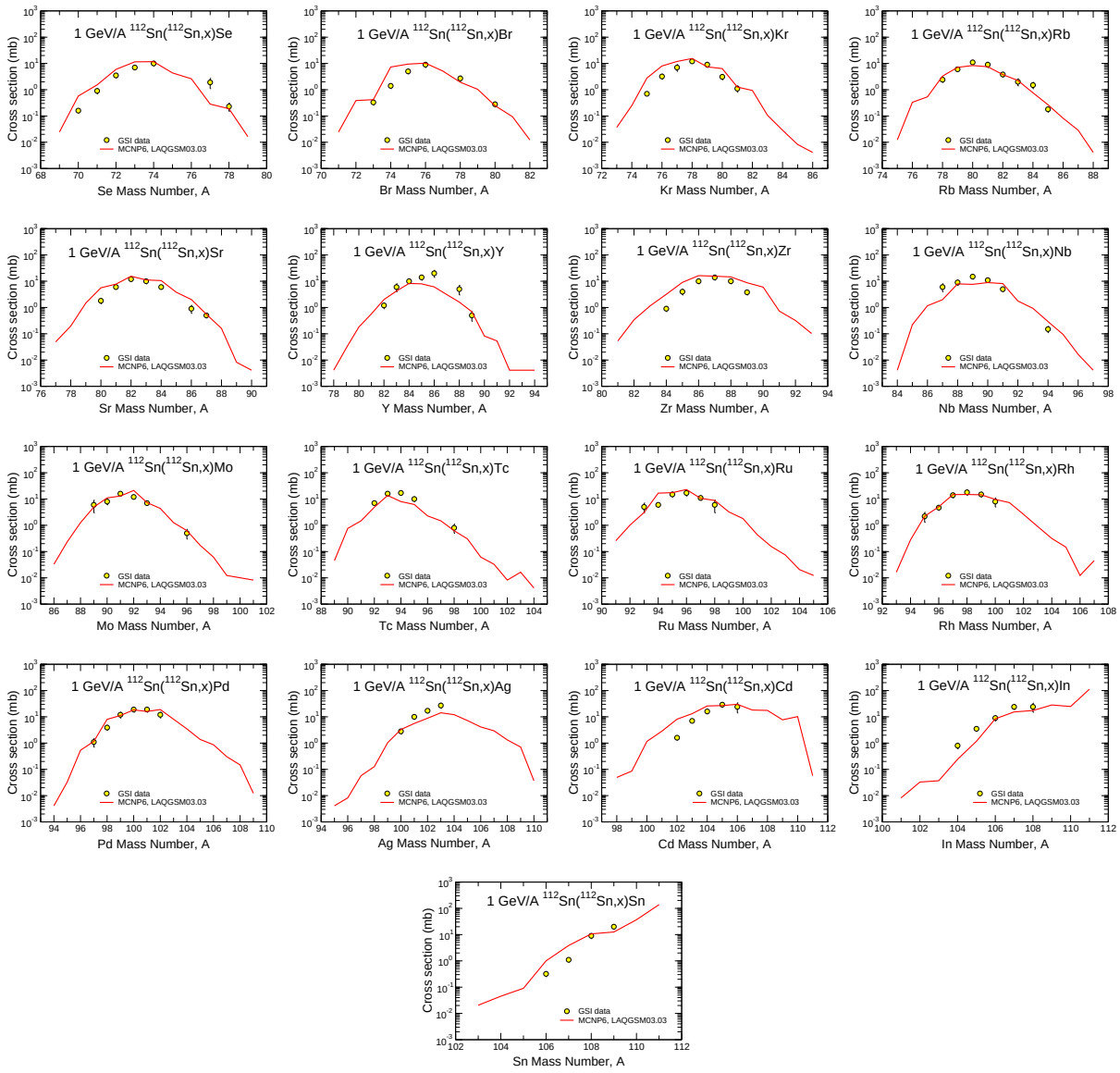

Figure 16: The same as in Fig. 16, but for products with Z from 34 to 50.

Besides the MCNP6 results, we show here also calculations by LAQGSM03.03 used as a stand alone code. We have compared all MCNP6 results for this test-problem with corresponding results by LAQGSM03.03 used as a stand alone code, but we limit ourself here with showing only the A- and Z-distributions of product yields from ^{112}Sn, shown below in Fig. 19, and for yields from ^{124}Sn, shown in Fig. 20, The MCNP6 results for the A- and Z-distributions are tabulated in the tables entitled "Summary by mass number" and "Summary by charge number" of the final output file Sn112_1AGeV_Sn112.mpi_c.o and are copied here also in separate files A-M6Laq.dat and Z-M6Laq.dat, respectively, presented in subdirectory */VALIDATION_LAQGSM/Experimental_data/SnSn_1GeVperA/. Similar results by LAQGSM03.03 used as a stand alone code are presented here in the files A-Laq.dat and Z-Laq.dat, respectively. Experimental data for A- and Z-distributions are presented in the files A112GSI.dat and Z112GSI.dat, respectively, in the same subdirectory.

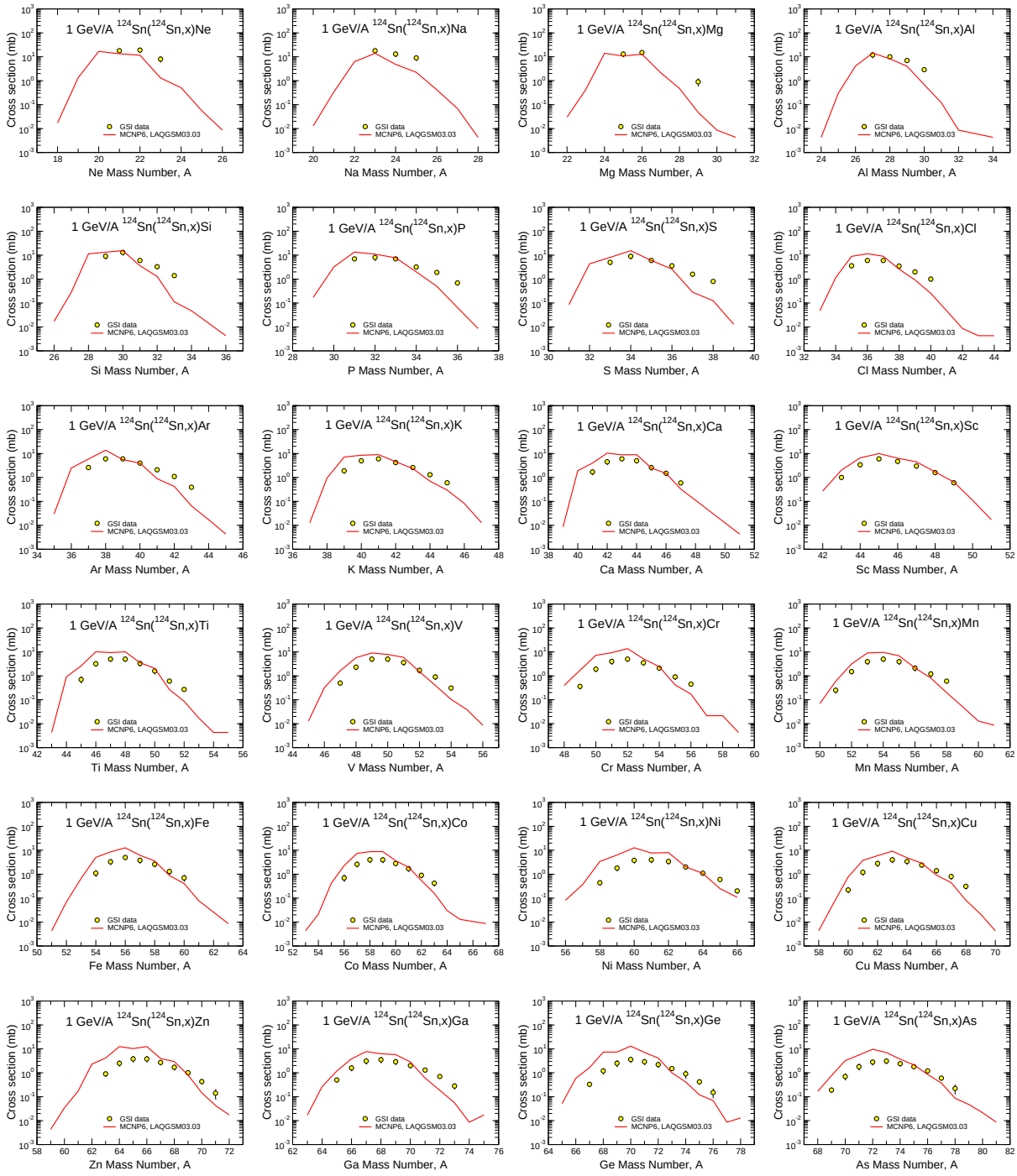

Figure 17: Isotopic cross sections of fragments with Z from 10 to 33 measured at GSI [76] in the reaction 1 GeV/A ^{124}Sn+^{124}Sn (circles) compared with MCNP6 calculations in parallel (MPI, red solid lines), as indicated in legends.

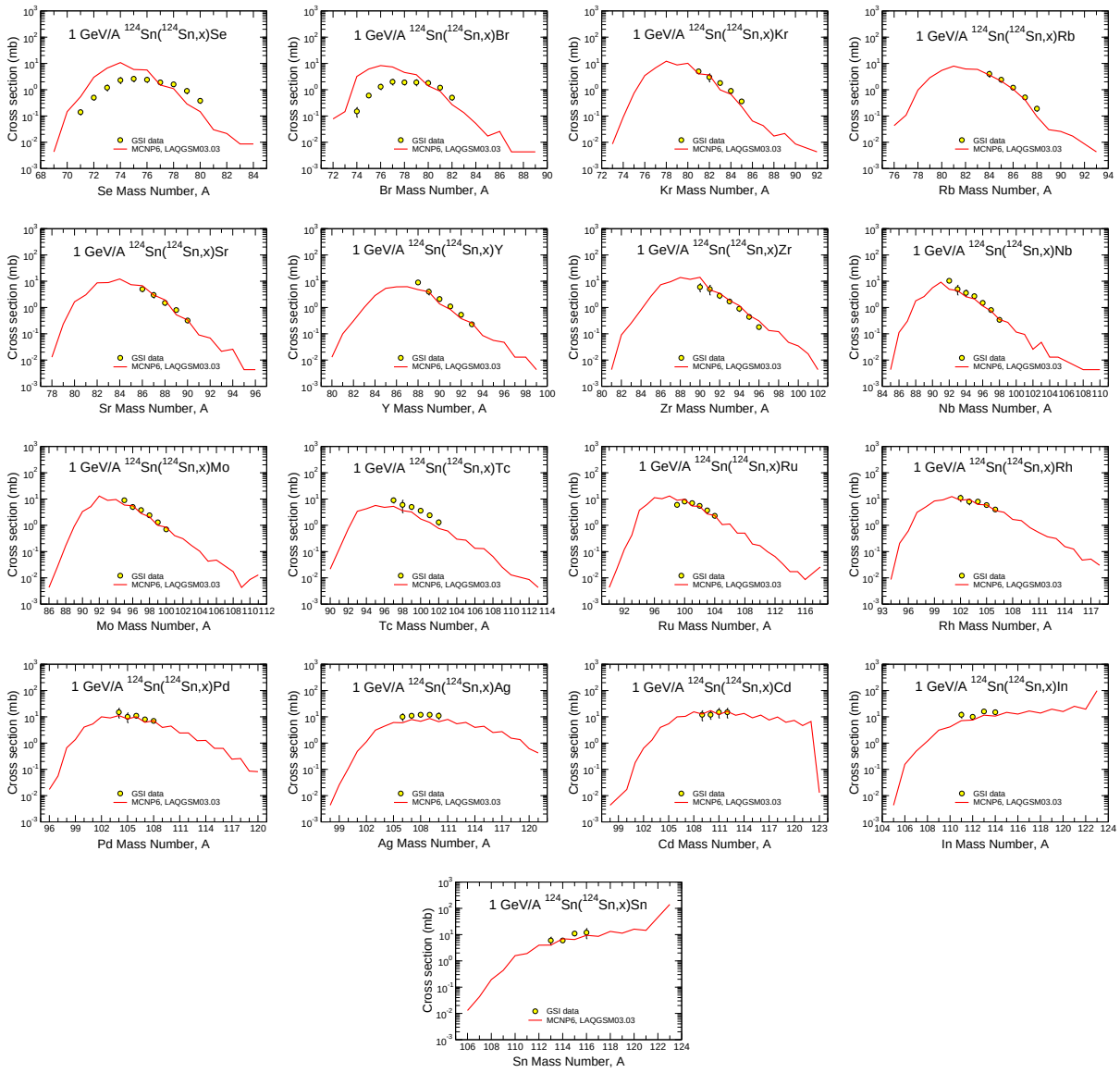

Figure 18: The same as in Fig. 19 but for products with Z from 34 to 50.

Templates to plot such results with xmgrace are presented in the files A112.fig and Z112.fig, respectively and the final pdf files with plots by xmgrace are A112.pdf and Z112.pdf, respectively, in subdirectory */VALIDATION_LAQGSM/Experimental_data/SnSn_1GeVperA/.

To investigate further the mechanisms of nuclide production in these reactions, in Ref. [77], we have calculated both reactions of this test-problem with a version of LAQGSM, LAQGSM03.S1 [78], which accounts for multifragmentation processes using the Statistical Multifragmentation Model (SMM) of Botvina et al. [60].

We found that for these reactions the results obtained with LAQGSM03.S1 are close to the values of the product cross-section yields calculated with LAQGSM03.03 or MCNP6. Examples of mass and charge distributions of products from the ^{112}Sn+^{112}Sn reaction calculated with LAQGSM03.S1 are compared with similar results by LAQGSM03.03 and by MCNP6 with LAQGSM03.03 in the lower plots of Fig. 1 of Ref. [77].

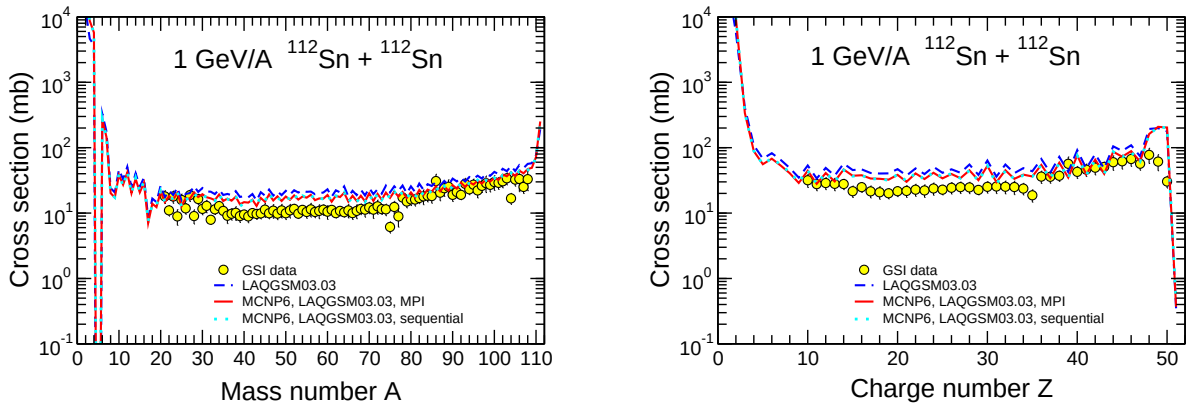

Figure 19: Experimental [76] mass and charge distributions of products from 1 GeV/A ^{112}Sn + ^{112}Sn (yellow filled circles) compared with results by LAQGSM03.03 used as a stand-alone code (blue dashed lines) and with MCNP6 calculations in parallel (MPI, red solid lines) and sequential (green dashed lines) modes using the LAQGSM03.03 event generator, as indicated.

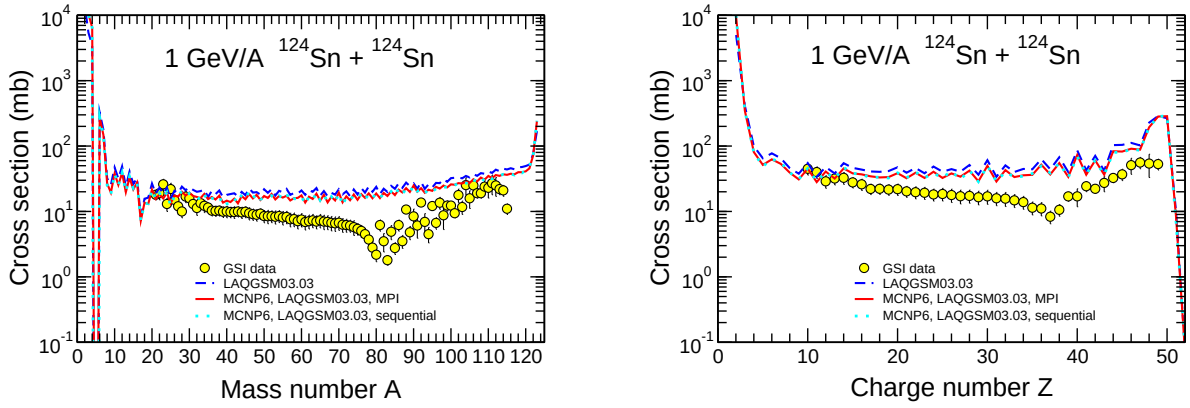

Figure 20: Experimental [76] mass and charge distributions of products from 1 GeV/A ^{124}Sn + ^{124}Sn (yellow filled circles) compared with results by LAQGSM03.03 used as a stand-alone code (blue dashed lines) and with MCNP6 calculations in parallel (MPI, red solid lines) and sequential (green dashed lines) modes using the LAQGSM03.03 event generator, as indicated.

A more detailed comparison of results by LAQGSM03.S1 and by LAQGSM03.03 as used in MCNP6 performed in Ref. [77] does not suggest an unambiguous signature of multifragmentation reactions in this data. We came to a similar conclusion in Ref. [79] while analyzing other comparable heavy-ion reactions. Mancusi et al. also made a similar conclusion from a study of 1-GeV proton-nucleus reactions [80].

4.3. p23000Te_Laq with inxc97

This MCNP6 problem is to test the applicability of MCNP6 using the LAQGSM03.03 event generator to describe radionuclide production from proton-induced reactions on tellurium at cosmic ray energies.

To be specific, in this test-problem, we calculate with MCNP6 using LAQGSM03.03 with the GENXS option the mass-number yield distribution of the products from a thin Te-target bombarded with 23-GeV protons and compare the results with recently measured experimental data. Such reactions are of interest to study rare events such as the interactions of solar neutrinos, dark matter particles, or rare processes, like double beta decay that are investigated in underground laboratories. The main goal of this test-problem is to investigate the applicability of MCNP6 to predict the radioactive isotopes that can be produced by cosmic ray exposure of TeO2 cryogenic detectors (or bolometers). We calculate this test-problem running MCNP6 in a sequential mode, as well as in parallel, with MPI, testing that MCNP6 provide the same results in both cases. In addition, we have utilized this test-problem to understand and to fix a problem observed while using the GENXS option of MCNP6 at ultra-relativistic energies (an initially unobserved "bug" in the GENXS option of MCNP6 at high-energies was found and fixed recently by Dick Prael). Last, this test-problem allows us to check if MCNP6 using LAQGSM03.03 with the GENXS option can provide in a single run results from a target with several isotopes (Te-nat has eight stable isotopes and we account for all of them in our example).

The 23 GeV proton irradiation was performed recently at CERN and the measured cross section are presented in Tables 2 and 3 of the paper [81].

After Dick Prael corrected the GENXS "bug" mentioned above, the MCNP6 results for this test-problem obtained in a parallel run with MPI coincide exactly with similar results obtained in a sequential run (see the figure with our results shown by the file p23000Te_A-2012.pdf in subdirectory */VaV/VALIDATION_LAQGSM/Experimental_data/p23000Te/ and also Fig. 21 below). Here, we present only the MPI results.

The main MCNP6 input file is **p23000Te_Laq** and the second, auxiliary, MCNP6 input file required by the GENXS option is **inxc97**, both presented in the Inputs subdirectory */VALIDATION_LAQGSM/Inputs/ and also shown below:

p23000Te_Laq:

```
MCNP6 test: p + Te by LAQGSM at 23 GeV, nevtype=66
C To evaluate cosmic-ray activation of tellurium
  1  1  1.0   -1 2 -3
  2  0        -4 (1:-2:3)
  3  0         4

c -------------------------------------------------------------
  1  cz  4.0
  2  pz  -1.0
  3  pz  1.0
  4  so  50.0

c -------------------------------------------------------------
```

```
dbcn 28j 1
  m1   52120 0.00096 52122 0.02603 52123 0.00908
       52124 0.04816 52125 0.07139 52126 0.18952
       52128 0.31687 52130 0.33799
  sdef erg = 23000 par = H dir = 1 pos = 0 0 0 vec 0 0 1
  imp:n 1 1 0
  imp:h 1 1 0
  phys:h 23100
  mode   h
LCA  2 1 5j -1 1j 1    $ use LAQGSM, nevtype = 66                    !!!
lcb  0 0 0 0 0 0
lea  2j 0
c  tropt genxs inxc97  nreact on  nescat off
  tropt genxs inxc97
c ---------------------------------------------------------------
  print 40 110 95
c  nps 1000
  nps 1000000
c  prdmp 2j -1
```

inxc97:

```
MCNP6 test: p + Te by LASQGSM03.03 at 23 GeV, nevtype=66
1 0 1 /
Cross Section Edit
50 0 9 /
5. 10. 15. 20. 25. 30. 35. 40. 45. 50. 55. 60. 65. 70. 75. 80.
85. 90. 95. 100. 120. /
1 5 6 7 8 21 22 23 24 /
```

The mass number distribution of product yields by MCNP6 (in units of barns) is tabulated in the table entitled "Summary by mass number" of the MCNP6 output file p23000Te_Laq.mpi.o presented in the Templates subdirectory /VALIDATION_LAQGSM/Templates/LINUX/ and is also copied in a separate file named M6Laq.mpi.dat, to help plotting with xmgrace the figure (see file p23000Te_A-2012.pdf) with our results. The file M6Laq.seq.dat presents similar results obtained in a sequential run, while the file p23000Te_A_exp.dat provides the experimental data by Barghouty et al. For historical reasons, we show here also the initial results obtained with the mentioned above GENXS "bug": Those initial, and wrong, results are presented in the file: p23000Te_a_Laq.dat, all shown in the same subdirectory.

A template for plotting our results with xmgrace is presented in the file p23000Te_A-2012.fig; the pdf file of the figure is: p23000Te_A-2012.pdf, presented here in Fig. 21.

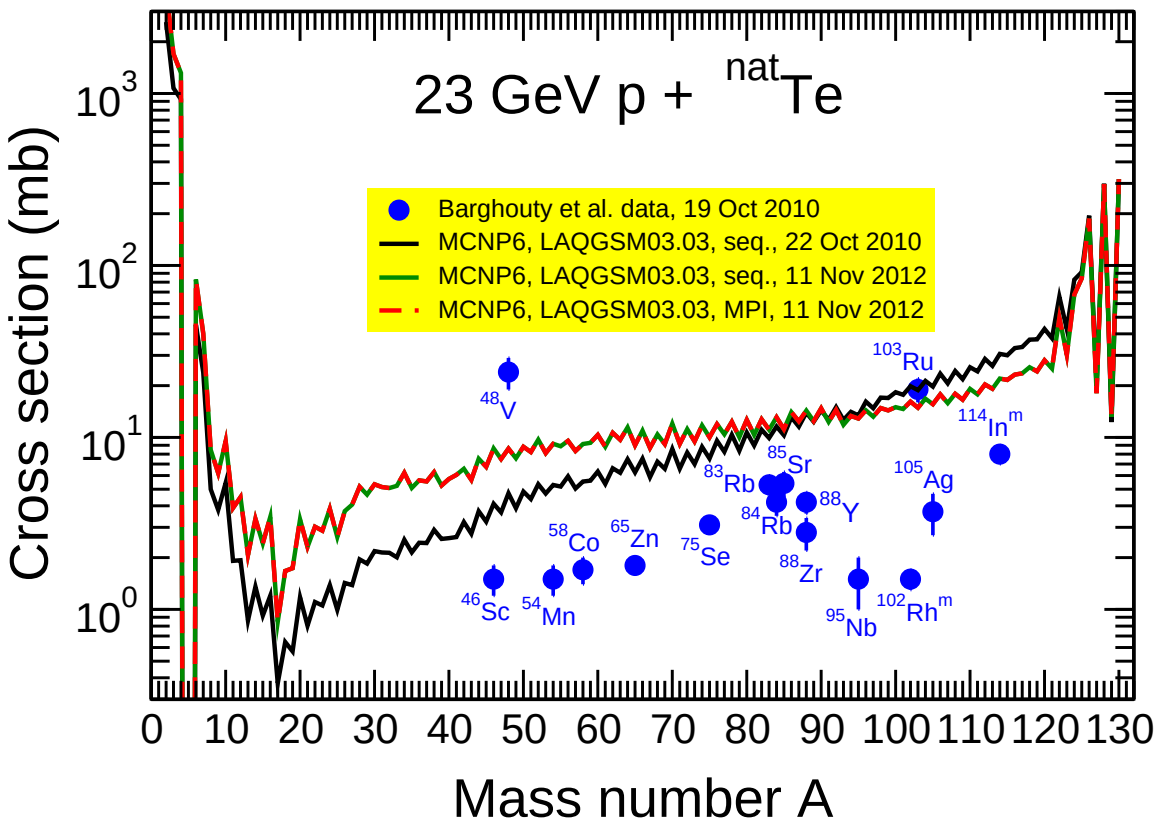

Figure 21: Mass number distributions of all product yields from the 23 GeV p + Te reaction calculated by MCNP6 using the LAQGSM03.03 event-generator in parallel (MPI, red dashed line) and sequential (green and black solid lines) compared with the cross sections of several isotopes from this reaction measured recently by Barghouty et al. [81]. The difference between results shown with the green (correct) and black (wrong) lines was caused by an intimal "bug" in the GENXS portion of MCNP6 while using LAQGSM03.03 at ultra-relativistic energies, fixed by Dr. Richard Prael later, as described in the text.

4.4. A) p400000Ta_REP; B) p800000Au_REP (both with with inxc97)

This problem is to test how MCNP6 using the LAQGSM03.03 event-generator predicts proton-induced fission cross section of preactinide nuclei at ultra-relativistic energies up to ~ 1 TeV.

To be exact, this test-problem is to calculate with MCNP6 using LAQGSM03.03 proton-induced fission cross section of ^{181}Ta and ^{197}Au at energies from 100 MeV to 800 GeV and to compare the results with predictions by LAQGSM03.03 used as stand alone code and with available experimental data. All MCNP6 calculations were done in parallel, with MPI. Such reactions are of interest for several astrophysical and space applications. This test-problem

is very similar to problem # 22 of the /VALIDATION_CEM/ test suite, A) p1000Ho_CEM; B) p1000Yb_CEM (both with inxs96), but is to test MCNP6 while using the LAQGSM03.03 event generator, including for reactions at much higher incident energies. In addition, this test-problem was needed to find and fix a "bug" in the GENXS portion of MCNP6 concerning a correct calculation of and printing in the MCNP6 output file the fission cross section while using LAQGSM03.03 with the GENXS option.

For this problem, we use not only the available experimental data on proton-induced fission cross sections of ^{181}Ta and ^{197}Au, but also the systematics by Prokofiev [57] that provide the best current estimations of the experimental fission cross sections for these nuclei in the energy region up to several GeV. It is convenient to show the files for ^{181}Ta and ^{197}Au fission cross sections in two separate subdirectories, namely,
/VALIDATION_LAQGSM/Experimental_data/p+Ta-Au_xfiss/pTa181/ and */pAu197/, respectively.

The easiest way to calculate fission cross sections with MCNP6 is to use the GENXS option for a single incident energy of protons; then, to perform as many calculations as needed changing only the proton energy on the SDEF card of the MCNP6 input. As all input files at different proton energies are exactly the same, with the only difference in the proton energy on the SDEF card, we present here only one example of MCNP6 input at output files at $T_p = 400$ GeV for ^{181}Ta and one example for ^{197}Au, at 800 GeV. The main MCNP6 input files for ^{181}Ta and ^{197}Au at these energies are **p400000Ta_REP** and **p800000Au_REP**, respectively. Recall that the GENXS option of MCNP6 requires a second, auxiliary, input file. For both our examples, it is the same, namely **inxc97**, used also in several other test-problems and shown explicitly in the previous sub-section. All three input files are presented in the subdirectory /VALIDATION_LAQGSM/Inputs/; both the main MCNP6 files are also shown below:

p400000Ta_REP:

```
MCNP6 test: p + Ta by LAQGSM03.03 at 400 GeV, nevtype=66
C To study Au fragmentation induced by very energetic projectiles;
c These calculations are done with corrections to MCNP6 by Dick Prael(REP)
c of 12/6/10 to account all fragments (not only 3) from Fermi break-up
  1  1  1.0   -1 2 -3
  2  0        -4 (1:-2:3)
  3  0         4

c -------------------------------------------------------------
  1  cz  4.0
  2  pz  -1.0
  3  pz  1.0
  4  so  50.0

c -------------------------------------------------------------
dbcn 28j 1
  m1 73181 1.0
  sdef erg = 400000 par = H dir = 1 pos = 0 0 0 vec 0 0 1
  imp:n 1 1 0
  imp:h 1 1 0
```

```
  phys:h 400100
  mode   h
LCA  2 1 5j -1 1j 1    $ use LAQGSM, nevtype = 66                    !!!
lcb  0 0 0 0 0 0
lea  2j 0
c  tropt genxs inxc98  nreact on  nescat off
  tropt genxs inxc97
c ---------------------------------------------------------------
  print 40 110 95
c  nps 1000
  nps 1000000
  prdmp 2j -1
```

p800000Au_REP:

```
MCNP6 test: p + Au by LAQGSM03.03 at 800 GeV, nevtype=66
C To study Au fragmentation induced by very energetic projectiles;
c These calculations are done with corrections to MCNP6 by Dick Prael(REP)
c of 12/6/10 to account all fragments (not only 3) from Fermi break-up
  1  1  1.0   -1 2 -3
  2  0        -4 (1:-2:3)
  3  0         4

c ---------------------------------------------------------------
  1  cz  4.0
  2  pz  -1.0
  3  pz  1.0
  4  so  50.0

c ---------------------------------------------------------------
dbcn 28j 1
  m1 79197 1.0
  sdef erg = 800000 par = H dir = 1 pos = 0 0 0 vec 0 0 1
  imp:n 1 1 0
  imp:h 1 1 0
  phys:h 800100
  mode   h
LCA  2 1 5j -1 1j 1    $ use LAQGSM, nevtype = 66                    !!!
lcb  0 0 0 0 0 0
lea  2j 0
c  tropt genxs inxc98  nreact on  nescat off
  tropt genxs inxc97
c ---------------------------------------------------------------
  print 40 110 95
c  nps 1000
  nps 1000000
  prdmp 2j -1
```

The output files for ^{181}Ta and ^{197}Au are p400000Ta_REP.mpi.o and p800000Au_REP.mpi.o, respectively, both presented in the subdirectory /VALIDATION_LAQGSM/Templates/LINUX/.

The fission cross section is printed in the output files in barns, two lines before the tables with residual nuclei yields. Files pTa181_M6REP.dat and M6_Laq_REP.dat, in subdirectories */VALIDATION_LAQGSM/Experimental_data/p+Ta-Au_xfiss/pTa181/ and */pAu197/, respectively, present fission cross sections at all energies calculated with MCNP6 for ^{181}Ta and ^{197}Au copied from the corresponding MCNP6 output files. For comparison, we show in the same subdirectory also examples of initial results, with the mentioned above "bug" in the calculation of fission cross sections with MCNP6 using LAQGSM03.03 with the GENXS option: Files pTa181_M6REP.dat and oldM6Laq.dat in the */pTa181/ and */pAu197/ subdirectories show such wrong results for ^{181}Ta and ^{197}Au, respectively.

The files pTa181_corrLAQ.fig and pAu197_corrLAQ.fig in subdirectories */pTa181/ and */pAu197/ are templates for plotting with xmgrace the fission cross section for ^{181}Ta and ^{197}Au at all incident energies of protons we calculated here. The final pdf files with figures for ^{181}Ta and ^{197}Au are pTa181_corrLAQ.pdf and pAu197_corrLAQ.pdf, respectively, shown below in Fig. 22.

All files with experimental data and with values predicted by the Prokofiev systematics for ^{181}Ta, in subdirectory */pTa181/, and for ^{197}Au, in subdirectory */pAu197/, have extensions "dat"; It is easy to understand what every file represents from its name, and also from comments provided in the beginning of all these files. A more detailed description of all references to these experimental data can be find in our paper [56].

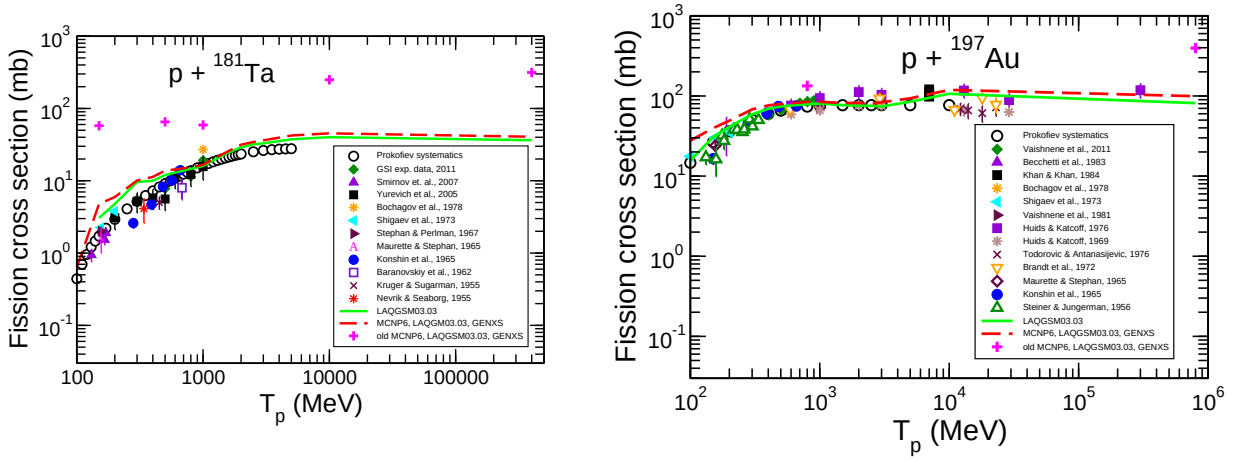

Figure 22: Prokofiev systematics [57] (open circles) and experimental proton-induced fission cross sections of ^{181}Ta and ^{197}Au (symbols, see detailed references in [56]) compared with our results by the updated MCNP6 using the LAQGSM03.03 event generator with the GENXS option, MPI (red dashed lines) and with calculations by LAQGSM03.03 used as a stand alone code (green lines), as indicated. For comparison, wrong initial results by an older, preliminary version of MCNP6 (called "Beta 1" [3]), before a "bug" in the calculation of the fission cross section with the GENXS option while using LAQGSM03.03 was fixed (see text) are shown as well with several magenta crosses.

5. Delayed Particle Test Suite

This Section is dedicated to problems on delayed neutron emission from various reactions. The first three test-problems are on delayed neutron emission from ^{235}U, ^{233}U, and ^{239}Pu thick targets after fission induced by thermal neutrons, involving the use of only data libraries and CINDER tables, while the last, 4th one, studies delayed neutrons emission at intermediate energies, from a thin highly enriched uranium (HEU) target bombarded with an 800-MeV proton beam, using also the CEM03.03 event-generator.

5.1. U235ACE and U235CINDER

This MCNP6 problem is to test the applicability of MCNP6 to describe delayed neutron emission from fission fragments for nuclear forensics applications pertaining to Special Nuclear Material (SNM) analysis. The Atomic Energy Act of 1954 defines special nuclear materials as plutonium, or uranium enriched in ^{233}U or ^{235}U. The current test-problem studies delayed neutron emission from ^{235}U, while the following two are dedicated to ^{233}U and ^{239}Pu.

SNM are tracked by international and national regulatory agencies, including the International Atomic Energy Agency. Since the early 1990s, nuclear material smuggling interceptions have been on the rise, and have included cases involving HEU, five of which occurred between July 2009 and June 2010 [82]. Delayed neutron counting (DNC) is a technique capable of determining the amount of fissile content in an unknown sample. Automated delayed neutron counting systems for mass determination of SNM have been developed to enhance nuclear forensics capabilities [83].

To be specific, this problem calculates the energy deposition per proton/triton pair (tally F6) averaged over a cell used to simulate the detector of the DNC system commissioned at the Royal Military College of Canada (RMCC) from a sample containing U-235.

The experimental data for this problem were measured at RMCC by PhD student Madison Theresa Sellers with collaborators using the SLOWPOKE-2 reactor as a source of predominately thermal neutrons. Madison converted the measured count rates into units of MeV/g (for one second interval) so that these values could be compared directly with the F6 tally results calculated by MCNP6. She kindly provided to us both the experimental values and the MCNP6 input files she used at RMCC to simulate her measurements. The publications [84] serve as current references for these measurements and simulations.

Experimental energy deposition in the detector in units of [MeV/g/s] are presented in the file U235.exp.dat of the subdirectory */DELAYED_PARTICLES/Experimental_data/RMC_U235/.

We have calculated this problem on the **Turing** supercomputer at LANL with MPI, as described in Sec. 2, using 4 nodes, 64 processors, in two different ways: accounting for up to 15 biased delayed neutrons from ACE data libraries (using 1015 for the 4th parameter of the phys:n card of the MCNP6 input file) and up to 15 biased delayed neutrons from CINDER tables (using 115 for the 4th parameter of the phys:n card of the MCNP6 input file). The input files for the ACE and CINDER calculations are **U235ACE** and **U235CINDER**, respectively, both presented in the subdirectory /DELAYED_PARTICLES/Inputs/ and both shown below:

U235ACE:

```
Modeling Delayed Neutron Emissions in RMC's DNC System
```

```
c Winter 2012
c
c --------------GEOMETRY----------------
c
c He-3 Detectors
c
c   Detector 1
   10  1000 -0.000511 -201 601 401          $Fill Gas
       imp:n=1 imp:e=1 imp:h=1 imp:t=1 imp:p=1
c
   11  2000    -7.92    201 -101 401        $S.S Container
       imp:n=1 imp:e=1 imp:h=1 imp:t=1 imp:p=1
c
c   Detector 2
   20  1000 -0.000511 -202 602 402
       imp:n=1 imp:e=1 imp:h=1 imp:t=1 imp:p=1
c
   21  2000    -7.92    202 -102 402
       imp:n=1 imp:e=1 imp:h=1 imp:t=1 imp:p=1
c
c   Detector 3
   30  1000 -0.000511 -203 603 403
       imp:n=1 imp:e=1 imp:h=1 imp:t=1 imp:p=1
c
   31  2000    -7.92    203 -103 403
       imp:n=1 imp:e=1 imp:h=1 imp:t=1 imp:p=1
c
c   Detector 4
   40  1000 -0.000511 -204 604 404
       imp:n=1 imp:e=1 imp:h=1 imp:t=1 imp:p=1
c
   41  2000    -7.92    204 -104 404
       imp:n=1 imp:e=1 imp:h=1 imp:t=1 imp:p=1
c
c   Detector 5
   50  1000 -0.000511 -205 605 405
       imp:n=1 imp:e=1 imp:h=1 imp:t=1 imp:p=1
c
   51  2000    -7.92    205 -105 405
       imp:n=1 imp:e=1 imp:h=1 imp:t=1 imp:p=1
c
c   Detector 6
   60  1000 -0.000511 -206 606 406
       imp:n=1 imp:e=1 imp:h=1 imp:t=1 imp:p=1
c
   61  2000    -7.92    206 -106 406
       imp:n=1 imp:e=1 imp:h=1 imp:t=1 imp:p=1
```

```
c
c Active Fill Area of Detectors
c
  14  1000 -0.000511 -601 401
       imp:n=1 imp:e=1 imp:h=1 imp:t=1 imp:p=1
c
  24  1000 -0.000511 -602 402
       imp:n=1 imp:e=1 imp:h=1 imp:t=1 imp:p=1
c
  34  1000 -0.000511 -603 403
       imp:n=1 imp:e=1 imp:h=1 imp:t=1 imp:p=1
c
  44  1000 -0.000511 -604 404
       imp:n=1 imp:e=1 imp:h=1 imp:t=1 imp:p=1
c
  54  1000 -0.000511 -605 405
       imp:n=1 imp:e=1 imp:h=1 imp:t=1 imp:p=1
c
  64  1000 -0.000511 -606 406
       imp:n=1 imp:e=1 imp:h=1 imp:t=1 imp:p=1
c
c
c Detector Anodes
c
   12    2000   -7.92            -401        $D1 anode
         imp:n=1 imp:e=1 imp:h=1 imp:t=1 imp:p=1
   22     2000  -7.92            -402        $D2 anode
         imp:n=1 imp:e=1 imp:h=1 imp:t=1 imp:p=1
   32     2000   -7.92           -403        $D3 anode
         imp:n=1 imp:e=1 imp:h=1 imp:t=1 imp:p=1
   42     2000   -7.92           -404        $D4 anode
         imp:n=1 imp:e=1 imp:h=1 imp:t=1 imp:p=1
   52     2000    -7.92          -405        $D5 anode
         imp:n=1 imp:e=1 imp:h=1 imp:t=1 imp:p=1
   62     2000   -7.92           -406        $D6 anode
         imp:n=1 imp:e=1 imp:h=1 imp:t=1 imp:p=1
c
c Detector Tops
c
   13  2000      -7.92  -301 401       $D1 top
         imp:n=1 imp:e=1 imp:h=1 imp:t=1 imp:p=1
   23  2000      -7.92  -302 402       $D2 top
         imp:n=1 imp:e=1 imp:h=1 imp:t=1 imp:p=1
   33  2000      -7.92  -303 403       $D3 top
         imp:n=1 imp:e=1 imp:h=1 imp:t=1 imp:p=1
   43  2000      -7.92  -304 404       $D4 top
         imp:n=1 imp:e=1 imp:h=1 imp:t=1 imp:p=1
```

```
   53  2000      -7.92  -305 405      $D5 top
         imp:n=1 imp:e=1 imp:h=1 imp:t=1 imp:p=1
   63  2000      -7.92  -306 406      $D6 top
         imp:n=1 imp:e=1 imp:h=1 imp:t=1 imp:p=1
c
c Outside Container
c
   37  2000      -7.92  -901 902                                $container outside
       imp:n=1 imp:e=1 imp:h=1 imp:t=1 imp:p=1
   17  6000      -0.93  -902 -901 101 102 103 104 105
                         106 301 302 303 304 305 306 801      $paraffin moderator
       imp:n=1 imp:e=1 imp:h=1 imp:t=1 imp:p=1
   18  3000     -0.0013 -903 901 902 801 101 102 103 104 105 106
                         301 302 303 304 803                  $air surrounding apparatus
                         305 306
       imp:n=1 imp:e=1 imp:h=1 imp:t=1 imp:p=1
   19     0              903                                  $geometry void
       imp:n=0 imp:e=0 imp:h=0 imp:t=0 imp:p=0
c
c Poly tubing
c
   27  4000   -0.94     -801 802 -903  882                    $PE outer tubing
       imp:n=1 imp:e=1 imp:h=1 imp:t=1 imp:p=1
   28  3000   -0.0013     -802 -903 507 508 509                $PE inner tubing
       imp:n=1 imp:e=1 imp:h=1 imp:t=1 imp:p=1
   29  3000   -0.0013     -882 -903 507 508 509                $PE inner tubing
       imp:n=1 imp:e=1 imp:h=1 imp:t=1 imp:p=1
c Pe vials
   47  4000   -0.94     -507 508 509  510                      $large vial
       imp:n=1 imp:e=1 imp:h=1 imp:t=1 imp:p=1
   48  3000   -0.0013        -508                              $bottom smaller vial
       imp:n=1 imp:e=1 imp:h=1 imp:t=1 imp:p=1
   49  5000  -0.9977 -509                                      $top smaller vial solution
       imp:n=1 imp:e=1 imp:h=1 imp:t=1 imp:p=1
c  59  3000  -0.0013        -510   509                        $air in top smaller vial
c       imp:n=1 imp:e=1 imp:h=1 imp:t=1 imp:p=1
   57  7000   -0.689   -803                                   $wooden stand
        imp:n=1 imp:e=1 imp:h=1 imp:t=1 imp:p=1
   58  3000    -0.0013     -510
         imp:n=1 imp:e=1 imp:h=1 imp:t=1 imp:p=1
c

c SURFACE CARDS
c These surfaces are used for active part inside detectors
  601       rcc 4 6.928 2.4939      0 0 31.115     2.45 $active area in detector 1
  602       rcc 8 0 2.4939          0 0 31.115     2.45 $active area in detector 2
  603       rcc 4 -6.928 2.4939     0 0 31.115     2.45 $active area in detector 3
```

```
  604       rcc -4 -6.928 2.4939    0 0 31.115     2.45 $active area in detector 4
  605       rcc -8 0 2.4939         0 0 31.115     2.45 $active area in detector 5
  606       rcc -4 6.928 2.4939     0 0 31.115     2.45 $active area in detector 6
c
  101       rcc 4 6.928 0.5    0 0 36.195    2.54  $ detector 1 outside
  102       rcc 8 0 0.5        0 0 36.195    2.54  $ detector 2 outside
  103       rcc 4 -6.928 0.5   0 0 36.195    2.54  $ detector 3 outside
  104       rcc -4 -6.928 0.5  0 0 36.195    2.54  $ detector 4 outside
  105       rcc -8 0 0.5       0 0 36.195    2.54  $ detector 5 outside
  106       rcc -4 6.928 0.5   0 0 36.195    2.54  $ detector 6 outside
c
c Inside the Detectors
c
c
  201       rcc 4 6.928 0.5889   0 0 36.0172  2.4511  $ detector 1 fill
  202       rcc 8 0 0.5889       0 0 36.0172  2.4511  $ detector 2 fill
  203       rcc 4 -6.928 0.5889  0 0 36.0172  2.4511  $ detector 3 fill
  204       rcc -4 -6.928 0.5889 0 0 36.0172  2.4511  $ detector 4 fill
  205       rcc -8 0 0.5889      0 0 36.0172  2.4511  $ detector 5 fill
  206       rcc -4 6.928 0.5889  0 0 36.0172  2.4511  $ detector 6 fill
c
c Detector Tops
c
  301       rcc 4 6.928 36.695    0 0 3.66  1.13  $ detector 1 top
  302       rcc 8 0 36.695        0 0 3.66  1.13  $ detector 2 top
  303       rcc 4 -6.928 36.695   0 0 3.66  1.13  $ detector 3 top
  304       rcc -4 -6.928 36.695  0 0 3.66  1.13  $ detector 4 top
  305       rcc -8 0 36.695       0 0 3.66  1.13  $ detector 5 top
  306       rcc -4 6.928 36.695   0 0 3.66  1.13  $ detector 6 top
c
c
c Detector Anode
c need to find the actual thickness of the anode
c Knoll original radius 0.008
  401       rcc 4 6.928 0.55   0 0 35.9  0.008  $detector 1 anode
  402       rcc 8 0 0.55       0 0 35.9  0.008  $detector 2 anode
  403       rcc 4 -6.928 0.55  0 0 35.9  0.008  $detector 3 anode
  404       rcc -4 -6.928 0.55 0 0 35.9  0.008  $detector 4 anode
  405       rcc -8 0 0.55      0 0 35.9  0.008  $detector 5 anode
  406       rcc -4 6.928 0.55  0 0 35.9  0.008  $detector 6 anode
c
  507       rcc 0 0 14.7       0 0 5.72  0.8509    $large vial outer
  508       rcc 0 0 15.1       0 0 2.2   0.4826    $bottom small vial
  509       rcc 0 0 17.3      0 0 1.38   0.4826    $top small vial solution
  510       rcc 0 0 18.7       0 0  0.82 0.4826    $air in the top vial
c
c
```

```
c Container & Paraffin
  901       rcc 0 0 0          0 0 34    15        $container outside
  902       rcc 0 0 0.5        0 0 33.5  14.5      $paraffin outside
  903       rcc 0 0 -20        0 0 64    35        $air around container
c
c Sample Tubing
  801       rcc 0 0 0.5        0 0 43    1.3       $PE tubing outer diameter bottom
  882       rcc 0 0 20.42      0 0 22.58 0.8509
  802       rcc 0 0 0.5        0 0 14.2    0.8509    $PE tubing inner diameter
c still need to add in the outer big container
c Wooden stand
  803       rcc 0 0 -5         0  0 4.9    18      $wooden stand
c

c MATERIAL AND SOURCE CARDS
c
mode  n h t
c
phys:n 3j 1015 j j 2 -1
c Large biasing in the number of delayed neutrons produced
phys:h j j 0 8j
c Mix and match tables and physics models for proton interactions
c
TOTNU
dbcn 28j 1 3j 1 $DN on,
c ------------------------------------------------------------------------
c                          MATERIAL DEFINITIONS
c
c .70c for calculations at room temperature
c negative fractions indicate wgt%
c
m1000    2003.70c              1  $He-3
c
m2000    24050.70c      -0.00793  $Steel, Stainless 304,
         24052.70c     -0.159032
         24053.70c     -0.018378
         24054.70c     -0.004661
         25055.70c         -0.02
         26054.70c     -0.039605
         26056.70c     -0.638496
         26057.70c      -0.01488
         26058.70c     -0.002019
         28058.70c     -0.064024
         28060.70c     -0.025321
         28061.70c     -0.001115
         28062.70c     -0.003599
         28064.70c     -0.000942
```

```
c
m3000    7014.70c      -0.755636    $Air at sea level
         8016.70c      -0.231475
        18036.70c        -3.9e-5
        18038.70c          -8e-6
        18040.70c      -0.012842
c
m4000    1001.70c      -0.143716    $Polyethylene
         6000.70c      -0.856284
mt4000   poly.10t                   $S(alpha,beta)
c
m5000
c $U-235, dissolved in HNO3/H20 mixture
c U-238 content is ignored in this current input deck
c Fissile mass of experimental runs has been increased 1000x
c This has been accounted for in the corresponding experimental data
         92235.70c       -2.14e-3
         1001.70c        -0.107
         8016.70c        -0.87786
         7014.70c        -0.013
mt5000  lwtr.10t                    $Light water scattering
c
m6000    1001.70c      -0.148605    $Paraffin
         6000.70c      -0.851395
mt6000   poly.10t
c
m7000    1001.70c      -0.057889    $wooden stand
         6000.70c      -0.482667
         8016.70c      -0.459440
c data cards
C nps 1e4
nps 1e8
c
c ----------------------------------
c                     SOURCE DEFINITION
c
c This file is specifically tailored to 2.14 ug U-235 sample irradiated for 60s in a
c thermal flux of 5.57e11 cm^-2 s^-1
sdef pos=0 0 18.4 par=n cel=49
     Rad=D2 Ext=D3 AXS 0 1 0
     erg=0.0253e-6 wgt=3.68e13 tme=d1
c
c from 0 - 60s MCNP models the neutron flux in the SLOWPOKE-2 reactor.
c
c The paraffin is not present in the experiments and therefore a correction to
c the neutron flux has been applied.
c
```

```
c A weight of 3.68e13 applied to the source yields the
c measured neutron flux of 5.57e11 1/cm^2/s in vial
c
c                          Time (sh) in sixty 1s interval
si1 H
      0e8 1e8 2e8 3e8 4e8 5e8 6e8 7e8 8e8 9e8
      10e8 11e8 12e8 13e8 14e8 15e8 16e8 17e8 18e8 19e8
      20e8 21e8 22e8 23e8 24e8 25e8 26e8 27e8 28e8 29e8
      30e8 31e8 32e8 33e8 34e8 35e8 36e8 37e8 38e8 39e8
      40e8 41e8 42e8 43e8 44e8 45e8 46e8 47e8 48e8 49e8
      50e8 51e8 52e8 53e8 54e8 55e8 56e8 57e8 58e8 59e8 60e8
sp1
      0 1 1 1 1 1 1 1 1 1
      1 1 1 1 1 1 1 1 1 1
      1 1 1 1 1 1 1 1 1 1
      1 1 1 1 1 1 1 1 1 1
      1 1 1 1 1 1 1 1 1 1
      1 1 1 1 1 1 1 1 1 1 1
c
c Source defined inside the PE vial
si2 H 0 0.4826
sp2 -21 1
si3 -1.1 1.1
c                        PARTICLE TIME, WEIGHT and ENERGY CUT-OFFS
cut:n 2400e8 j 0 0
cut:h 2400e8 1e-3 1e-6
cut:t 2400e8 1e-3 1e-6
c
F4:n 49
T4: 0 179i 180e8 2400e8
c The neutron flux in cell 49 should be 5.5 cm^-2 s^-1 for the first sixty
c seconds of the run
c Energy Deposition in the detector as a function time
F6:h,t (14 24 34 44 54 64)
t6 60e8 179i 240e8 2400e8
```

U235CINDER:

```
Modeling Delayed Neutron Emissions in RMC's DNC System
c Winter 2012
c
c --------------GEOMETRY----------------
c
c He-3 Detectors
c
c   Detector 1
   10  1000 -0.000511 -201 601 401          $Fill Gas
```

```
       imp:n=1 imp:e=1 imp:h=1 imp:t=1 imp:p=1
c
   11  2000    -7.92    201 -101 401        $S.S Container
       imp:n=1 imp:e=1 imp:h=1 imp:t=1 imp:p=1
c
c   Detector 2
   20  1000 -0.000511 -202 602 402
       imp:n=1 imp:e=1 imp:h=1 imp:t=1 imp:p=1
c
   21  2000    -7.92    202 -102 402
       imp:n=1 imp:e=1 imp:h=1 imp:t=1 imp:p=1
c
c   Detector 3
   30  1000 -0.000511 -203 603 403
       imp:n=1 imp:e=1 imp:h=1 imp:t=1 imp:p=1
c
   31  2000    -7.92    203 -103 403
       imp:n=1 imp:e=1 imp:h=1 imp:t=1 imp:p=1
c
c   Detector 4
   40  1000 -0.000511 -204 604 404
       imp:n=1 imp:e=1 imp:h=1 imp:t=1 imp:p=1
c
   41  2000    -7.92    204 -104 404
       imp:n=1 imp:e=1 imp:h=1 imp:t=1 imp:p=1
c
c   Detector 5
   50  1000 -0.000511 -205 605 405
       imp:n=1 imp:e=1 imp:h=1 imp:t=1 imp:p=1
c
   51  2000    -7.92    205 -105 405
       imp:n=1 imp:e=1 imp:h=1 imp:t=1 imp:p=1
c
c   Detector 6
   60  1000 -0.000511 -206 606 406
       imp:n=1 imp:e=1 imp:h=1 imp:t=1 imp:p=1
c
   61  2000    -7.92    206 -106 406
       imp:n=1 imp:e=1 imp:h=1 imp:t=1 imp:p=1
c
c Active Fill Area of Detectors
c
  14  1000 -0.000511 -601 401
       imp:n=1 imp:e=1 imp:h=1 imp:t=1 imp:p=1
c
  24  1000 -0.000511 -602 402
       imp:n=1 imp:e=1 imp:h=1 imp:t=1 imp:p=1
```

```
c
  34  1000 -0.000511 -603 403
       imp:n=1 imp:e=1 imp:h=1 imp:t=1 imp:p=1
c
  44  1000 -0.000511 -604 404
       imp:n=1 imp:e=1 imp:h=1 imp:t=1 imp:p=1
c
  54  1000 -0.000511 -605 405
       imp:n=1 imp:e=1 imp:h=1 imp:t=1 imp:p=1
c
  64  1000 -0.000511 -606 406
       imp:n=1 imp:e=1 imp:h=1 imp:t=1 imp:p=1
c
c
c Detector Anodes
c
   12    2000   -7.92             -401        $D1 anode
         imp:n=1 imp:e=1 imp:h=1 imp:t=1 imp:p=1
   22     2000  -7.92             -402        $D2 anode
         imp:n=1 imp:e=1 imp:h=1 imp:t=1 imp:p=1
   32     2000   -7.92            -403        $D3 anode
         imp:n=1 imp:e=1 imp:h=1 imp:t=1 imp:p=1
   42     2000   -7.92            -404        $D4 anode
         imp:n=1 imp:e=1 imp:h=1 imp:t=1 imp:p=1
   52     2000    -7.92           -405        $D5 anode
         imp:n=1 imp:e=1 imp:h=1 imp:t=1 imp:p=1
   62     2000   -7.92            -406        $D6 anode
         imp:n=1 imp:e=1 imp:h=1 imp:t=1 imp:p=1
c
c Detector Tops
c
   13  2000      -7.92  -301 401       $D1 top
         imp:n=1 imp:e=1 imp:h=1 imp:t=1 imp:p=1
   23  2000      -7.92  -302 402       $D2 top
         imp:n=1 imp:e=1 imp:h=1 imp:t=1 imp:p=1
   33  2000      -7.92  -303 403       $D3 top
         imp:n=1 imp:e=1 imp:h=1 imp:t=1 imp:p=1
   43  2000      -7.92  -304 404       $D4 top
         imp:n=1 imp:e=1 imp:h=1 imp:t=1 imp:p=1
   53  2000      -7.92  -305 405      $D5 top
         imp:n=1 imp:e=1 imp:h=1 imp:t=1 imp:p=1
   63  2000      -7.92  -306 406      $D6 top
         imp:n=1 imp:e=1 imp:h=1 imp:t=1 imp:p=1
c
c Outside Container
c
   37  2000      -7.92  -901 902                                $container outside
```

```
        imp:n=1 imp:e=1 imp:h=1 imp:t=1 imp:p=1
   17  6000      -0.93  -902 -901 101 102 103 104 105
                         106 301 302 303 304 305 306 801      $paraffin moderator
        imp:n=1 imp:e=1 imp:h=1 imp:t=1 imp:p=1
   18  3000     -0.0013 -903 901 902 801 101 102 103 104 105 106
                         301 302 303 304 803                  $air surrounding apparatus
                         305 306
        imp:n=1 imp:e=1 imp:h=1 imp:t=1 imp:p=1
   19     0              903                                  $geometry void
        imp:n=0 imp:e=0 imp:h=0 imp:t=0 imp:p=0
c
c Poly tubing
c
   27  4000   -0.94     -801 802 -903  882                   $PE outer tubing
        imp:n=1 imp:e=1 imp:h=1 imp:t=1 imp:p=1
   28  3000   -0.0013     -802 -903 507 508 509               $PE inner tubing
        imp:n=1 imp:e=1 imp:h=1 imp:t=1 imp:p=1
   29  3000   -0.0013     -882 -903 507 508 509               $PE inner tubing
        imp:n=1 imp:e=1 imp:h=1 imp:t=1 imp:p=1
c Pe vials
   47  4000   -0.94     -507 508 509  510                    $large vial
        imp:n=1 imp:e=1 imp:h=1 imp:t=1 imp:p=1
   48  3000   -0.0013        -508                            $bottom smaller vial
        imp:n=1 imp:e=1 imp:h=1 imp:t=1 imp:p=1
   49  5000  -0.9977 -509                                    $top smaller vial solution
        imp:n=1 imp:e=1 imp:h=1 imp:t=1 imp:p=1
c  59  3000  -0.0013        -510   509                      $air in top smaller vial
c       imp:n=1 imp:e=1 imp:h=1 imp:t=1 imp:p=1
   57  7000   -0.689   -803                                  $wooden stand
         imp:n=1 imp:e=1 imp:h=1 imp:t=1 imp:p=1
   58  3000    -0.0013     -510
          imp:n=1 imp:e=1 imp:h=1 imp:t=1 imp:p=1
c

c SURFACE CARDS
c These surfaces are used for active part inside detectors
  601       rcc 4 6.928 2.4939      0 0 31.115     2.45 $active area in detector 1
  602       rcc 8 0 2.4939          0 0 31.115     2.45 $active area in detector 2
  603       rcc 4 -6.928 2.4939     0 0 31.115     2.45 $active area in detector 3
  604       rcc -4 -6.928 2.4939    0 0 31.115     2.45 $active area in detector 4
  605       rcc -8 0 2.4939         0 0 31.115     2.45 $active area in detector 5
  606       rcc -4 6.928 2.4939     0 0 31.115     2.45 $active area in detector 6
c
  101       rcc 4 6.928 0.5    0 0 36.195    2.54  $ detector 1 outside
  102       rcc 8 0 0.5        0 0 36.195    2.54  $ detector 2 outside
  103       rcc 4 -6.928 0.5   0 0 36.195    2.54  $ detector 3 outside
  104       rcc -4 -6.928 0.5  0 0 36.195    2.54  $ detector 4 outside
```

```
  105       rcc -8 0 0.5       0 0 36.195    2.54  $ detector 5 outside
  106       rcc -4 6.928 0.5   0 0 36.195    2.54  $ detector 6 outside
c
c Inside the Detectors
c
c
  201       rcc 4 6.928 0.5889   0 0 36.0172  2.4511  $ detector 1 fill
  202       rcc 8 0 0.5889       0 0 36.0172  2.4511  $ detector 2 fill
  203       rcc 4 -6.928 0.5889  0 0 36.0172  2.4511  $ detector 3 fill
  204       rcc -4 -6.928 0.5889 0 0 36.0172  2.4511  $ detector 4 fill
  205       rcc -8 0 0.5889      0 0 36.0172  2.4511  $ detector 5 fill
  206       rcc -4 6.928 0.5889  0 0 36.0172  2.4511  $ detector 6 fill
c
c Detector Tops
c
  301       rcc 4 6.928 36.695    0 0 3.66  1.13  $ detector 1 top
  302       rcc 8 0 36.695        0 0 3.66  1.13  $ detector 2 top
  303       rcc 4 -6.928 36.695   0 0 3.66  1.13  $ detector 3 top
  304       rcc -4 -6.928 36.695  0 0 3.66  1.13  $ detector 4 top
  305       rcc -8 0 36.695       0 0 3.66  1.13  $ detector 5 top
  306       rcc -4 6.928 36.695   0 0 3.66  1.13  $ detector 6 top
c
c
c Detector Anode
c need to find the actual thickness of the anode
c Knoll original radius 0.008
  401       rcc 4 6.928 0.55   0 0 35.9  0.008  $detector 1 anode
  402       rcc 8 0 0.55       0 0 35.9  0.008  $detector 2 anode
  403       rcc 4 -6.928 0.55  0 0 35.9  0.008  $detector 3 anode
  404       rcc -4 -6.928 0.55 0 0 35.9  0.008  $detector 4 anode
  405       rcc -8 0 0.55      0 0 35.9  0.008  $detector 5 anode
  406       rcc -4 6.928 0.55  0 0 35.9  0.008  $detector 6 anode
c
  507       rcc 0 0 14.7       0 0 5.72  0.8509    $large vial outer
  508       rcc 0 0 15.1       0 0 2.2   0.4826    $bottom small vial
  509       rcc 0 0 17.3      0 0 1.38   0.4826    $top small vial solution
  510       rcc 0 0 18.7       0 0  0.82 0.4826    $air in the top vial
c
c
c Container & Paraffin
  901       rcc 0 0 0          0 0 34    15        $container outside
  902       rcc 0 0 0.5        0 0 33.5  14.5      $paraffin outside
  903       rcc 0 0 -20        0 0 64    35        $air around container
c
c Sample Tubing
  801       rcc 0 0 0.5        0 0 43    1.3       $PE tubing outer diameter bottom
  882       rcc 0 0 20.42      0 0 22.58 0.8509
```

```
  802       rcc 0 0 0.5        0 0 14.2    0.8509    $PE tubing inner diameter
c still need to add in the outer big container
c Wooden stand
  803       rcc 0 0 -5         0  0 4.9    18      $wooden stand
c

c MATERIAL AND SOURCE CARDS
c
mode  n h t
c
phys:n 3j 115 j j 2 -1
c Large biasing in the number of delayed neutrons produced
phys:h j j 0 8j
c Mix and match tables and physics models for proton interactions
c
TOTNU
dbcn 28j 1 3j 1 $DN on,
c ------------------------------------------------------------------------
c                          MATERIAL DEFINITIONS
c
c .70c for calculations at room temperature
c negative fractions indicate wgt%
c
m1000    2003.70c              1  $He-3
c
m2000    24050.70c      -0.00793  $Steel, Stainless 304,
         24052.70c     -0.159032
         24053.70c     -0.018378
         24054.70c     -0.004661
         25055.70c         -0.02
         26054.70c     -0.039605
         26056.70c     -0.638496
         26057.70c      -0.01488
         26058.70c     -0.002019
         28058.70c     -0.064024
         28060.70c     -0.025321
         28061.70c     -0.001115
         28062.70c     -0.003599
         28064.70c     -0.000942
c
m3000    7014.70c      -0.755636    $Air at sea level
         8016.70c      -0.231475
        18036.70c        -3.9e-5
        18038.70c           -8e-6
        18040.70c      -0.012842
c
m4000    1001.70c      -0.143716    $Polyethylene
```

```
         6000.70c      -0.856284
mt4000   poly.10t                  $S(alpha,beta)
c
m5000
c $U-235, dissolved in HNO3/H20 mixture
c U-238 content is ignored in this current input deck
c Fissile mass of experimental runs has been increased 1000x
c This has been accounted for in the corresponding experimental data
         92235.70c       -2.14e-3
         1001.70c        -0.107
         8016.70c        -0.87786
         7014.70c        -0.013
mt5000  lwtr.10t                   $Light water scattering
c
m6000    1001.70c      -0.148605    $Paraffin
         6000.70c      -0.851395
mt6000   poly.10t
c
m7000    1001.70c      -0.057889    $wooden stand
         6000.70c      -0.482667
         8016.70c      -0.459440
c data cards
C nps 1e4
nps 1e8
c
c ----------------------------------
c                     SOURCE DEFINITION
c
c This file is specifically tailored to 2.14 ug U-235 sample irradiated for 60s in a
c thermal flux of 5.57e11 cm^-2 s^-1
sdef pos=0 0 18.4 par=n cel=49
     Rad=D2 Ext=D3 AXS 0 1 0
     erg=0.0253e-6 wgt=3.68e13 tme=d1
c
c from 0 - 60s MCNP models the neutron flux in the SLOWPOKE-2 reactor.
c
c The paraffin is not present in the experiments and therefore a correction to
c the neutron flux has been applied.
c
c A weight of 3.68e13 applied to the source yields the
c measured neutron flux of 5.57e11 1/cm^2/s in vial
c
c                         Time (sh) in sixty 1s interval
si1 H
      0e8 1e8 2e8 3e8 4e8 5e8 6e8 7e8 8e8 9e8
      10e8 11e8 12e8 13e8 14e8 15e8 16e8 17e8 18e8 19e8
      20e8 21e8 22e8 23e8 24e8 25e8 26e8 27e8 28e8 29e8
```

```
      30e8 31e8 32e8 33e8 34e8 35e8 36e8 37e8 38e8 39e8
      40e8 41e8 42e8 43e8 44e8 45e8 46e8 47e8 48e8 49e8
      50e8 51e8 52e8 53e8 54e8 55e8 56e8 57e8 58e8 59e8 60e8
sp1
      0 1 1 1 1 1 1 1 1
      1 1 1 1 1 1 1 1 1
      1 1 1 1 1 1 1 1 1
      1 1 1 1 1 1 1 1 1
      1 1 1 1 1 1 1 1 1
      1 1 1 1 1 1 1 1 1 1
c
c Source defined inside the PE vial
si2 H 0 0.4826
sp2 -21 1
si3 -1.1 1.1
c                        PARTICLE TIME, WEIGHT and ENERGY CUT-OFFS
cut:n 2400e8 j 0 0
cut:h 2400e8 1e-3 1e-6
cut:t 2400e8 1e-3 1e-6
c
F4:n 49
T4: 0 179i 180e8 2400e8
c The neutron flux in cell 49 should be 5.5 cm^-2 s^-1 for the first sixty
c seconds of the run
c Energy Deposition in the detector as a function time
F6:h,t (14 24 34 44 54 64)
t6 60e8 179i 240e8 2400e8
```

The MCNP6 output files for the ACE and CINDER cases are U235ACE.mpi.o and U235CINDER.mpi.o, respectively, both presented in the subdirectory /DELAYED_PARTICLES/Templetes/LINUX/.

Note that the experimental values are tabulated as a function of time after irradiation; the duration of the irradiation was 60 s. We need to properly account for this while extracting the corresponding values from the F6 tally of the MCNP6 output files tabulated as functions of the time (in shakes; 1 shake = 10^{-8} s) from the beginning of irradiation. In other words, we need to account that the time of 6E+9 shakes in the F6 tally corresponds to the time of 0 seconds after irradiation. Extracted from the MCNP6 output files, values of the energy deposition in units of [MeV/g/s] as functions of the time after irradiation are presented in the files U235ACE.mpi.dat and U235CINDER.mpi.dat of the subdirectory */DELAYED_PARTICLES/Experimental_data/RMC_U235/, for the case of ACE and CINDER calculations, respectively.

We plotted our results with xmgrace in two different ways: using a linear scale for the y-axis (used for F6 [MeV/g/s]) and a logarithmic one. Templates for the linear and logarithmic plotting with xmgrace are presented in the files U235ACE.lin.fig and U235ACE.log.fig, respectively, of the same subdirectory. The pdf files of figures for the linear and logarithmic plotting are U235ACE.lin.pdf and U235ACE.log.pdf, respectively, both presented in the same subdirectory, and also shown below in Fig. 23.

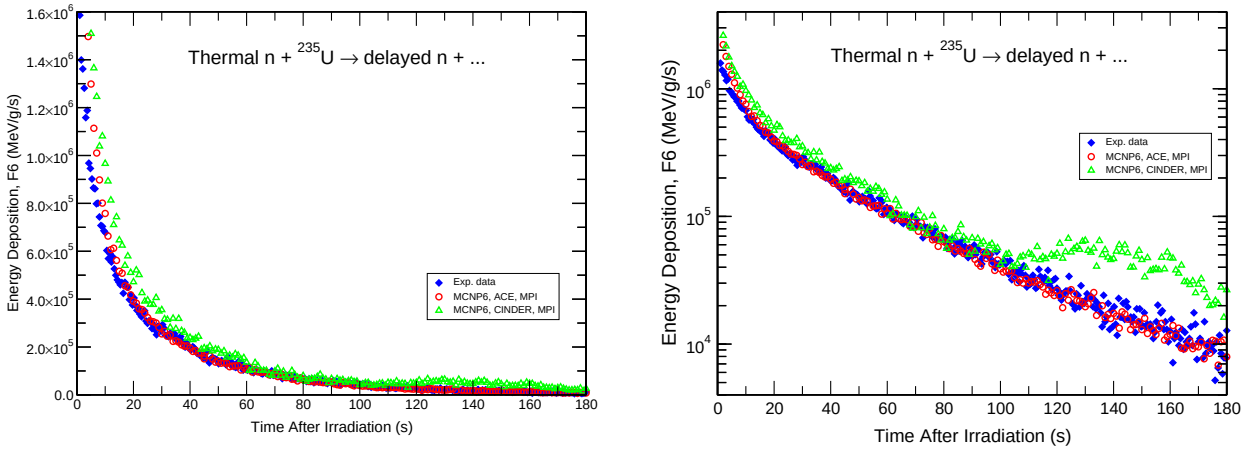

Figure 23: Comparison of the measured [84] energy deposition by delayed neutrons from fission of ^{235}U (filled blue diamonds) with MCNP6 simulation results using the ACE (ENDF/B-VII.0) data libraries (red open circles) and CINDER (lib00c, Oct 2, 2000) tables (green open triangles) as functions of the time after irradiation plotted using linear and logarithmic scales. The significant deference between CIDER and ACE results in the time region above $\sim$ 120 seconds was caused by a too coarse time bins structure in CINDER tables used by MCNP6, a deficiency found and fixed in MCNP6 later by Dr. Michael R. James (see text).

From the results presented in Fig. 23 we can see a reasonable good agreement between the measured data and our MCNP6 calculations, both using the ACE data libraries and the CINDER tables, especially if we plot our results in linear scale, as shown on the left plot. However, if we plot exactly the same results using a logarithmic scale, we can see a much bigger disagreement between the measured data and the CINDER results than for the MCNP6 results obtained using the ACE data libraries, for times after irradiation longer than $\sim$ 120 seconds. Such "increase of disagreement" between calculations and measured data depending on how we present our results is quite interesting and instructive: If we would like to stress the disagreement, we would use only the logarithmic scale, while if we were not completely honest and would like to hide our disagreement for some reasons, we would chose the linear scale. This is why we need to be very carefully when comparing measured data and calculations, using as many as possible different representations, formats, and scales.

A special analysis by Dr. Michael R. James, his colleagues, and by Madison Sellers of the reason for the observed disagreement between the MCNP6 results obtained with the ACE data library and with CINDER tables, as can be seen in Fig. 23, has shown that it was caused by a too coarse time bins structure in CINDER tables used by MCNP6. Mike James fixed this deficiency in MCNP6 recently. Now, the calculations with CINDER agree much better with the measured data and with the results obtained using the ACE data library, as we were informed very recently in a personal communication to us from Madison Sellers.

5.2. U233ACE and U233CINDER

This MCNP6 problem is to test the applicability of MCNP6 to describe delayed neutron emission from fission fragments for nuclear forensics applications pertaining to Special Nuclear Material (SNM) analysis. The Atomic Energy Act of 1954 defines special nuclear materials as plutonium, or uranium enriched in ^{233}U or ^{235}U. The current test-problem studies delayed neutron emission from ^{233}U, while the previous one was dedicated to ^{235}U and the following example is on ^{239}Pu.

SNM are tracked by international and national regulatory agencies, including the International Atomic Energy Agency. Since the early 1990s, nuclear material smuggling interceptions have been on the rise, and have included cases involving HEU, five of which occurred between July 2009 and June 2010 [82]. Delayed neutron counting (DNC) is a technique capable of determining the amount of fissile content in an unknown sample. Automated delayed neutron counting systems for mass determination of SNM are developed lately to enhance nuclear forensics capabilities [83].

To be specific, this problem calculates the energy deposition per proton/triton pair (tally F6) averaged over a cell used to simulate the detector of the DNC system commissioned at the Royal Military College of Canada (RMCC) from a sample containing U-233.

The experimental data for this problem were measured at RMCC by PhD student Madison Theresa Sellers with collaborators using the SLOWPOKE-2 reactor as a source of predominately thermal neutrons. Madison converted the measured count rates into units of MeV/g (for one second interval) so that these values could be compared directly with the F6 tally results calculated by MCNP6. She kindly provided to us both the experimental values and the MCNP6 input files she used at RMCC to simulate her measurements. The publications [84] serve as current references for these measurements and simulations.

Experimental energy deposition in the detector in units of [MeV/g/s] are presented in the file U233.exp.dat of the subdirectory */DELAYED_PARTICLES/Experimental_data/RMC_U233/.

This test-problem is very similar to the previous one on ^{235}U, discussed above in subsection 5.1, but for completeness sake, we provide here all the details. We have calculated this problem on the **Turing** supercomputer at LANL with MPI, as described in Sec. 2, using 4 nodes, 64 processors, in two different ways: accounting for up to 15 biased delayed neutrons from ACE data libraries (using 1015 for the 4th parameter of the phys:n card of the MCNP6 input file) and up to 15 biased delayed neutrons from CINDER tables (using 115 for the 4th parameter of the phys:n card of the MCNP6 input file). The input files for the ACE and CINDER calculations are **U233ACE** and **U233CINDER**, respectively, both presented in the subdirectory /DELAYED_PARTICLES/Inputs/ and both shown below:

U233ACE:

```
Modeling Delayed Neutron Emissions in RMC's DNC System
c Winter 2012
c
c --------------GEOMETRY---------------
c
c He-3 Detectors
c
c   Detector 1
```

```
   10  1000 -0.000511 -201 601 401          $Fill Gas
       imp:n=1 imp:e=1 imp:h=1 imp:t=1 imp:p=1
c
   11  2000    -7.92    201 -101 401        $S.S Container
       imp:n=1 imp:e=1 imp:h=1 imp:t=1 imp:p=1
c
c   Detector 2
   20  1000 -0.000511 -202 602 402
       imp:n=1 imp:e=1 imp:h=1 imp:t=1 imp:p=1
c
   21  2000    -7.92    202 -102 402
       imp:n=1 imp:e=1 imp:h=1 imp:t=1 imp:p=1
c
c   Detector 3
   30  1000 -0.000511 -203 603 403
       imp:n=1 imp:e=1 imp:h=1 imp:t=1 imp:p=1
c
   31  2000    -7.92    203 -103 403
       imp:n=1 imp:e=1 imp:h=1 imp:t=1 imp:p=1
c
c   Detector 4
   40  1000 -0.000511 -204 604 404
       imp:n=1 imp:e=1 imp:h=1 imp:t=1 imp:p=1
c
   41  2000    -7.92    204 -104 404
       imp:n=1 imp:e=1 imp:h=1 imp:t=1 imp:p=1
c
c   Detector 5
   50  1000 -0.000511 -205 605 405
       imp:n=1 imp:e=1 imp:h=1 imp:t=1 imp:p=1
c
   51  2000    -7.92    205 -105 405
       imp:n=1 imp:e=1 imp:h=1 imp:t=1 imp:p=1
c
c   Detector 6
   60  1000 -0.000511 -206 606 406
       imp:n=1 imp:e=1 imp:h=1 imp:t=1 imp:p=1
c
   61  2000    -7.92    206 -106 406
       imp:n=1 imp:e=1 imp:h=1 imp:t=1 imp:p=1
c
c Active Fill Area of Detectors
c
  14  1000 -0.000511 -601 401
       imp:n=1 imp:e=1 imp:h=1 imp:t=1 imp:p=1
c
  24  1000 -0.000511 -602 402
```

```
      imp:n=1 imp:e=1 imp:h=1 imp:t=1 imp:p=1
c
  34  1000 -0.000511 -603 403
      imp:n=1 imp:e=1 imp:h=1 imp:t=1 imp:p=1
c
  44  1000 -0.000511 -604 404
      imp:n=1 imp:e=1 imp:h=1 imp:t=1 imp:p=1
c
  54  1000 -0.000511 -605 405
      imp:n=1 imp:e=1 imp:h=1 imp:t=1 imp:p=1
c
  64  1000 -0.000511 -606 406
      imp:n=1 imp:e=1 imp:h=1 imp:t=1 imp:p=1
c
c
c Detector Anodes
c
   12    2000   -7.92            -401        $D1 anode
         imp:n=1 imp:e=1 imp:h=1 imp:t=1 imp:p=1
   22     2000  -7.92            -402        $D2 anode
         imp:n=1 imp:e=1 imp:h=1 imp:t=1 imp:p=1
   32     2000   -7.92            -403        $D3 anode
         imp:n=1 imp:e=1 imp:h=1 imp:t=1 imp:p=1
   42     2000   -7.92            -404        $D4 anode
         imp:n=1 imp:e=1 imp:h=1 imp:t=1 imp:p=1
   52     2000    -7.92           -405        $D5 anode
         imp:n=1 imp:e=1 imp:h=1 imp:t=1 imp:p=1
   62     2000   -7.92            -406        $D6 anode
         imp:n=1 imp:e=1 imp:h=1 imp:t=1 imp:p=1
c
c Detector Tops
c
   13  2000      -7.92  -301 401       $D1 top
         imp:n=1 imp:e=1 imp:h=1 imp:t=1 imp:p=1
   23  2000      -7.92  -302 402       $D2 top
         imp:n=1 imp:e=1 imp:h=1 imp:t=1 imp:p=1
   33  2000      -7.92  -303 403       $D3 top
         imp:n=1 imp:e=1 imp:h=1 imp:t=1 imp:p=1
   43  2000      -7.92  -304 404       $D4 top
         imp:n=1 imp:e=1 imp:h=1 imp:t=1 imp:p=1
   53  2000      -7.92  -305 405      $D5 top
         imp:n=1 imp:e=1 imp:h=1 imp:t=1 imp:p=1
   63  2000      -7.92  -306 406      $D6 top
         imp:n=1 imp:e=1 imp:h=1 imp:t=1 imp:p=1
c
c Outside Container
c
```

```
   37  2000      -7.92  -901 902                                $container outside
       imp:n=1 imp:e=1 imp:h=1 imp:t=1 imp:p=1
   17  6000      -0.93  -902 -901 101 102 103 104 105
                         106 301 302 303 304 305 306 801       $paraffin moderator
       imp:n=1 imp:e=1 imp:h=1 imp:t=1 imp:p=1
   18  3000     -0.0013 -903 901 902 801 101 102 103 104 105 106
                         301 302 303 304 803                   $air surrounding apparatus
                         305 306
       imp:n=1 imp:e=1 imp:h=1 imp:t=1 imp:p=1
   19     0               903                                  $geometry void
       imp:n=0 imp:e=0 imp:h=0 imp:t=0 imp:p=0
c
c Poly tubing
c
   27  4000   -0.94     -801 802 -903  882                     $PE outer tubing
       imp:n=1 imp:e=1 imp:h=1 imp:t=1 imp:p=1
   28  3000   -0.0013     -802 -903 507 508 509                $PE inner tubing
       imp:n=1 imp:e=1 imp:h=1 imp:t=1 imp:p=1
   29  3000   -0.0013     -882 -903 507 508 509                $PE inner tubing
       imp:n=1 imp:e=1 imp:h=1 imp:t=1 imp:p=1
c Pe vials
   47  4000   -0.94     -507 508 509  510                      $large vial
       imp:n=1 imp:e=1 imp:h=1 imp:t=1 imp:p=1
   48  3000   -0.0013        -508                              $bottom smaller vial
       imp:n=1 imp:e=1 imp:h=1 imp:t=1 imp:p=1
   49  5000  -0.9977 -509                                      $top smaller vial solution
       imp:n=1 imp:e=1 imp:h=1 imp:t=1 imp:p=1
c  59  3000  -0.0013        -510   509                        $air in top smaller vial
c       imp:n=1 imp:e=1 imp:h=1 imp:t=1 imp:p=1
   57  7000   -0.689   -803                                    $wooden stand
        imp:n=1 imp:e=1 imp:h=1 imp:t=1 imp:p=1
   58  3000    -0.0013     -510
         imp:n=1 imp:e=1 imp:h=1 imp:t=1 imp:p=1
c

c SURFACE CARDS
c These surfaces are used for active part inside detectors
  601       rcc 4 6.928 2.4939      0 0 31.115     2.45 $active area in detector 1
  602       rcc 8 0 2.4939          0 0 31.115     2.45 $active area in detector 2
  603       rcc 4 -6.928 2.4939     0 0 31.115     2.45 $active area in detector 3
  604       rcc -4 -6.928 2.4939    0 0 31.115     2.45 $active area in detector 4
  605       rcc -8 0 2.4939         0 0 31.115     2.45 $active area in detector 5
  606       rcc -4 6.928 2.4939     0 0 31.115     2.45 $active area in detector 6
c
  101       rcc 4 6.928 0.5    0 0 36.195    2.54  $ detector 1 outside
  102       rcc 8 0 0.5        0 0 36.195    2.54  $ detector 2 outside
  103       rcc 4 -6.928 0.5   0 0 36.195    2.54  $ detector 3 outside
```

```
  104       rcc -4 -6.928 0.5  0 0 36.195    2.54  $ detector 4 outside
  105       rcc -8 0 0.5       0 0 36.195    2.54  $ detector 5 outside
  106       rcc -4 6.928 0.5   0 0 36.195    2.54  $ detector 6 outside
c
c Inside the Detectors
c
c
  201       rcc 4 6.928 0.5889   0 0 36.0172  2.4511  $ detector 1 fill
  202       rcc 8 0 0.5889       0 0 36.0172  2.4511  $ detector 2 fill
  203       rcc 4 -6.928 0.5889  0 0 36.0172  2.4511  $ detector 3 fill
  204       rcc -4 -6.928 0.5889 0 0 36.0172  2.4511  $ detector 4 fill
  205       rcc -8 0 0.5889      0 0 36.0172  2.4511  $ detector 5 fill
  206       rcc -4 6.928 0.5889  0 0 36.0172  2.4511  $ detector 6 fill
c
c Detector Tops
c
  301       rcc 4 6.928 36.695    0 0 3.66  1.13  $ detector 1 top
  302       rcc 8 0 36.695        0 0 3.66  1.13  $ detector 2 top
  303       rcc 4 -6.928 36.695   0 0 3.66  1.13  $ detector 3 top
  304       rcc -4 -6.928 36.695  0 0 3.66  1.13  $ detector 4 top
  305       rcc -8 0 36.695       0 0 3.66  1.13  $ detector 5 top
  306       rcc -4 6.928 36.695   0 0 3.66  1.13  $ detector 6 top
c
c
c Detector Anode
c need to find the actual thickness of the anode
c Knoll original radius 0.008
  401       rcc 4 6.928 0.55   0 0 35.9  0.008  $detector 1 anode
  402       rcc 8 0 0.55       0 0 35.9  0.008  $detector 2 anode
  403       rcc 4 -6.928 0.55  0 0 35.9  0.008  $detector 3 anode
  404       rcc -4 -6.928 0.55 0 0 35.9  0.008  $detector 4 anode
  405       rcc -8 0 0.55      0 0 35.9  0.008  $detector 5 anode
  406       rcc -4 6.928 0.55  0 0 35.9  0.008  $detector 6 anode
c
  507       rcc 0 0 14.7       0 0 5.72  0.8509    $large vial outer
  508       rcc 0 0 15.1       0 0 2.2   0.4826    $bottom small vial
  509       rcc 0 0 17.3      0 0 1.38   0.4826    $top small vial solution
  510       rcc 0 0 18.7       0 0  0.82 0.4826    $air in the top vial
c
c
c Container & Paraffin
  901       rcc 0 0 0          0 0 34    15        $container outside
  902       rcc 0 0 0.5        0 0 33.5  14.5      $paraffin outside
  903       rcc 0 0 -20        0 0 64    35        $air around container
c
c Sample Tubing
  801       rcc 0 0 0.5        0 0 43    1.3       $PE tubing outer diameter bottom
```

```
  882       rcc 0 0 20.42      0 0 22.58 0.8509
  802       rcc 0 0 0.5        0 0 14.2    0.8509    $PE tubing inner diameter
c still need to add in the outer big container
c Wooden stand
  803       rcc 0 0 -5         0  0 4.9    18      $wooden stand
c

c MATERIAL AND SOURCE CARDS
c
mode  n h t
c
phys:n 3j 1015 j j 2 -1
c Large biasing in the number of delayed neutrons produced
phys:h j j 0 8j
c Mix and match tables and physics models for proton interactions
c
TOTNU
dbcn 28j 1 3j 1 $DN on,
c ------------------------------------------------------------------------
c                          MATERIAL DEFINITIONS
c
c .70c for calculations at room temperature
c negative fractions indicate wgt%
c
m1000    2003.70c              1  $He-3
c
m2000    24050.70c      -0.00793  $Steel, Stainless 304,
         24052.70c     -0.159032
         24053.70c     -0.018378
         24054.70c     -0.004661
         25055.70c         -0.02
         26054.70c     -0.039605
         26056.70c     -0.638496
         26057.70c      -0.01488
         26058.70c     -0.002019
         28058.70c     -0.064024
         28060.70c     -0.025321
         28061.70c     -0.001115
         28062.70c     -0.003599
         28064.70c     -0.000942
c
m3000    7014.70c      -0.755636    $Air at sea level
         8016.70c      -0.231475
        18036.70c        -3.9e-5
        18038.70c           -8e-6
        18040.70c      -0.012842
c
```

```
m4000    1001.70c      -0.143716    $Polyethylene
         6000.70c      -0.856284
mt4000   poly.10t                   $S(alpha,beta)
c
m5000
c $U-233, dissolved in HNO3/H20 mixture
c
c Fissile mass of experimental runs has been increased 1000x
c This has been accounted for in the corresponding experimental data
         92233.70c       -1.63e-3
         1001.70c        -0.107
         8016.70c        -0.87837
         7014.70c        -0.013
mt5000  lwtr.10t                    $Light water scattering
c
m6000    1001.70c      -0.148605    $Paraffin
         6000.70c      -0.851395
mt6000   poly.10t
c
m7000    1001.70c      -0.057889    $wooden stand
         6000.70c      -0.482667
         8016.70c      -0.459440
c data cards
nps 1e8
c
c ------------------------------------
c                     SOURCE DEFINITION
c
c This file is specifically tailored to 1.63 ug U-233 sample irradiated for 60s in a
c thermal flux of 5.57e11 cm^-2 s^-1
sdef pos=0 0 18.4 par=n cel=49
     Rad=D2 Ext=D3 AXS 0 1 0
     erg=0.0253e-6 wgt=3.68e13 tme=d1
c
c from 0 - 60s MCNP models the neutron flux in the SLOWPOKE-2 reactor.
c
c The paraffin is not present in the experiments and therefore a correction to
c the neutron flux has been applied.
c
c A weight of 3.68e13 applied to the source yields the
c measured neutron flux of 5.57e11 1/cm^2/s in vial
c
c                         Time (sh) in sixty 1s interval
si1 H
      0e8 1e8 2e8 3e8 4e8 5e8 6e8 7e8 8e8 9e8
      10e8 11e8 12e8 13e8 14e8 15e8 16e8 17e8 18e8 19e8
      20e8 21e8 22e8 23e8 24e8 25e8 26e8 27e8 28e8 29e8
```

```
      30e8 31e8 32e8 33e8 34e8 35e8 36e8 37e8 38e8 39e8
      40e8 41e8 42e8 43e8 44e8 45e8 46e8 47e8 48e8 49e8
      50e8 51e8 52e8 53e8 54e8 55e8 56e8 57e8 58e8 59e8 60e8
sp1
      0 1 1 1 1 1 1 1 1
      1 1 1 1 1 1 1 1 1
      1 1 1 1 1 1 1 1 1
      1 1 1 1 1 1 1 1 1
      1 1 1 1 1 1 1 1 1
      1 1 1 1 1 1 1 1 1 1
c
c Source defined inside the PE vial
si2 H 0 0.4826
sp2 -21 1
si3 -1.1 1.1
c                        PARTICLE TIME, WEIGHT and ENERGY CUT-OFFS
cut:n 2400e8 j 0 0
cut:h 2400e8 1e-3 1e-6
cut:t 2400e8 1e-3 1e-6
c
F4:n 49
T4: 0 179i 180e8 2400e8
c The neutron flux in cell 49 should be 5.5 cm^-2 s^-1 for the first sixty
c seconds of the run
c Energy Deposition in the detector as a function time
F6:h,t (14 24 34 44 54 64)
t6 60e8 179i 240e8 2400e8
```

U233CINDER:

```
Modeling Delayed Neutron Emissions in RMC's DNC System
c Winter 2012
c
c --------------GEOMETRY----------------
c
c He-3 Detectors
c
c   Detector 1
   10  1000 -0.000511 -201 601 401          $Fill Gas
       imp:n=1 imp:e=1 imp:h=1 imp:t=1 imp:p=1
c
   11  2000    -7.92    201 -101 401        $S.S Container
       imp:n=1 imp:e=1 imp:h=1 imp:t=1 imp:p=1
c
c   Detector 2
   20  1000 -0.000511 -202 602 402
       imp:n=1 imp:e=1 imp:h=1 imp:t=1 imp:p=1
```

```
c
   21  2000    -7.92    202 -102 402
       imp:n=1 imp:e=1 imp:h=1 imp:t=1 imp:p=1
c
c   Detector 3
   30  1000 -0.000511 -203 603 403
       imp:n=1 imp:e=1 imp:h=1 imp:t=1 imp:p=1
c
   31  2000    -7.92    203 -103 403
       imp:n=1 imp:e=1 imp:h=1 imp:t=1 imp:p=1
c
c   Detector 4
   40  1000 -0.000511 -204 604 404
       imp:n=1 imp:e=1 imp:h=1 imp:t=1 imp:p=1
c
   41  2000    -7.92    204 -104 404
       imp:n=1 imp:e=1 imp:h=1 imp:t=1 imp:p=1
c
c   Detector 5
   50  1000 -0.000511 -205 605 405
       imp:n=1 imp:e=1 imp:h=1 imp:t=1 imp:p=1
c
   51  2000    -7.92    205 -105 405
       imp:n=1 imp:e=1 imp:h=1 imp:t=1 imp:p=1
c
c   Detector 6
   60  1000 -0.000511 -206 606 406
       imp:n=1 imp:e=1 imp:h=1 imp:t=1 imp:p=1
c
   61  2000    -7.92    206 -106 406
       imp:n=1 imp:e=1 imp:h=1 imp:t=1 imp:p=1
c
c Active Fill Area of Detectors
c
  14  1000 -0.000511 -601 401
       imp:n=1 imp:e=1 imp:h=1 imp:t=1 imp:p=1
c
  24  1000 -0.000511 -602 402
       imp:n=1 imp:e=1 imp:h=1 imp:t=1 imp:p=1
c
  34  1000 -0.000511 -603 403
       imp:n=1 imp:e=1 imp:h=1 imp:t=1 imp:p=1
c
  44  1000 -0.000511 -604 404
       imp:n=1 imp:e=1 imp:h=1 imp:t=1 imp:p=1
c
  54  1000 -0.000511 -605 405
```

```
      imp:n=1 imp:e=1 imp:h=1 imp:t=1 imp:p=1
c
  64  1000 -0.000511 -606 406
      imp:n=1 imp:e=1 imp:h=1 imp:t=1 imp:p=1
c
c
c Detector Anodes
c
   12    2000   -7.92            -401        $D1 anode
         imp:n=1 imp:e=1 imp:h=1 imp:t=1 imp:p=1
   22     2000  -7.92            -402        $D2 anode
         imp:n=1 imp:e=1 imp:h=1 imp:t=1 imp:p=1
   32     2000   -7.92           -403        $D3 anode
         imp:n=1 imp:e=1 imp:h=1 imp:t=1 imp:p=1
   42     2000   -7.92           -404        $D4 anode
         imp:n=1 imp:e=1 imp:h=1 imp:t=1 imp:p=1
   52     2000    -7.92          -405        $D5 anode
         imp:n=1 imp:e=1 imp:h=1 imp:t=1 imp:p=1
   62     2000   -7.92           -406        $D6 anode
         imp:n=1 imp:e=1 imp:h=1 imp:t=1 imp:p=1
c
c Detector Tops
c
   13  2000      -7.92  -301 401       $D1 top
         imp:n=1 imp:e=1 imp:h=1 imp:t=1 imp:p=1
   23  2000      -7.92  -302 402       $D2 top
         imp:n=1 imp:e=1 imp:h=1 imp:t=1 imp:p=1
   33  2000      -7.92  -303 403       $D3 top
         imp:n=1 imp:e=1 imp:h=1 imp:t=1 imp:p=1
   43  2000      -7.92  -304 404       $D4 top
         imp:n=1 imp:e=1 imp:h=1 imp:t=1 imp:p=1
   53  2000      -7.92  -305 405      $D5 top
         imp:n=1 imp:e=1 imp:h=1 imp:t=1 imp:p=1
   63  2000      -7.92  -306 406      $D6 top
         imp:n=1 imp:e=1 imp:h=1 imp:t=1 imp:p=1
c
c Outside Container
c
   37  2000      -7.92  -901 902                              $container outside
       imp:n=1 imp:e=1 imp:h=1 imp:t=1 imp:p=1
   17  6000      -0.93  -902 -901 101 102 103 104 105
                         106 301 302 303 304 305 306 801      $paraffin moderator
       imp:n=1 imp:e=1 imp:h=1 imp:t=1 imp:p=1
   18  3000     -0.0013 -903 901 902 801 101 102 103 104 105 106
                         301 302 303 304 803                  $air surrounding apparatus
                         305 306
       imp:n=1 imp:e=1 imp:h=1 imp:t=1 imp:p=1
```

```
   19     0              903                                   $geometry void
        imp:n=0 imp:e=0 imp:h=0 imp:t=0 imp:p=0
c
c Poly tubing
c
   27  4000   -0.94     -801 802 -903  882                     $PE outer tubing
        imp:n=1 imp:e=1 imp:h=1 imp:t=1 imp:p=1
   28  3000   -0.0013     -802 -903 507 508 509                $PE inner tubing
        imp:n=1 imp:e=1 imp:h=1 imp:t=1 imp:p=1
   29  3000   -0.0013     -882 -903 507 508 509                $PE inner tubing
        imp:n=1 imp:e=1 imp:h=1 imp:t=1 imp:p=1
c Pe vials
   47  4000   -0.94     -507 508 509  510                      $large vial
        imp:n=1 imp:e=1 imp:h=1 imp:t=1 imp:p=1
   48  3000   -0.0013        -508                              $bottom smaller vial
        imp:n=1 imp:e=1 imp:h=1 imp:t=1 imp:p=1
   49  5000  -0.9977 -509                                      $top smaller vial solution
        imp:n=1 imp:e=1 imp:h=1 imp:t=1 imp:p=1
c  59  3000  -0.0013        -510   509                        $air in top smaller vial
c       imp:n=1 imp:e=1 imp:h=1 imp:t=1 imp:p=1
   57  7000   -0.689   -803                                    $wooden stand
         imp:n=1 imp:e=1 imp:h=1 imp:t=1 imp:p=1
   58  3000    -0.0013     -510
          imp:n=1 imp:e=1 imp:h=1 imp:t=1 imp:p=1
c

c SURFACE CARDS
c These surfaces are used for active part inside detectors
  601       rcc 4 6.928 2.4939      0 0 31.115     2.45 $active area in detector 1
  602       rcc 8 0 2.4939          0 0 31.115     2.45 $active area in detector 2
  603       rcc 4 -6.928 2.4939     0 0 31.115     2.45 $active area in detector 3
  604       rcc -4 -6.928 2.4939    0 0 31.115     2.45 $active area in detector 4
  605       rcc -8 0 2.4939         0 0 31.115     2.45 $active area in detector 5
  606       rcc -4 6.928 2.4939     0 0 31.115     2.45 $active area in detector 6
c
  101       rcc 4 6.928 0.5    0 0 36.195    2.54  $ detector 1 outside
  102       rcc 8 0 0.5        0 0 36.195    2.54  $ detector 2 outside
  103       rcc 4 -6.928 0.5   0 0 36.195    2.54  $ detector 3 outside
  104       rcc -4 -6.928 0.5  0 0 36.195    2.54  $ detector 4 outside
  105       rcc -8 0 0.5       0 0 36.195    2.54  $ detector 5 outside
  106       rcc -4 6.928 0.5   0 0 36.195    2.54  $ detector 6 outside
c
c Inside the Detectors
c
c
  201       rcc 4 6.928 0.5889   0 0 36.0172  2.4511  $ detector 1 fill
  202       rcc 8 0 0.5889       0 0 36.0172  2.4511  $ detector 2 fill
```

```
  203       rcc 4 -6.928 0.5889  0 0 36.0172  2.4511  $ detector 3 fill
  204       rcc -4 -6.928 0.5889 0 0 36.0172  2.4511  $ detector 4 fill
  205       rcc -8 0 0.5889      0 0 36.0172  2.4511  $ detector 5 fill
  206       rcc -4 6.928 0.5889  0 0 36.0172  2.4511  $ detector 6 fill
c
c Detector Tops
c
  301       rcc 4 6.928 36.695    0 0 3.66  1.13  $ detector 1 top
  302       rcc 8 0 36.695        0 0 3.66  1.13  $ detector 2 top
  303       rcc 4 -6.928 36.695   0 0 3.66  1.13  $ detector 3 top
  304       rcc -4 -6.928 36.695  0 0 3.66  1.13  $ detector 4 top
  305       rcc -8 0 36.695       0 0 3.66  1.13  $ detector 5 top
  306       rcc -4 6.928 36.695   0 0 3.66  1.13  $ detector 6 top
c
c
c Detector Anode
c need to find the actual thickness of the anode
c Knoll original radius 0.008
  401       rcc 4 6.928 0.55   0 0 35.9  0.008  $detector 1 anode
  402       rcc 8 0 0.55       0 0 35.9  0.008  $detector 2 anode
  403       rcc 4 -6.928 0.55  0 0 35.9  0.008  $detector 3 anode
  404       rcc -4 -6.928 0.55 0 0 35.9  0.008  $detector 4 anode
  405       rcc -8 0 0.55      0 0 35.9  0.008  $detector 5 anode
  406       rcc -4 6.928 0.55  0 0 35.9  0.008  $detector 6 anode
c
  507       rcc 0 0 14.7       0 0 5.72  0.8509    $large vial outer
  508       rcc 0 0 15.1       0 0 2.2   0.4826    $bottom small vial
  509       rcc 0 0 17.3      0 0 1.38   0.4826    $top small vial solution
  510       rcc 0 0 18.7       0 0  0.82 0.4826    $air in the top vial
c
c
c Container & Paraffin
  901       rcc 0 0 0          0 0 34    15        $container outside
  902       rcc 0 0 0.5        0 0 33.5  14.5      $paraffin outside
  903       rcc 0 0 -20        0 0 64    35        $air around container
c
c Sample Tubing
  801       rcc 0 0 0.5        0 0 43    1.3       $PE tubing outer diameter bottom
  882       rcc 0 0 20.42      0 0 22.58 0.8509
  802       rcc 0 0 0.5        0 0 14.2    0.8509    $PE tubing inner diameter
c still need to add in the outer big container
c Wooden stand
  803       rcc 0 0 -5         0  0 4.9    18      $wooden stand
c

c MATERIAL AND SOURCE CARDS
c
```

```
mode  n h t
c
phys:n 3j 115 j j 2 -1
c Large biasing in the number of delayed neutrons produced
phys:h j j 0 8j
c Mix and match tables and physics models for proton interactions
c
TOTNU
dbcn 28j 1 3j 1 $DN on,
c ------------------------------------------------------------------------
c                          MATERIAL DEFINITIONS
c
c .70c for calculations at room temperature
c negative fractions indicate wgt%
c
m1000    2003.70c              1  $He-3
c
m2000    24050.70c      -0.00793  $Steel, Stainless 304,
         24052.70c     -0.159032
         24053.70c     -0.018378
         24054.70c     -0.004661
         25055.70c         -0.02
         26054.70c     -0.039605
         26056.70c     -0.638496
         26057.70c      -0.01488
         26058.70c     -0.002019
         28058.70c     -0.064024
         28060.70c     -0.025321
         28061.70c     -0.001115
         28062.70c     -0.003599
         28064.70c     -0.000942
c
m3000    7014.70c      -0.755636    $Air at sea level
         8016.70c      -0.231475
        18036.70c        -3.9e-5
        18038.70c          -8e-6
        18040.70c      -0.012842
c
m4000    1001.70c      -0.143716    $Polyethylene
         6000.70c      -0.856284
mt4000   poly.10t                   $S(alpha,beta)
c
m5000
c $U-233, dissolved in HNO3/H20 mixture
c
c Fissile mass of experimental runs has been increased 1000x
c This has been accounted for in the corresponding experimental data
```

```
         92233.70c       -1.63e-3
         1001.70c        -0.107
         8016.70c        -0.87837
         7014.70c        -0.013
mt5000  lwtr.10t                    $Light water scattering
c
m6000    1001.70c      -0.148605    $Paraffin
         6000.70c      -0.851395
mt6000   poly.10t
c
m7000    1001.70c      -0.057889    $wooden stand
         6000.70c      -0.482667
         8016.70c      -0.459440
c data cards
nps 1e8
c
c ----------------------------------
c                       SOURCE DEFINITION
c
c This file is specifically tailored to 1.63 ug U-233 sample irradiated for 60s in a
c thermal flux of 5.57e11 cm^-2 s^-1
sdef pos=0 0 18.4 par=n cel=49
     Rad=D2 Ext=D3 AXS 0 1 0
     erg=0.0253e-6 wgt=3.68e13 tme=d1
c
c from 0 - 60s MCNP models the neutron flux in the SLOWPOKE-2 reactor.
c
c The paraffin is not present in the experiments and therefore a correction to
c the neutron flux has been applied.
c
c A weight of 3.68e13 applied to the source yields the
c measured neutron flux of 5.57e11 1/cm^2/s in vial
c
c                           Time (sh) in sixty 1s interval
si1 H
      0e8 1e8 2e8 3e8 4e8 5e8 6e8 7e8 8e8 9e8
      10e8 11e8 12e8 13e8 14e8 15e8 16e8 17e8 18e8 19e8
      20e8 21e8 22e8 23e8 24e8 25e8 26e8 27e8 28e8 29e8
      30e8 31e8 32e8 33e8 34e8 35e8 36e8 37e8 38e8 39e8
      40e8 41e8 42e8 43e8 44e8 45e8 46e8 47e8 48e8 49e8
      50e8 51e8 52e8 53e8 54e8 55e8 56e8 57e8 58e8 59e8 60e8
sp1
      0 1 1 1 1 1 1 1 1
      1 1 1 1 1 1 1 1 1
      1 1 1 1 1 1 1 1 1
      1 1 1 1 1 1 1 1 1
      1 1 1 1 1 1 1 1 1
```

```
      1 1 1 1 1 1 1 1 1 1 1
c
c Source defined inside the PE vial
si2 H 0 0.4826
sp2 -21 1
si3 -1.1 1.1
c                          PARTICLE TIME, WEIGHT and ENERGY CUT-OFFS
cut:n 2400e8 j 0 0
cut:h 2400e8 1e-3 1e-6
cut:t 2400e8 1e-3 1e-6
c
F4:n 49
T4: 0 179i 180e8 2400e8
c The neutron flux in cell 49 should be 5.5 cm^-2 s^-1 for the first sixty
c seconds of the run
c Energy Deposition in the detector as a function time
F6:h,t (14 24 34 44 54 64)
t6 60e8 179i 240e8 2400e8
```

The MCNP6 output files for the ACE and CINDER cases are U233ACE.mpi.o and U233CINDER.mpi.o, respectively, both presented in the subdirectory /DELAYED_PARTICLES/Templetes/LINUX/.

Note that the experimental values are tabulated as a function of time after irradiation; the duration of the irradiation was 60 s. We need to properly account for this while extracting the corresponding values from the F6 tally of the MCNP6 output files tabulated as functions of the time (in shakes; 1 shake = 10^{-8} s) from the beginning of irradiation. In other words, we need to account that the time of 6E+9 shakes in the F6 tally corresponds to the time of 0 seconds after irradiation. Extracted from the MCNP6 output files, values of the energy deposition in units of [MeV/g/s] as functions of the time after irradiation are presented in the files U233ACE.mpi.dat and U233CINDER.mpi.dat of the subdirectory */DELAYED_PARTICLES/Experimental_data/RMC_U233/, for the case of ACE and CINDER calculations, respectively.

We plotted our results with xmgrace in two different ways: using a linear scale for the y-axis (used for F6 [MeV/g/s]) and a logarithmic one. Templates for the linear and logarithmic plotting with xmgrace are presented in the files U233ACE.lin.fig and U233ACE.log.fig, respectively, of the same subdirectory. The pdf files of figures for the linear and logarithmic plotting are U233ACE.lin.pdf and U233ACE.log.pdf, respectively, both presented in the same subdirectory, and also shown below in Fig. 24.

From the results presented in Fig. 24 we can see a reasonable good agreement between the measured data and our MCNP6 calculations, both using the ACE data libraries and the CINDER tables, especially if we plot our results in linear scale, as shown on the left plot. However, if we plot exactly the same results using a logarithmic scale, we can see a much bigger disagreement between the measured data and the CINDER results than for the MCNP6 results obtained using the ACE data libraries, for times after irradiation longer than $\sim$ 120 seconds. Such "increase of disagreement" between calculations and measured data depending on how we present our results is quite interesting and instructive: If we would like to stress the disagreement, we would use only the logarithmic scale, while if we were not completely honest

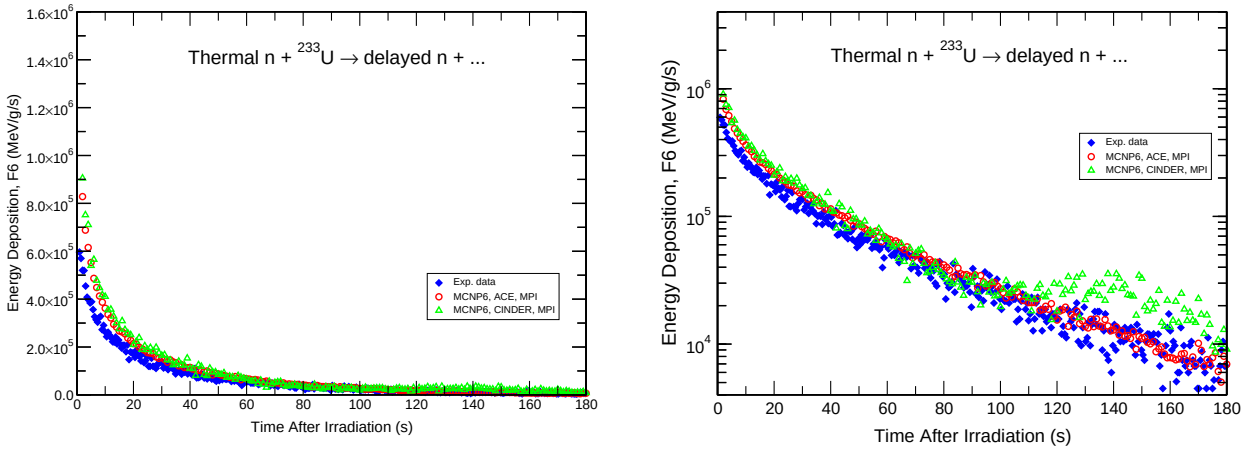

Figure 24: The same as in Fig. 23, but for delay neutrons from ^{233}U.

and would like to hide our disagreement for some reasons, we would chose the linear scale. This is why we need to be very carefully when comparing measured data and calculations, using as many as possible different representations, formats, and scales.

A special analysis by Dr. Michael R. James, his colleagues, and by Madison Sellers of the reason for the observed disagreement between the MCNP6 results obtained with the ACE data library and with CINDER tables, as can be seen in Fig. 24, has shown that it was caused by a too coarse time bins structure in CINDER tables used by MCNP6. Mike James fixed this deficiency in MCNP6 recently. Now, the calculations with CINDER agree much better with the measured data and with the results obtained using the ACE data library, as we were informed very recently in a personal communication to us from Madison Sellers.

5.3. Pu239ACE and Pu239CINDER

This MCNP6 problem is to test the applicability of MCNP6 to describe delayed neutron emission from fission fragments for nuclear forensics applications pertaining to Special Nuclear Material (SNM) analysis. The Atomic Energy Act of 1954 defines special nuclear materials as plutonium, or uranium enriched in ^{233}U or ^{235}U. The current test-problem studies delayed neutron emission from ^{239}Pu, while the previous ones were dedicated to ^{235}U and ^{235}U.

SNM are tracked by international and national regulatory agencies, including the International Atomic Energy Agency. Since the early 1990s, nuclear material smuggling interceptions have been on the rise, and have included cases involving HEU, five of which occurred between July 2009 and June 2010 [82]. Delayed neutron counting (DNC) is a technique capable of determining the amount of fissile content in an unknown sample. Automated delayed neutron counting systems for mass determination of SNM are developed lately to enhance nuclear forensics capabilities [83].

To be specific, this problem calculates the energy deposition per proton/triton pair (tally F6) averaged over a cell used to simulate the detector of the DNC system commissioned at the Royal Military College of Canada (RMCC) from a sample containing U-233.

The experimental data for this problem were measured at RMCC by PhD student Madison Theresa Sellers with collaborators using the SLOWPOKE-2 reactor as a source of predominately thermal neutrons. Madison converted the measured count rates into units of MeV/g (for one

second interval) so that these values could be compared directly with the F6 tally results calculated by MCNP6. She kindly provided to us both the experimental values and the MCNP6 input files she used at RMCC to simulate her measurements. The publications [84] serve as current references for these measurements and simulations.

Experimental energy deposition in the detector in units of [MeV/g/s] are presented in the file Pu239.exp.dat of the subdirectory */DELAYED_PARTICLES/Experimental_data/RMC_Pu239/.

This test-problem is very similar to the previous ones on ^{235}U and ^{233}U, discussed above in sub-sections 5.1 and 5.2, but for completeness sake, we provide here all the details. We have calculated this problem on the **Turing** supercomputer at LANL with MPI, as described in Sec. 2, using 4 nodes, 64 processors, in two different ways: accounting for up to 15 biased delayed neutrons from ACE data libraries (using 1015 for the 4th parameter of the phys:n card of the MCNP6 input file) and up to 15 biased delayed neutrons from CINDER tables (using 115 for the 4th parameter of the phys:n card of the MCNP6 input file). The input files for the ACE and CINDER calculations are **Pu239ACE** and **Pu239CINDER**, respectively, both presented in the subdirectory /DELAYED_PARTICLES/Inputs/ and both shown below:

Pu239ACE:

```
Modeling Delayed Neutron Emissions in RMC's DNC System
c Winter 2012
c
c --------------GEOMETRY----------------
c
c He-3 Detectors
c
c   Detector 1
   10  1000 -0.000511 -201 601 401          $Fill Gas
       imp:n=1 imp:e=1 imp:h=1 imp:t=1 imp:p=1
c
   11  2000    -7.92    201 -101 401        $S.S Container
       imp:n=1 imp:e=1 imp:h=1 imp:t=1 imp:p=1
c
c   Detector 2
   20  1000 -0.000511 -202 602 402
       imp:n=1 imp:e=1 imp:h=1 imp:t=1 imp:p=1
c
   21  2000    -7.92    202 -102 402
       imp:n=1 imp:e=1 imp:h=1 imp:t=1 imp:p=1
c
c   Detector 3
   30  1000 -0.000511 -203 603 403
       imp:n=1 imp:e=1 imp:h=1 imp:t=1 imp:p=1
c
   31  2000    -7.92    203 -103 403
       imp:n=1 imp:e=1 imp:h=1 imp:t=1 imp:p=1
c
c   Detector 4
```

```
   40  1000 -0.000511 -204 604 404
       imp:n=1 imp:e=1 imp:h=1 imp:t=1 imp:p=1
c
   41  2000    -7.92    204 -104 404
       imp:n=1 imp:e=1 imp:h=1 imp:t=1 imp:p=1
c
c   Detector 5
   50  1000 -0.000511 -205 605 405
       imp:n=1 imp:e=1 imp:h=1 imp:t=1 imp:p=1
c
   51  2000    -7.92    205 -105 405
       imp:n=1 imp:e=1 imp:h=1 imp:t=1 imp:p=1
c
c   Detector 6
   60  1000 -0.000511 -206 606 406
       imp:n=1 imp:e=1 imp:h=1 imp:t=1 imp:p=1
c
   61  2000    -7.92    206 -106 406
       imp:n=1 imp:e=1 imp:h=1 imp:t=1 imp:p=1
c
c Active Fill Area of Detectors
c
  14  1000 -0.000511 -601 401
       imp:n=1 imp:e=1 imp:h=1 imp:t=1 imp:p=1
c
  24  1000 -0.000511 -602 402
       imp:n=1 imp:e=1 imp:h=1 imp:t=1 imp:p=1
c
  34  1000 -0.000511 -603 403
       imp:n=1 imp:e=1 imp:h=1 imp:t=1 imp:p=1
c
  44  1000 -0.000511 -604 404
       imp:n=1 imp:e=1 imp:h=1 imp:t=1 imp:p=1
c
  54  1000 -0.000511 -605 405
       imp:n=1 imp:e=1 imp:h=1 imp:t=1 imp:p=1
c
  64  1000 -0.000511 -606 406
       imp:n=1 imp:e=1 imp:h=1 imp:t=1 imp:p=1
c
c
c Detector Anodes
c
   12    2000   -7.92            -401        $D1 anode
         imp:n=1 imp:e=1 imp:h=1 imp:t=1 imp:p=1
   22     2000  -7.92            -402        $D2 anode
         imp:n=1 imp:e=1 imp:h=1 imp:t=1 imp:p=1
```

```
   32     2000   -7.92           -403        $D3 anode
          imp:n=1 imp:e=1 imp:h=1 imp:t=1 imp:p=1
   42     2000   -7.92           -404        $D4 anode
          imp:n=1 imp:e=1 imp:h=1 imp:t=1 imp:p=1
   52     2000    -7.92          -405        $D5 anode
          imp:n=1 imp:e=1 imp:h=1 imp:t=1 imp:p=1
   62     2000   -7.92           -406        $D6 anode
          imp:n=1 imp:e=1 imp:h=1 imp:t=1 imp:p=1
c
c Detector Tops
c
   13  2000      -7.92  -301 401       $D1 top
         imp:n=1 imp:e=1 imp:h=1 imp:t=1 imp:p=1
   23  2000      -7.92  -302 402       $D2 top
         imp:n=1 imp:e=1 imp:h=1 imp:t=1 imp:p=1
   33  2000      -7.92  -303 403       $D3 top
         imp:n=1 imp:e=1 imp:h=1 imp:t=1 imp:p=1
   43  2000      -7.92  -304 404       $D4 top
         imp:n=1 imp:e=1 imp:h=1 imp:t=1 imp:p=1
   53  2000      -7.92  -305 405      $D5 top
         imp:n=1 imp:e=1 imp:h=1 imp:t=1 imp:p=1
   63  2000      -7.92  -306 406      $D6 top
         imp:n=1 imp:e=1 imp:h=1 imp:t=1 imp:p=1
c
c Outside Container
c
   37  2000      -7.92  -901 902                                $container outside
       imp:n=1 imp:e=1 imp:h=1 imp:t=1 imp:p=1
   17  6000      -0.93  -902 -901 101 102 103 104 105
                         106 301 302 303 304 305 306 801      $paraffin moderator
       imp:n=1 imp:e=1 imp:h=1 imp:t=1 imp:p=1
   18  3000     -0.0013 -903 901 902 801 101 102 103 104 105 106
                         301 302 303 304 803                  $air surrounding apparatus
                         305 306
       imp:n=1 imp:e=1 imp:h=1 imp:t=1 imp:p=1
   19     0               903                                 $geometry void
       imp:n=0 imp:e=0 imp:h=0 imp:t=0 imp:p=0
c
c Poly tubing
c
   27  4000   -0.94     -801 802 -903  882                    $PE outer tubing
       imp:n=1 imp:e=1 imp:h=1 imp:t=1 imp:p=1
   28  3000   -0.0013     -802 -903 507 508 509                $PE inner tubing
       imp:n=1 imp:e=1 imp:h=1 imp:t=1 imp:p=1
   29  3000   -0.0013     -882 -903 507 508 509                $PE inner tubing
       imp:n=1 imp:e=1 imp:h=1 imp:t=1 imp:p=1
c Pe vials
```

```
   47  4000   -0.94     -507 508 509  510                    $large vial
       imp:n=1 imp:e=1 imp:h=1 imp:t=1 imp:p=1
   48  3000   -0.0013        -508                            $bottom smaller vial
       imp:n=1 imp:e=1 imp:h=1 imp:t=1 imp:p=1
   49  5000  -0.9977 -509                                    $top smaller vial solution
       imp:n=1 imp:e=1 imp:h=1 imp:t=1 imp:p=1
c  59  3000  -0.0013        -510   509                      $air in top smaller vial
c       imp:n=1 imp:e=1 imp:h=1 imp:t=1 imp:p=1
   57  7000   -0.689   -803                                  $wooden stand
        imp:n=1 imp:e=1 imp:h=1 imp:t=1 imp:p=1
   58  3000    -0.0013     -510
         imp:n=1 imp:e=1 imp:h=1 imp:t=1 imp:p=1
c

c SURFACE CARDS
c These surfaces are used for active part inside detectors
  601       rcc 4 6.928 2.4939      0 0 31.115     2.45 $active area in detector 1
  602       rcc 8 0 2.4939          0 0 31.115     2.45 $active area in detector 2
  603       rcc 4 -6.928 2.4939     0 0 31.115     2.45 $active area in detector 3
  604       rcc -4 -6.928 2.4939    0 0 31.115     2.45 $active area in detector 4
  605       rcc -8 0 2.4939         0 0 31.115     2.45 $active area in detector 5
  606       rcc -4 6.928 2.4939     0 0 31.115     2.45 $active area in detector 6
c
  101       rcc 4 6.928 0.5    0 0 36.195    2.54  $ detector 1 outside
  102       rcc 8 0 0.5        0 0 36.195    2.54  $ detector 2 outside
  103       rcc 4 -6.928 0.5   0 0 36.195    2.54  $ detector 3 outside
  104       rcc -4 -6.928 0.5  0 0 36.195    2.54  $ detector 4 outside
  105       rcc -8 0 0.5       0 0 36.195    2.54  $ detector 5 outside
  106       rcc -4 6.928 0.5   0 0 36.195    2.54  $ detector 6 outside
c
c Inside the Detectors
c
c
  201       rcc 4 6.928 0.5889   0 0 36.0172  2.4511  $ detector 1 fill
  202       rcc 8 0 0.5889       0 0 36.0172  2.4511  $ detector 2 fill
  203       rcc 4 -6.928 0.5889  0 0 36.0172  2.4511  $ detector 3 fill
  204       rcc -4 -6.928 0.5889 0 0 36.0172  2.4511  $ detector 4 fill
  205       rcc -8 0 0.5889      0 0 36.0172  2.4511  $ detector 5 fill
  206       rcc -4 6.928 0.5889  0 0 36.0172  2.4511  $ detector 6 fill
c
c Detector Tops
c
  301       rcc 4 6.928 36.695    0 0 3.66  1.13  $ detector 1 top
  302       rcc 8 0 36.695        0 0 3.66  1.13  $ detector 2 top
  303       rcc 4 -6.928 36.695   0 0 3.66  1.13  $ detector 3 top
  304       rcc -4 -6.928 36.695  0 0 3.66  1.13  $ detector 4 top
  305       rcc -8 0 36.695       0 0 3.66  1.13  $ detector 5 top
```

```
  306       rcc -4 6.928 36.695   0 0 3.66  1.13  $ detector 6 top
c
c
c Detector Anode
c need to find the actual thickness of the anode
c Knoll original radius 0.008
  401       rcc 4 6.928 0.55   0 0 35.9  0.008  $detector 1 anode
  402       rcc 8 0 0.55       0 0 35.9  0.008  $detector 2 anode
  403       rcc 4 -6.928 0.55  0 0 35.9  0.008  $detector 3 anode
  404       rcc -4 -6.928 0.55 0 0 35.9  0.008  $detector 4 anode
  405       rcc -8 0 0.55      0 0 35.9  0.008  $detector 5 anode
  406       rcc -4 6.928 0.55  0 0 35.9  0.008  $detector 6 anode
c
  507       rcc 0 0 14.7       0 0 5.72  0.8509    $large vial outer
  508       rcc 0 0 15.1       0 0 2.2   0.4826    $bottom small vial
  509       rcc 0 0 17.3      0 0 1.38   0.4826    $top small vial solution
  510       rcc 0 0 18.7       0 0  0.82 0.4826    $air in the top vial
c
c
c Container & Paraffin
  901       rcc 0 0 0          0 0 34    15        $container outside
  902       rcc 0 0 0.5        0 0 33.5  14.5      $paraffin outside
  903       rcc 0 0 -20        0 0 64    35        $air around container
c
c Sample Tubing
  801       rcc 0 0 0.5        0 0 43    1.3       $PE tubing outer diameter bottom
  882       rcc 0 0 20.42      0 0 22.58 0.8509
  802       rcc 0 0 0.5        0 0 14.2    0.8509    $PE tubing inner diameter
c still need to add in the outer big container
c Wooden stand
  803       rcc 0 0 -5         0  0 4.9    18      $wooden stand
c

c MATERIAL AND SOURCE CARDS
c
mode  n h t
c
phys:n 3j 1015 j j 2 -1
c Large biasing in the number of delayed neutrons produced
phys:h j j 0 8j
c Mix and match tables and physics models for proton interactions
c
TOTNU
dbcn 28j 1 3j 1 $DN on,
c ---------------------------------------------------------------------
c                          MATERIAL DEFINITIONS
c
```

```
c .70c for calculations at room temperature
c negative fractions indicate wgt%
c
m1000    2003.70c              1  $He-3
c
m2000    24050.70c      -0.00793  $Steel, Stainless 304,
         24052.70c     -0.159032
         24053.70c     -0.018378
         24054.70c     -0.004661
         25055.70c         -0.02
         26054.70c     -0.039605
         26056.70c     -0.638496
         26057.70c      -0.01488
         26058.70c     -0.002019
         28058.70c     -0.064024
         28060.70c     -0.025321
         28061.70c     -0.001115
         28062.70c     -0.003599
         28064.70c     -0.000942
c
m3000    7014.70c      -0.755636    $Air at sea level
         8016.70c      -0.231475
        18036.70c        -3.9e-5
        18038.70c          -8e-6
        18040.70c      -0.012842
c
m4000    1001.70c      -0.143716    $Polyethylene
         6000.70c      -0.856284
mt4000   poly.10t                   $S(alpha,beta)
c
m5000
c $Plutonium-239, dissolved in HNO3/H20 mixture
c Fissile mass of experimental runs has been increased 1000x
c This has been accounted for in the corresponding experimental data
         94239.70c       -0.88e-3
         1001.70c        -0.107
         8016.70c        -0.87912
         7014.70c        -0.013
mt5000  lwtr.10t                    $Light water scattering
c
m6000    1001.70c      -0.148605    $Paraffin
         6000.70c      -0.851395
mt6000   poly.10t
c
m7000    1001.70c      -0.057889    $wooden stand
         6000.70c      -0.482667
         8016.70c      -0.459440
```

```
c data cards
nps 1e8
c
c ----------------------------------
c                      SOURCE DEFINITION
c
c This file is specifically tailored to 0.88 ug Pu-239 sample irradiated for 60s in a
c thermal flux of 5.57e11 cm^-2 s^-1
sdef pos=0 0 18.4 par=n cel=49
     Rad=D2 Ext=D3 AXS 0 1 0
     erg=0.0253e-6 wgt=3.68e13 tme=d1
c
c from 0 - 60s MCNP models the neutron flux in the SLOWPOKE-2 reactor.
c
c The paraffin is not present in the experiments and therefore a correction to
c the neutron flux has been applied.
c
c A weight of 3.68e13 applied to the source yields the
c measured neutron flux of 5.57e11 1/cm^2/s in vial
c
c                          Time (sh) in sixty 1s interval
si1 H
      0e8 1e8 2e8 3e8 4e8 5e8 6e8 7e8 8e8 9e8
      10e8 11e8 12e8 13e8 14e8 15e8 16e8 17e8 18e8 19e8
      20e8 21e8 22e8 23e8 24e8 25e8 26e8 27e8 28e8 29e8
      30e8 31e8 32e8 33e8 34e8 35e8 36e8 37e8 38e8 39e8
      40e8 41e8 42e8 43e8 44e8 45e8 46e8 47e8 48e8 49e8
      50e8 51e8 52e8 53e8 54e8 55e8 56e8 57e8 58e8 59e8 60e8
sp1
      0 1 1 1 1 1 1 1 1
      1 1 1 1 1 1 1 1 1 1
      1 1 1 1 1 1 1 1 1 1
      1 1 1 1 1 1 1 1 1 1
      1 1 1 1 1 1 1 1 1 1
      1 1 1 1 1 1 1 1 1 1 1
c
c Source defined inside the PE vial
si2 H 0 0.4826
sp2 -21 1
si3 -1.1 1.1
c                        PARTICLE TIME, WEIGHT and ENERGY CUT-OFFS
cut:n 2400e8 j 0 0
cut:h 2400e8 1e-3 1e-6
cut:t 2400e8 1e-3 1e-6
c
F4:n 49
T4: 0 179i 180e8 2400e8
```

```
c The neutron flux in cell 49 should be 5.5 cm^-2 s^-1 for the first sixty
c seconds of the run
c Energy Deposition in the detector as a function time
F6:h,t (14 24 34 44 54 64)
t6 60e8 179i 240e8 2400e8
```

Pu239CINDER:

```
Modeling Delayed Neutron Emissions in RMC's DNC System
c Winter 2012
c
c --------------GEOMETRY---------------
c
c He-3 Detectors
c
c   Detector 1
   10  1000 -0.000511 -201 601 401          $Fill Gas
       imp:n=1 imp:e=1 imp:h=1 imp:t=1 imp:p=1
c
   11  2000    -7.92    201 -101 401        $S.S Container
       imp:n=1 imp:e=1 imp:h=1 imp:t=1 imp:p=1
c
c   Detector 2
   20  1000 -0.000511 -202 602 402
       imp:n=1 imp:e=1 imp:h=1 imp:t=1 imp:p=1
c
   21  2000    -7.92    202 -102 402
       imp:n=1 imp:e=1 imp:h=1 imp:t=1 imp:p=1
c
c   Detector 3
   30  1000 -0.000511 -203 603 403
       imp:n=1 imp:e=1 imp:h=1 imp:t=1 imp:p=1
c
   31  2000    -7.92    203 -103 403
       imp:n=1 imp:e=1 imp:h=1 imp:t=1 imp:p=1
c
c   Detector 4
   40  1000 -0.000511 -204 604 404
       imp:n=1 imp:e=1 imp:h=1 imp:t=1 imp:p=1
c
   41  2000    -7.92    204 -104 404
       imp:n=1 imp:e=1 imp:h=1 imp:t=1 imp:p=1
c
c   Detector 5
   50  1000 -0.000511 -205 605 405
       imp:n=1 imp:e=1 imp:h=1 imp:t=1 imp:p=1
c
```

```
   51  2000    -7.92    205 -105 405
       imp:n=1 imp:e=1 imp:h=1 imp:t=1 imp:p=1
c
c   Detector 6
   60  1000 -0.000511 -206 606 406
       imp:n=1 imp:e=1 imp:h=1 imp:t=1 imp:p=1
c
   61  2000    -7.92    206 -106 406
       imp:n=1 imp:e=1 imp:h=1 imp:t=1 imp:p=1
c
c Active Fill Area of Detectors
c
  14  1000 -0.000511 -601 401
       imp:n=1 imp:e=1 imp:h=1 imp:t=1 imp:p=1
c
  24  1000 -0.000511 -602 402
       imp:n=1 imp:e=1 imp:h=1 imp:t=1 imp:p=1
c
  34  1000 -0.000511 -603 403
       imp:n=1 imp:e=1 imp:h=1 imp:t=1 imp:p=1
c
  44  1000 -0.000511 -604 404
       imp:n=1 imp:e=1 imp:h=1 imp:t=1 imp:p=1
c
  54  1000 -0.000511 -605 405
       imp:n=1 imp:e=1 imp:h=1 imp:t=1 imp:p=1
c
  64  1000 -0.000511 -606 406
       imp:n=1 imp:e=1 imp:h=1 imp:t=1 imp:p=1
c
c
c Detector Anodes
c
   12    2000   -7.92            -401        $D1 anode
         imp:n=1 imp:e=1 imp:h=1 imp:t=1 imp:p=1
   22     2000  -7.92            -402        $D2 anode
         imp:n=1 imp:e=1 imp:h=1 imp:t=1 imp:p=1
   32     2000   -7.92           -403        $D3 anode
         imp:n=1 imp:e=1 imp:h=1 imp:t=1 imp:p=1
   42     2000   -7.92           -404        $D4 anode
         imp:n=1 imp:e=1 imp:h=1 imp:t=1 imp:p=1
   52     2000    -7.92          -405        $D5 anode
         imp:n=1 imp:e=1 imp:h=1 imp:t=1 imp:p=1
   62     2000   -7.92           -406        $D6 anode
         imp:n=1 imp:e=1 imp:h=1 imp:t=1 imp:p=1
c
c Detector Tops
```

```
c
   13  2000      -7.92  -301 401       $D1 top
         imp:n=1 imp:e=1 imp:h=1 imp:t=1 imp:p=1
   23  2000      -7.92  -302 402       $D2 top
         imp:n=1 imp:e=1 imp:h=1 imp:t=1 imp:p=1
   33  2000      -7.92  -303 403       $D3 top
         imp:n=1 imp:e=1 imp:h=1 imp:t=1 imp:p=1
   43  2000      -7.92  -304 404       $D4 top
         imp:n=1 imp:e=1 imp:h=1 imp:t=1 imp:p=1
   53  2000      -7.92  -305 405      $D5 top
         imp:n=1 imp:e=1 imp:h=1 imp:t=1 imp:p=1
   63  2000      -7.92  -306 406      $D6 top
         imp:n=1 imp:e=1 imp:h=1 imp:t=1 imp:p=1
c
c Outside Container
c
   37  2000      -7.92  -901 902                              $container outside
       imp:n=1 imp:e=1 imp:h=1 imp:t=1 imp:p=1
   17  6000      -0.93  -902 -901 101 102 103 104 105
                         106 301 302 303 304 305 306 801      $paraffin moderator
       imp:n=1 imp:e=1 imp:h=1 imp:t=1 imp:p=1
   18  3000     -0.0013 -903 901 902 801 101 102 103 104 105 106
                         301 302 303 304 803                  $air surrounding apparatus
                         305 306
       imp:n=1 imp:e=1 imp:h=1 imp:t=1 imp:p=1
   19     0               903                                 $geometry void
       imp:n=0 imp:e=0 imp:h=0 imp:t=0 imp:p=0
c
c Poly tubing
c
   27  4000   -0.94     -801 802 -903  882                    $PE outer tubing
       imp:n=1 imp:e=1 imp:h=1 imp:t=1 imp:p=1
   28  3000   -0.0013     -802 -903 507 508 509               $PE inner tubing
       imp:n=1 imp:e=1 imp:h=1 imp:t=1 imp:p=1
   29  3000   -0.0013     -882 -903 507 508 509               $PE inner tubing
       imp:n=1 imp:e=1 imp:h=1 imp:t=1 imp:p=1
c Pe vials
   47  4000   -0.94     -507 508 509  510                     $large vial
       imp:n=1 imp:e=1 imp:h=1 imp:t=1 imp:p=1
   48  3000   -0.0013        -508                             $bottom smaller vial
       imp:n=1 imp:e=1 imp:h=1 imp:t=1 imp:p=1
   49  5000  -0.9977 -509                                     $top smaller vial solution
       imp:n=1 imp:e=1 imp:h=1 imp:t=1 imp:p=1
c  59  3000  -0.0013        -510   509                       $air in top smaller vial
c       imp:n=1 imp:e=1 imp:h=1 imp:t=1 imp:p=1
   57  7000   -0.689   -803                                   $wooden stand
        imp:n=1 imp:e=1 imp:h=1 imp:t=1 imp:p=1
```

```
   58  3000    -0.0013     -510
         imp:n=1 imp:e=1 imp:h=1 imp:t=1 imp:p=1
c

c SURFACE CARDS
c These surfaces are used for active part inside detectors
  601       rcc 4 6.928 2.4939      0 0 31.115     2.45 $active area in detector 1
  602       rcc 8 0 2.4939          0 0 31.115     2.45 $active area in detector 2
  603       rcc 4 -6.928 2.4939     0 0 31.115     2.45 $active area in detector 3
  604       rcc -4 -6.928 2.4939    0 0 31.115     2.45 $active area in detector 4
  605       rcc -8 0 2.4939         0 0 31.115     2.45 $active area in detector 5
  606       rcc -4 6.928 2.4939     0 0 31.115     2.45 $active area in detector 6
c
  101       rcc 4 6.928 0.5    0 0 36.195    2.54  $ detector 1 outside
  102       rcc 8 0 0.5        0 0 36.195    2.54  $ detector 2 outside
  103       rcc 4 -6.928 0.5   0 0 36.195    2.54  $ detector 3 outside
  104       rcc -4 -6.928 0.5  0 0 36.195    2.54  $ detector 4 outside
  105       rcc -8 0 0.5       0 0 36.195    2.54  $ detector 5 outside
  106       rcc -4 6.928 0.5   0 0 36.195    2.54  $ detector 6 outside
c
c Inside the Detectors
c
c
  201       rcc 4 6.928 0.5889   0 0 36.0172  2.4511  $ detector 1 fill
  202       rcc 8 0 0.5889       0 0 36.0172  2.4511  $ detector 2 fill
  203       rcc 4 -6.928 0.5889  0 0 36.0172  2.4511  $ detector 3 fill
  204       rcc -4 -6.928 0.5889 0 0 36.0172  2.4511  $ detector 4 fill
  205       rcc -8 0 0.5889      0 0 36.0172  2.4511  $ detector 5 fill
  206       rcc -4 6.928 0.5889  0 0 36.0172  2.4511  $ detector 6 fill
c
c Detector Tops
c
  301       rcc 4 6.928 36.695    0 0 3.66  1.13  $ detector 1 top
  302       rcc 8 0 36.695        0 0 3.66  1.13  $ detector 2 top
  303       rcc 4 -6.928 36.695   0 0 3.66  1.13  $ detector 3 top
  304       rcc -4 -6.928 36.695  0 0 3.66  1.13  $ detector 4 top
  305       rcc -8 0 36.695       0 0 3.66  1.13  $ detector 5 top
  306       rcc -4 6.928 36.695   0 0 3.66  1.13  $ detector 6 top
c
c
c Detector Anode
c need to find the actual thickness of the anode
c Knoll original radius 0.008
  401       rcc 4 6.928 0.55   0 0 35.9  0.008  $detector 1 anode
  402       rcc 8 0 0.55       0 0 35.9  0.008  $detector 2 anode
  403       rcc 4 -6.928 0.55  0 0 35.9  0.008  $detector 3 anode
  404       rcc -4 -6.928 0.55 0 0 35.9  0.008  $detector 4 anode
```

```
  405       rcc -8 0 0.55      0 0 35.9  0.008  $detector 5 anode
  406       rcc -4 6.928 0.55  0 0 35.9  0.008  $detector 6 anode
c
  507       rcc 0 0 14.7       0 0 5.72  0.8509    $large vial outer
  508       rcc 0 0 15.1       0 0 2.2   0.4826    $bottom small vial
  509       rcc 0 0 17.3      0 0 1.38   0.4826    $top small vial solution
  510       rcc 0 0 18.7       0 0  0.82 0.4826    $air in the top vial
c
c
c Container & Paraffin
  901       rcc 0 0 0          0 0 34    15        $container outside
  902       rcc 0 0 0.5        0 0 33.5  14.5      $paraffin outside
  903       rcc 0 0 -20        0 0 64    35        $air around container
c
c Sample Tubing
  801       rcc 0 0 0.5        0 0 43    1.3       $PE tubing outer diameter bottom
  882       rcc 0 0 20.42      0 0 22.58 0.8509
  802       rcc 0 0 0.5        0 0 14.2    0.8509    $PE tubing inner diameter
c still need to add in the outer big container
c Wooden stand
  803       rcc 0 0 -5         0  0 4.9    18      $wooden stand
c

c MATERIAL AND SOURCE CARDS
c
mode  n h t
c
phys:n 3j 115 j j 2 -1
c Large biasing in the number of delayed neutrons produced
phys:h j j 0 8j
c Mix and match tables and physics models for proton interactions
c
TOTNU
dbcn 28j 1 3j 1 $DN on,
c ---------------------------------------------------------------------
c                          MATERIAL DEFINITIONS
c
c .70c for calculations at room temperature
c negative fractions indicate wgt%
c
m1000    2003.70c              1  $He-3
c
m2000    24050.70c      -0.00793  $Steel, Stainless 304,
         24052.70c     -0.159032
         24053.70c     -0.018378
         24054.70c     -0.004661
         25055.70c         -0.02
```

```
         26054.70c     -0.039605
         26056.70c     -0.638496
         26057.70c      -0.01488
         26058.70c     -0.002019
         28058.70c     -0.064024
         28060.70c     -0.025321
         28061.70c     -0.001115
         28062.70c     -0.003599
         28064.70c     -0.000942
c
m3000    7014.70c      -0.755636    $Air at sea level
         8016.70c      -0.231475
        18036.70c        -3.9e-5
        18038.70c          -8e-6
        18040.70c      -0.012842
c
m4000    1001.70c      -0.143716    $Polyethylene
         6000.70c      -0.856284
mt4000   poly.10t                   $S(alpha,beta)
c
m5000
c $Plutonium-239, dissolved in HNO3/H20 mixture
c Fissile mass of experimental runs has been increased 1000x
c This has been accounted for in the corresponding experimental data
         94239.70c       -0.88e-3
         1001.70c        -0.107
         8016.70c        -0.87912
         7014.70c        -0.013
mt5000  lwtr.10t                    $Light water scattering
c
m6000    1001.70c      -0.148605    $Paraffin
         6000.70c      -0.851395
mt6000   poly.10t
c
m7000    1001.70c      -0.057889    $wooden stand
         6000.70c      -0.482667
         8016.70c      -0.459440
c data cards
nps 1e8
c
c ----------------------------------
c                     SOURCE DEFINITION
c
c This file is specifically tailored to 0.88 ug Pu-239 sample irradiated for 60s in a
c thermal flux of 5.57e11 cm^-2 s^-1
sdef pos=0 0 18.4 par=n cel=49
     Rad=D2 Ext=D3 AXS 0 1 0
```

```
     erg=0.0253e-6 wgt=3.68e13 tme=d1
c
c from 0 - 60s MCNP models the neutron flux in the SLOWPOKE-2 reactor.
c
c The paraffin is not present in the experiments and therefore a correction to
c the neutron flux has been applied.
c
c A weight of 3.68e13 applied to the source yields the
c measured neutron flux of 5.57e11 1/cm^2/s in vial
c
c                          Time (sh) in sixty 1s interval
si1 H
      0e8 1e8 2e8 3e8 4e8 5e8 6e8 7e8 8e8 9e8
      10e8 11e8 12e8 13e8 14e8 15e8 16e8 17e8 18e8 19e8
      20e8 21e8 22e8 23e8 24e8 25e8 26e8 27e8 28e8 29e8
      30e8 31e8 32e8 33e8 34e8 35e8 36e8 37e8 38e8 39e8
      40e8 41e8 42e8 43e8 44e8 45e8 46e8 47e8 48e8 49e8
      50e8 51e8 52e8 53e8 54e8 55e8 56e8 57e8 58e8 59e8 60e8
sp1
      0 1 1 1 1 1 1 1 1
      1 1 1 1 1 1 1 1 1 1
      1 1 1 1 1 1 1 1 1 1
      1 1 1 1 1 1 1 1 1 1
      1 1 1 1 1 1 1 1 1 1
      1 1 1 1 1 1 1 1 1 1 1
c
c Source defined inside the PE vial
si2 H 0 0.4826
sp2 -21 1
si3 -1.1 1.1
c                        PARTICLE TIME, WEIGHT and ENERGY CUT-OFFS
cut:n 2400e8 j 0 0
cut:h 2400e8 1e-3 1e-6
cut:t 2400e8 1e-3 1e-6
c
F4:n 49
T4: 0 179i 180e8 2400e8
c The neutron flux in cell 49 should be 5.5 cm^-2 s^-1 for the first sixty
c seconds of the run
c Energy Deposition in the detector as a function time
F6:h,t (14 24 34 44 54 64)
t6 60e8 179i 240e8 2400e8
```

The MCNP6 output files for the ACE and CINDER cases are Pu239ACE.mpi.o and Pu239CINDER.mpi.o, respectively, both presented in the subdirectory /DELAYED_PARTICLES/Templetes/LINUX/.

Note that the experimental values are tabulated as a function of time after irradiation;

the duration of the irradiation was 60 s. We need to properly account for this while extracting the corresponding values from the F6 tally of the MCNP6 output files tabulated as functions of the time (in shakes; 1 shake = 10^{-8} s) from the beginning of irradiation. In other words, we need to account that the time of 6E+9 shakes in the F6 tally corresponds to the time of 0 seconds after irradiation. Extracted from the MCNP6 output files, values of the energy deposition in units of [MeV/g/s] as functions of the time after irradiation are presented in the files Pu239ACE.mpi.dat and Pu239CINDER.mpi.dat of the subdirectory */DELAYED_PARTICLES/Experimental_data/RMC_Pu239/, for the case of ACE and CINDER calculations, respectively.

We plotted our results with xmgrace in two different ways: using a linear scale for the y-axis (used for F6 [MeV/g/s]) and a logarithmic one. Templates for the linear and logarithmic plotting with xmgrace are presented in the files Pu239ACE.lin.fig and Pu239ACE.log.fig, respectively, of the same subdirectory. The pdf files of figures for the linear and logarithmic plotting are Pu239ACE.lin.pdf and Pu239ACE.log.pdf, respectively, both presented in the same subdirectory, and also shown below in Fig. 25.

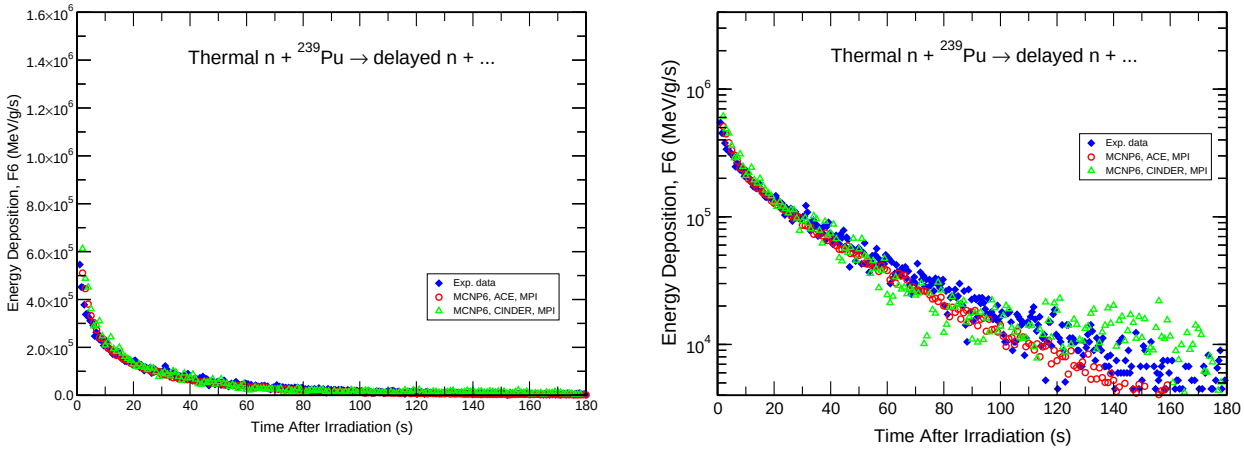

Figure 25: The same as in Fig. 23, but for delay neutrons from ^{239}Pu.

From the results presented in Fig. 25 we can see a reasonable good agreement between the measured data and our MCNP6 calculations, both using the ACE data libraries and the CINDER tables, especially if we plot our results in linear scale, as shown on the left plot. However, if we plot exactly the same results using a logarithmic scale, we can see a much bigger disagreement between the measured data and the CINDER results than for the MCNP6 results obtained using the ACE data libraries, for times after irradiation longer than $\sim$ 120 seconds. Such "increase of disagreement" between calculations and measured data depending on how we present our results is quite interesting and instructive: We need to be very carefully when comparing measured data and calculations, using as many as possible different representations, formats, and scales.

A special analysis by Dr. Michael R. James, his colleagues, and by Madison Sellers of the reason for the observed disagreement between the MCNP6 results obtained with the ACE data library and with CINDER tables, as can be seen in Fig. 25, has shown that it was caused by a too coarse time bins structure in CINDER tables used by MCNP6. Mike James fixed this deficiency in MCNP6 recently. Now, the calculations with CINDER agree much better with the measured data and with the results obtained using the ACE data library, as we were informed very recently in a personal communication to us from Madison Sellers.

5.4. heu_point + tally_u.dat (+ inp_3e8)

This MCNP6 problem is to test the applicability of MCNP6 in applications on active interrogation using intermediate-energy ($\sim$ 1 GeV) beams of protons. To be specific, this problem calculates delayed neutron emission [angular distributions as well as integrated spectra and total multiplicities] (tally F1 - number of delayed neutrons crossing a surface) as a function of time after irradiating a thin highly enriched uranium (HEU) target bombarded with an 800-MeV proton beam.

The experimental data relevant to this test-problem (more exactly, delayed neutron cross sections from thin targets of a variety of isotopes, including ^{235}U and ^{238}U of interest to our current problem) were measured with short single pulses of up to 10^{11} 800 MeV-protons at the LANSCE accelerator of LANL. Measured delayed neutron cross sections from thin targets of many different isotopes bombarded with 800-MeV protons are presented in several figures of the papers [85].

We have extracted the ^{235}U data from an enlarged version of Fig. 6 of the second paper in Ref. [85], and the data on ^{238}U, from enlarged Fig. 7 of the same paper. The ^{235}U and ^{238}U experimental delayed neutron emission integrated spectra in units of [mb/sec] are presented in the files p800U235dnexp.dat and p800U238dnexp.dat of the subdirectory */DELAYED_PARTICLES/Experimental_data/p800HEU_DN/.

We calculated this problem on the **Turing** supercomputer at LANL with MPI, using 4 nodes, 64 processors, as described in Sec. 2. Because the cross sections of delayed neutron emission from our reactions are quite small, in order to get the desired uncertainty (nps=3×10^8), we had to calculate our problem in several steps, with the "continue" option, as described in Sec. 2.

The main MCNP6 input file for this problem is **heu_point**. It uses a separate little file with the specification of the tallies we want to calculate, named **tally_u.dat**. Finally, during the second, third, and forth runs with the "continue" option, we used a two-line auxiliary input file called **inp_3e8**. All these files are presented in subdirectory /DELAYED_PARTICLES/Inputs/ and are also shown below.

heu_point:

```
Cross sections 'point' method, uranium
1 18 -18.239 -1   imp:n,p,h=1
2 0         1 -2  imp:n,p,h=1
3 0           2  imp:n,p,h=0

1 so .01
2 so      100.0

mode n p h / z | d t s a
sdef par=h erg=800.0 vec 0 0 1 dir 1
lca 7j -2 1
c phys:n 800 j j -101 j 1     $ delayed analog sampling models $Old, MCNPX
phys:n 800 j j -101 j      $ delayed analog sampling models
cut:n j j 0 0
phys:p j j j -1 j -101      $ analog photonuclear & multigoup delayed gammas
```

```
cut:p j j 0 0
phys:h 800
phys:/ 400
phys:| 400
phys:d 100
phys:t 100
phys:s 100
phys:a 100
act nonfiss=all
c
print
c nps 2100000000
c nps 10000000
nps 50000000
prdmp j 5000000 1 2 5000000
c
c   HEU + NB, density = 18.239 gm/cc
m18
       plib=04p  nlib=70c hlib=25h  pnlib=71u elib =03e
       92235 .93 92238 .07
mx18:n   j j
mx18:p   j j
mx18:h   model model
DBCN 28j 1
c
read file tally_u.dat
```

tally_u.dat:

```
c
*c0 175 165 155 145 125 105 85 65 45 35 25 15 5 0 t
c
f1:n 1
ft1 frv 0 0 1
fq1 c t
t1 0.0 0.5e8 249i 250.5e8
c
f11:n 1
e11 1e-8 99log 800.0
ft11 frv 0 0 1
fq11 c e
c
f111:n 1
t111 1 199log 1e13
ft111 frv 0 0 1
fq111 c t
c
```

```
f1111:n 1
t1111 0.0 1e8 1e10
ft1111 frv 0 0 1
e1111 0.0 99i 3.0
c
f21:n 1
e21 0.0 99i 800.0
ft21 tag 3
fu21 -1 92235.00000 92238.00000 10 T
c ft21 frv 0 0 1
fq21 c e
t21 0 1e8 1e15
c21 0 1
c
f2:n 1
ft2 frv 0 0 1
fq2 c t
t2 0.0 0.5e8 249i 250.5e8
c
c



tmesh
rmesh11:h flux
cora11 -10.0 99i 10.0
corb11 -10 10
corc11 -10.0 99i 10.0
endmd
```

inp_3e8:

```
continue
nps 300000000
```

The first MCNP6 output file for this problem is heu_point.mpi.o. The last (fourth) output file is heu_point.mpi_c3.o. They are both presented, together with the final MCTAL file, heu_point.mpi_c3.m, in subdirectory */DELAYED_PARTICLES/Templetes/LINUX/.

Note that the experimental delayed neutron spectra are presented in [mb/sec] as functions of the time after irradiation in seconds. The F1 tally in this problem provides us integrated (and angular) delayed neutron currents as functions of time in shakes (1 shake = $10^{-}8$ sec). Extracted from the MCNP6 output file values of integrated (total) delayed neutron current (F1) for our HEU material, in units of [neutrons/shake] (and per incident proton), as a function of the time (already converted in seconds) are copied in the file heu-800M6.dat presented in subdirectory */DELAYED_PARTICLES/Experimental_data/p800HEU_DN/.

We plotted our results with xmgrace. A template for plotting our MCNP6 HEU results together with the experimental data for ^{235}U and ^{238}U is presented in the file p800HEU_dn.fig

of the same subdirectory. The pdf file of the figure with comparison of our MCNP6 HEU calculation with available measurements for ^{235}U and ^{238}U is p800HEU_dn.pdf, presented in the same subdirectory, and also shown below in Fig. 26.

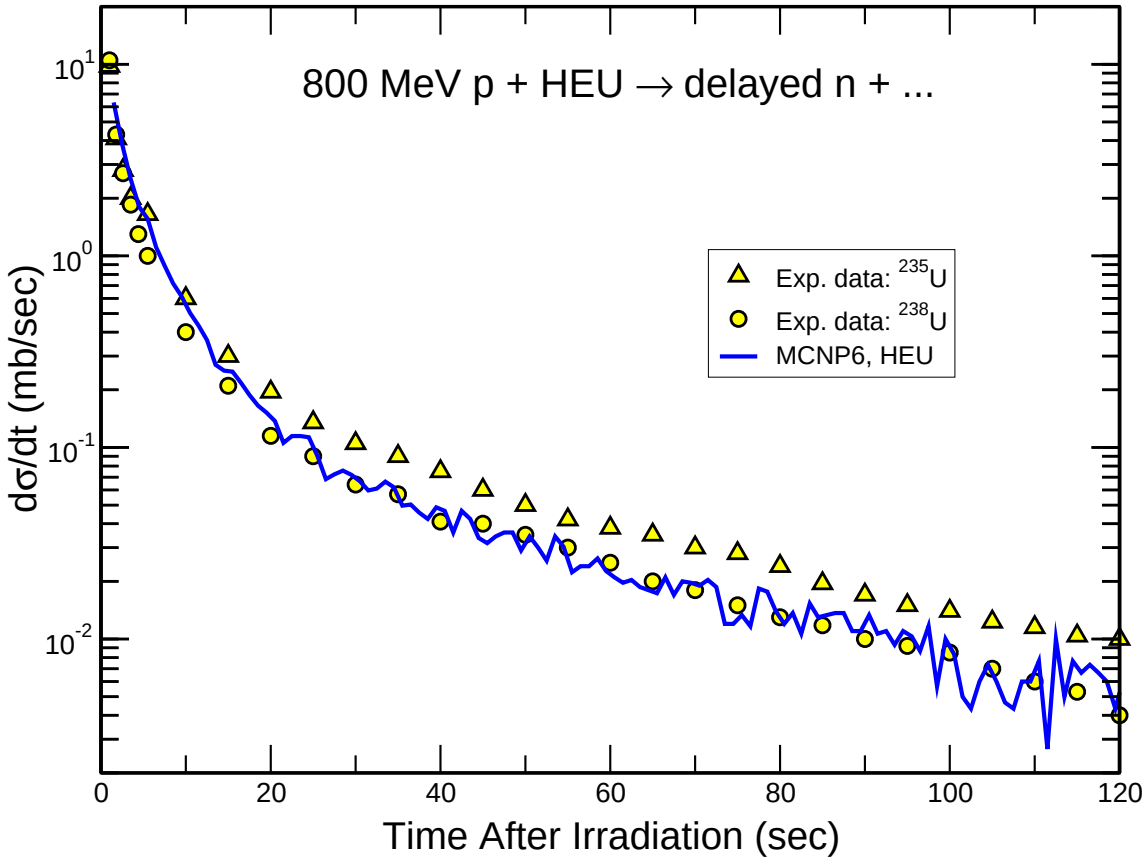

Figure 26: Comparison of the measured [85] time-dependent delayed-neutron production cross sections for the 800 MeV protons on ^{235}U and ^{238}U with calculations by MCNP6 in parallel, with MPI, for a HEU target, as indicated in legend.

From Fig. 26, we can see that, just as expected, MCNP6 predicts delayed neutron emission from our HEU target bombarded with 800 MeV protons in good agreement with the measured data for ^{235}U and ^{238}U [85]. This fact may serve as a proof that MCNP6 can be an useful tool in applications on active interrogation using intermediate-energy ($\sim$ 1 GeV) beams of protons.

6. Testing the Production Release Version 1 of MCNP6

In his Section we V&V the latest, first production, version of MCNP6 [6] on 26 reactions induced by intermediate-energy protons and heavy-ions on various targets. These 26 examples are grouped in 5 test-problems described in the following subsections.

6.1. ^{12}C + ^{9}Be at 0.3, 0.6, 0.95, and 1.993 GeV/A

This MCNP6 problem is to test the applicability of MCNP6 using the LAQGSM03.03 event generator to describe double-differential spectra of protons at 3.5 degrees produced in interactions of ^{12}C ions with ^{9}Be at 0.3, 0.6, 0.95, and 1.992 GeV/nucleon. Production of high-energy particles in forward directions is of interest for many different applications, like shielding for missions in space, at accelerators, medical (cancer treatment with heavy ions), etc. Such reactions are also of a great academic interest in studying the production in inverse kinematics of the so-called "cumulative particles", i.e., energetic particles in the kinematic region forbidden in the interaction of free nucleons.

The experimental data for this problem were measured at the accelerator complex TWAC (Tera-Watt Accumulator) ITEP, Russia and are published in the form of invariant cross sections at incident energies of 0.6, 0.95, and 1.992 GeV/nucleon in Figs. 3-5 of the paper [86]. Dr. Anna Petrovna Krutenkova, the main co-author of this work, kindly converted the invariant spectra into more convenient to us double-differential spectra and sent us numerical values of their data at the published incident energies of 0.6, 0.95, and 1.992 GeV/nucleon, as well as preliminary results on yet unpublished measurements at 0.3 GeV/nucleon.

Experimental proton spectra at 0.3, 0.6, 0.95, and 1.992 GeV/A are presented here in the files 300-exp.dat, 600-exp.dat, 950-exp.dat, and 1992-exp.dat, respectively, in subdirectory */VALIDATION_LAQGSM/Experimental_data/C12+Be9_p/.

We calculate with MCNP6 these spectra using the GENXS option in parallel, with MPI as well as, for comparison, in a sequential mode. The main MCNP6 input files at 0.3, 0.6, 0.95, and 1.992 GeV/A are **C300Be**, **C600Be**, **C950Be**, and **C1992Be.long**, respectively. For the second input files required by the GENXS option we use the same file **inxc88** at 0.3, 0.6, 0.95 GeV/A and the file **inxc99** at 1.992 GeV/A. Note that because in the */VALIDATION_LAQGSM/Inputs/ subdirectory there is already another **inxc88** file from the LAQGSM test-problem # 18, we renamed our present "inxc88" file here as "inx88a"; users can rename it back to "inxc88" in their working directory, while running these examples, in order to get an output file looking exactly as our. All input files are presented in subdirectory */VALIDATION_LAQGSM/Inputs/. We list below only **C1992Be.long**, **inxc99**, and **inx88a**, as **C300Be**, **C600Be**, and **C950Be**, differ from **C1992Be.long** only by the values of the incident energy (in MeV), defined by parameter **erg** on the **sdef** card.

C1992Be.long:

```
MCNP6 test: p-spectra from 1.992 GeV C+Be by LAQGSM03.03
  1  1  1.0   -1 2 -3
  2  0        -4 (1:-2:3)
  3  0         4
```

```
c ------------------------------------------------------------
  1  cz  4.0
  2  pz  -1.0
  3  pz  1.0
  4  so  50.0

c ------------------------------------------------------------
dbcn 28j 1
  m1 04009  1.0
  sdef erg=23904 par=06012 dir=1 pos=0 0 0 vec 0 0 1
  imp:n 1 1 0
  imp:h 1 1 0
  phys:n 42008
  phys:h 42008
  phys:/ 42008
  phys:* 42008
  phys:z 42008
  phys:k 42008
  phys:? 42008
  phys:q 42008
  phys:g 42008
  phys:d 42008
  phys:t 42008
  phys:s 42008
  phys:a 42008
  phys:# 42008
  mode  n h / * z k ? q g d t s a #
LCA  2 1 5j -1 1j 1 66   $ use LAQGSM, nevtype = 6: LCA(11)=66        !!!
lcb  0 0 0 0 0 0
lea  2j 0
  tropt genxs inxc99 nreact on  nescat off
c ------------------------------------------------------------
  print 40 110 95
  nps 10000000
c  nps 700000
c  prdmp 2j -1
```

inxc99:

```
MCNP6 test: p-spectra from 1992 MeV C+Be by LAQGSM03.03
1 0 0 /
Cross Section Edit
200 -4 11 /
   1.     3.     5.     7.     9.    11.    13.    15.    17.    19.
  22.    27.    32.    37.    42.    47.    52.    57.    62.    67.
  72.    77.    82.    87.    92.    97.   105.   125.   135.   145.
 155.   165.   175.   185.   195.   205.   215.   225.   235.   245.
```

```
 255.   265.   275.   285.   295.   305.   315.   325.   335.   345.
 355.   365.   375.   385.   395.   405.   415.   425.   435.   445.
 455.   465.   475.   485.   495.   505.   515.   525.   535.   545.
 555.   565.   575.   585.   595.   605.   615.   625.   635.   645.
 655.   665.   675.   685.   695.   705.   715.   725.   735.   745.
 755.   765.   775.   785.   795.   805.   815.   825.   835.   845.
 855.   865.   875.   885.   895.   905.   915.   925.   935.   945.
 955.   965.   975.   985.   995.  1025.  1075.  1125.  1175.  1225.
1275.  1325.  1375.  1425.  1475.  1525.  1575.  1625.  1675.  1725.
1775.  1825.  1875.  1925.  1975.  2025.  2075.  2125.  2175.  2225.
2275.  2325.  2375.  2425.  2475.  2525.  2575.  2625.  2675.  2725.
2775.  2825.  2875.  2925.  2975.  3025.  3075.  3125.  3175.  3225.
3275.  3325.  3375.  3425.  3475.  3525.  3575.  3625.  3675.  3725.
3775.  3825.  3875.  3925.  3975.  4025.  4075.  4125.  4275.  4325.
4373.  4425.  4475.  4525.  4575.  4625.  4675.  4725.  4775.  4825.
4875.  4925.  4975.  5025.  5075.  5125.  5175.  5225.  5275.  5325. /
30. 6.5 0.5 0./
1 5 6 7 15 16 19 21 22 23 24 /
```

inx88a:

```
MCNP6 test: p-spectra from 0.3 - 2 GeV C+Be by LAQGSM03.03
1 0 0 /
Cross Section Edit
150 -4 11 /
   1.     3.     5.     7.     9.    11.    13.    15.    17.    19.
  22.    27.    32.    37.    42.    47.    52.    57.    62.    67.
  72.    77.    82.    87.    92.    97.   105.   125.   135.   145.
 155.   165.   175.   185.   195.   205.   215.   225.   235.   245.
 255.   265.   275.   285.   295.   305.   315.   325.   335.   345.
 355.   365.   375.   385.   395.   405.   415.   425.   435.   445.
 455.   465.   475.   485.   495.   505.   515.   525.   535.   545.
 555.   565.   575.   585.   595.   605.   615.   625.   635.   645.
 655.   665.   675.   685.   695.   705.   715.   725.   735.   745.
 755.   765.   775.   785.   795.   805.   815.   825.   835.   845.
 855.   865.   875.   885.   895.   905.   915.   925.   935.   945.
 955.   965.   975.   985.   995.  1025.  1075.  1125.  1175.  1225.
1275.  1325.  1375.  1425.  1475.  1525.  1575.  1625.  1675.  1725.
1775.  1825.  1875.  1925.  1975.  2025.  2075.  2125.  2175.  2225. /
30. 6.5 0.5 0./
1 5 6 7 15 16 19 21 22 23 24 /
```

Proton double-differential spectra calculated in a sequential mode by MCNP6 using LAQGSM03.03 with the GENXS option at 3.5 ± 3 degrees at 0.3, 0.6, 0.95, and 1.992 GeV/A are tabulated in units of [b/sr/MeV] in the 3d pairs of columns of the "proton production cross section" table of the MCNP6 output files C300Be.o, C600Be.o, C950Be.o, and C1992Be.long.o, respectively, presented in subdirectory */VALIDATION_LAQGSM/Templates/LINUX/ and are copied in

separate files 300-GENXS.dat, 600-GENXS.dat, 950-GENXS.dat, and 1992-GENXS.dat in subdirectory */VALIDATION_LAQGSM/Experimental_data/C12+Be9_p/, to make it easier plotting such spectra with xmgrace. Similar spectra calculated with MPI, as described in Sec. 2, are tabulated in similar tables of the output files C300Be.mpi.o, C600Be.mpi.o, 950Be.mpi.o, and C1992Be.long.mpi.o, respectively, and are copied here in separate files 300-GENXS.mpi.dat, 600-GENXS.mpi.dat, 950-GENXS.mpi.dat, and 1992-GENXS.long.mpi.dat, in the same subdirectories. All the output files are presented in subdirectory /VALIDATION_LAQGSM/Templates/LINUX/.

Besides the MCNP6 results, we show here for comparison also calculations by LAQGSM03.03 used as a stand alone code. Proton double-differential spectra at 3.5 ± 3 degrees at 0.3, 0.6, 0.95, and 1.992 GeV/A by LAQGSM03.03 used as a stand alone code are presented here in the files 300-L13.dat, 600-L13.dat, 950-L13.dat, and 1992-L13.dat, respectively.

The file C_Be_p_ITEP.MPI.fig is a template for plotting the proton spectra with xmgrace at all four incident energies. The pdf file of the figure with these spectra is C_Be_p_ITEP.MPI.pdf. It is provided in subdirectory */VALIDATION_LAQGSM/Experimental_data/C12+Be9_p/ and is shown below in Fig. 27.

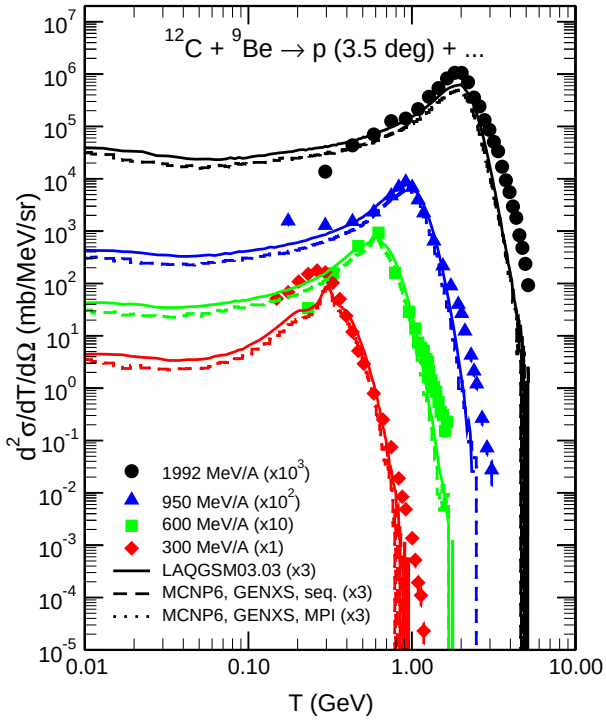

Figure 27: Comparison of the measured [86] proton spectra at 3.5 degrees from 0.3, 0.6, 0.95, and 1.993 GeV/nucleon ^{12}C + ^{9}Be reactions (symbols) with results by LAQGSM03.03 [16] used as a stand alone code (solid lines) and with calculations by the production version of MCNP6 [6], using the LAQGSM03.03 event generator, performed in sequential (dashed lines) and parallel, with MPI (dotted lines) modes using the GENXS option [63], as indicated in legend. Note that the experimental data were provided to us by the authors of the measurements [86] only in relative units; we had to multiply our LAQGSM03.03 and MCNP6 results calculated in absolute values by a factor of three, in order to get an agreement with the experimental data plotted in the relative units.

From Fig. 25 we can see that the production, Version 1, of MCNP6 using LAQGSM03.03 describes quite well the measured proton spectra at 600, 950, and 1992 MeV/A. As expected, the results obtained in a sequential run are practically the same as the ones obtained with MPI, with only some tiny differences in the last digits of some calculated values, not seen at all in the scale of our figure.

We see that the results by MCNP6 using LAQGSM03.03 calculated with the GENXS option [63] agree well with similar results obtained by LAQGSM03.03, but are a little lower (absolute normalization). This is OK and just as expected, because, as already explained above in Sec. 4.1, in the "Beta 3" version of MCNP6 [5], Dr. Richard E. Prael changed the absolute normalization of the nucleus-nucleus reactions calculated with the GENXS option [63], to match the approximation adopted by MCNPX [8]: It agrees quite well with the total reaction cross sections for nucleus-nucleus reactions predicted by LAQGSM03.03 [16] used as a stand alone code, but it is a little lower.

In the case of the incident energy of 300 MeV/nucleon, our results differ significantly from the preliminary and unpublished yet experimental data in the quasi-elastic peak. We do not understand yet this disagreement. One possible explanation could be that LAQGSM03.03 does not account for α-clustering of ^{12}C, and the clustering effects should be stronger al lower energies. But the difference we got looks too big to us to be explained only by the neglecting of clustering effects. We can not exclude that there are some problems with these preliminary and unpublished yet data; could be that in their "final" version, when published by their author, the measured data will look a little different and agree better with our predictions.

6.2. 230 MeV/A ^{4}He + Al and Cu

This MCNP6 problem is to test the applicability of MCNP6 using the LAQGSM03.03 event generator to describe neutron spectra from thin Al and Cu targets bombarded with 230 MeV/nucleon ^{4}He. Accurate prediction of such data is important for medical applications, space missions, and design and operation of rare isotope research facilities.

A direct "trigger" for this test-problem was the recent "Final Report on Benchmarking Heavy Ion Transport Codes FLUKA, HETC-HEDS, MARS15, MCNPX, and PHITS, DE-FG02-08ER41548, 2013" by R. M. Ronningen et al. [89] where not so good results by an old version MCNPX using an old version of LAQGSM were shown and much more worse results by a version of MARS15 using a version of LAQGSM were published: We need to check how the production version of MCNP6 using the latest version of our LAQGSM03.03 describes such reactions.

The experimental data for this problem were measured at the Heavy Ion Medical Accelerator in the Chiba (HIMAC) facility of the National Institute of Radiological Science (NIRS), Japan and are published as figures in the paper [87]. They are provided in a tabulated form on the CD-ROM accompanying the book by Takahashi Nakamura and Lawrence Heilbronn [88]; part of these data are also available already in EXFOR.

Experimental neutron spectra from Al at 5, 10, 20, 30, 40, 60, and 80 degrees are presented in subdirectory */VALIDATION_LAQGSM/Experimental_data/230He+AlCu/ in the files He230Al.5.e.dat, He230Al.10.e.dat, He230Al.20.e.dat, He230Al.30.e.dat, He230Al.40.e.dat, He230Al.60.e.dat, and He230Al.80.e.dat, respectively. We do not present there explicitly similar experimental data for the Cu target: They are included in the xmgrace template of the figure for Cu, He230Cu.fig, can by found in the cited above literature, and are shown in our

figures He230Cu.ps and He230AlCu.pdf.

We calculate with MCNP6 these spectra using the GENXS option in parallel, with MPI, as described in Sec. 2. The main MCNP6 input files for Al and Cu are **He230Al_n** and **He230Cu_n**, respectively. In our current calculations, we assume that the Al target consists of only ^{27}Al ions and the Cu one, of only ^{64}Cu ions: our past extensive experience shows that the spectra calculated from a Cu target with a natural abundance of ^{63}Cu and ^{65}Cu, would be almost the same as results for ^{64}Cu. For the second input files required by the GENXS option we use the same file, **in-xe**, for both Al and Cu. All input files are presented in subdirectory */VALIDATION_LAQGSM/Inputs/. We show below only the input files for Al, **He230Al_n** and **in-xe**,

He230Al_n:

```
MCNP6 test: p-spectra from 230 MeV/A He4 + Al27 by LAQGSM03.03
  1  1  1.0   -1 2 -3
  2  0        -4 (1:-2:3)
  3  0         4

c -------------------------------------------------------------
  1  cz  4.0
  2  pz  -1.0
  3  pz  1.0
  4  so  50.0

c -------------------------------------------------------------
dbcn 28j 1
  m1 13027  1.0
  sdef erg=920 par=02004 dir=1 pos=0 0 0 vec 0 0 1
  imp:n 1 1 0
  imp:h 1 1 0
  phys:n 53008
  phys:h 53000
  phys:/ 53008
  phys:* 53008
  phys:z 53008
  phys:k 53008
  phys:? 53008
  phys:q 53008
  phys:g 53008
  phys:d 53008
  phys:t 53008
  phys:s 53008
  phys:a 53008
  phys:# 53008
  mode  n h / * z k ? q g d t s a #
LCA  2 1 5j -1 1j 1 66   $ use LAQGSM, nevtype = 66: LCA(11)=66 !!!
lcb  0 0 0 0 0 0
```

```
lea  2j 0
  tropt genxs in-xe  nreact on  nescat off
c ------------------------------------------------------------
  print 40 110 95
  nps 10000000
c  nps 700000
c  prdmp 2j -1
```

in-xe:

```
MCNP6 test: n-spectra from 400 MeV/A Xe132 + Li7 by LAQGSM03.03
1 0 0 /
Cross Section Edit
150 -14 1 /
   1.     3.     5.     7.     9.    11.    13.    15.    17.    19.
  22.    27.    32.    37.    42.    47.    52.    57.    62.    67.
  72.    77.    82.    87.    92.    97.   105.   125.   135.   145.
 155.   165.   175.   185.   195.   205.   215.   225.   235.   245.
 255.   265.   275.   285.   295.   305.   315.   325.   335.   345.
 355.   365.   375.   385.   395.   405.   415.   425.   435.   445.
 455.   465.   475.   485.   495.   505.   515.   525.   535.   545.
 555.   565.   575.   585.   595.   605.   615.   625.   635.   645.
 655.   665.   675.   685.   695.   705.   715.   725.   735.   745.
 755.   765.   775.   785.   795.   805.   815.   825.   835.   845.
 855.   865.   875.   885.   895.   905.   915.   925.   935.   945.
 955.   965.   975.   985.   995.  1025.  1075.  1125.  1175.  1225.
1275.  1325.  1375.  1425.  1475.  1525.  1575.  1625.  1675.  1725.
1775.  1825.  1875.  1925.  1975.  2025.  2075.  2125.  2175.  2225.
2275.  2325.  2375.  2425.  2475.  2525.  2575.  2625.  2675.  2725. /
82.5 77.5 62.5 57.5 42.5 37.5 32.5 27.5 22.5 17.5 12.5 7.5 0.5 0./
1 /
```

as the file **He230Cu_n** for Cu differs from the shown above file **He230Al_n** only by the material card, **m1**, which for Cu looks like:

```
  m1 29064  1.0
```

Neutron double-differential spectra calculated by MCNP6 using LAQGSM03.03 with the GENXS option at 80, 60, and 40 ($\pm$2.5) degrees are tabulated in units of [b/sr/MeV] in the 2nd, 4th, and 6th pairs of columns of the first part of the "neutron production cross section" table (with the neutron energy tabulated in MeV in the 1st column) of the MCNP6 output files He230Al_n.mpi.o and He230Cu_n.mpi.o for Al and Cu, respectively. Similar neutron spectra at 30, 20, 10, and 5 ($\pm$2.5) degrees are tabulated in units of [b/sr/MeV] in the 1st, 3rd, 5th, and 6th pairs of columns of the second part of the same "neutron production cross section" table (with the neutron energy tabulated in MeV in the 1st column) of the MCNP6 output files He230Al_n.mpi.o and He230Cu_n.mpi.o for Al and Cu, respectively. Both output files are presented in subdirectory */VALIDATION_LAQGSM/Templates/LINUX/. For convenience of plotting these spectra with xmgrace, the MCNP6 neutron spectra at 5, 10, 20, 30, 40, 60, and 80

degrees are copied from the MCNP6 output files into separate files. We present in subdirectory */VALIDATION_LAQGSM/Experimental_data/230He+AlCu/ such files explicitly only for Al, they are: 5.genxs.dat, 10.genxs.dat, 20.genxs.dat, 30.genxs.dat, 40.genxs.dat, 60.genxs.dat, and 80.genxs.dat. We do not show there explicitly such files for Cu: They are included in the template for the xmgrace figure, He230Cu.fig.

Besides the MCNP6 results, we show here for comparison also calculations by LAQGSM03.03 used as a stand alone code. Neutron double-differential spectra at 5, 10, 20, 30, 40, 60, and 80 (±2.5) degrees by LAQGSM03.03 used as a stand alone code for Al are presented here in the files 5.laq.dat, 10.laq.dat, 20.laq.dat, 30.laq.dat, 40.laq.dat, 60.laq.dat, and 80.laq.dat. We do not show here explicitly such files for Cu: They are included in the template for the xmgrace figure, He230Cu.fig.

The files He230Al.fig and He230Cu.fig are templates for plotting the Al and Cu spectra with xmgrace at all seven angles for which we have data. The Postscript files produced by xmgrace, He230Al.ps and He230Cu.ps, are merged in a single figure with the LaTeX file He230AlCu.tex. The final pdf file from LaTeX with spectra for both Al and Cu targets is He230AlCu.pdf presented together with all other relevant files in subdirectory /VALIDATION_LAQGSM/Experimental_data/230He+AlCu/ and also shown below in Fig. 28.

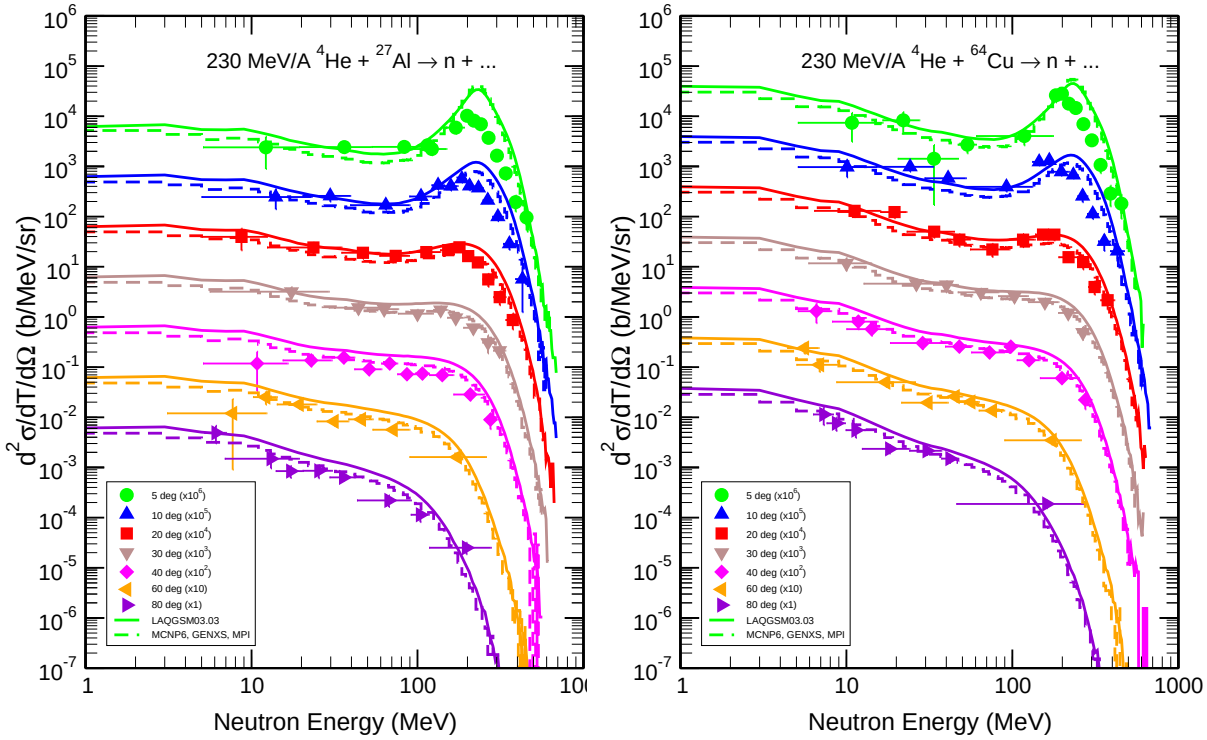

Figure 28: Comparison of the measured [87, 88] neutron spectra at 5, 10, 20, 30, 40, 60, and 80 degrees from 230 MeV/nucleon ^{4}He interactions with ^{27}Al and ^{64}Cu (symbols) with results by LAQGSM03.03 [16] used as a stand alone code (solid lines; 10^7 simulated inelastic events) and with calculations by the production version 1.0 of MCNP6 [6], using the LAQGSM03.03 event generator performed in parallel, with MPI (dashed lines; 10^7 simulated inelastic events) using the GENXS option [63], as indicated in legends.

From Fig. 28 we can see that the production version 1 of MCNP6 [6] using LAQGSM03.03 describes well the measured neutron spectra from these reactions.

We see that the results by MCNP6 using LAQGSM03.03 calculated with the GENXS option [63] agree well with similar results obtained by LAQGSM03.03 used as a stand alone code, but are a little lower (absolute normalization). This is OK and is just as expected, because, as already explained above in Sec. 4.1, in the "Beta 3" version of MCNP6 [5], Dr. Richard E. Prael changed the absolute normalization of the nucleus-nucleus reactions calculated with the GENXS option [63], to match the approximation adopted by MCNPX [8]: It agrees quite well with the total reaction cross sections for nucleus-nucleus reactions predicted by LAQGSM03.03 [16] used as a stand alone code, but it is a little lower.

Let us mention that similar good results for such spectra were obtained [90] very recently at Fermi National Accelerator Laboratory (FNAL) by Gudima, Mokhov, and Striganov with the MARS15 transport code using several (different from our LAQGSM03.03 [16]) versions of LAQGSM. Our current good results together with similar results from Ref. [90] make questionable the quite poor results by a version of LAQGSM used in a version of MCNPX and much worse results by MARS15 using a version of LAQGSM published in Ref. [89]. We can assume together with the authors of Ref. [90] that either some errors were present in the input files used in the calculations performed in Ref. [89], or the compilation of MARS15 was done on their machine with some problems, or some other problems were involved in obtaining the questionable results presented in Ref. [89]. On August 20, 2013, we have urged the authors of Ref. [89] to resolve this issue and somehow revise and re-distribute their Report to its readers/users.

6.3. 400 MeV/A ^{14}N, ^{84}Kr, and ^{132}Xe + Li, C, CH_2, Al, Cu, and Pb

This MCNP6 problem is to test the applicability of MCNP6 using the LAQGSM03.03 event generator to describe neutron spectra from thin Li, C, polyethylene (CH2), Al, Cu, and Pb targets bombarded with 400 MeV/A ^{14}N, ^{84}Kr, and ^{132}Xe beams. Accurate prediction of such data is important for medical applications, space missions, and design and operation of rare isotope research facilities.

A direct "trigger" for this test-problem was the recent "Final Report on Benchmarking Heavy Ion Transport Codes FLUKA, HETC-HEDS, MARS15, MCNPX, and PHITS, DE-FG02-08ER41548, 2013" by R. M. Ronningen et al. [89] where not so good results by an old version MCNPX using an old version of LAQGSM were shown and much more worse results by a version of MARS15 using a version of LAQGSM were published: We need to check how the production version of MCNP6 using the latest version of our LAQGSM03.03 describes such reactions.

The experimental data for this problem were measured at the Heavy Ion Medical Accelerator in the Chiba (HIMAC) facility of the National Institute of Radiological Science (NIRS), Japan and are published as figures in the paper [87]. They are provided in a tabulated form on the CD-ROM accompanying the book by Takahashi Nakamura and Lawrence Heilbronn [88]; part of these data are also available already in EXFOR.

Experimental n-spectra from C at 5, 10, 20, 30, 40, 60, and 80 degrees are presented in the files N400C.5.e.dat, N400C.10.e.dat, N400C.20.e.dat, N400C.30.e.dat, N400C.40.e.dat, N400C.60.e.dat, and N400C.80.e.dat, respectively. We do not present there explicitly similar experimental data for the Cu target for reactions induced by ^{14}N, and we do not show

explicitly data for all reactions induced by ^{84}Kr and ^{132}Xe ions: All these data are included in the xmgrace templates of the figures: N400Cu.fig, Kr400Li.fig, Kr400C.fig, Kr400CH2.fig, Kr400Al.fig, Kr400Cu.fig, Kr400Pb.fig, Xe400Li.fig, Xe400C.fig, Xe400CH2.fig, Xe400Al.fig, Xe400Cu.fig, and Xe400Pb.fig, can by found in the cited above literature, and are shown in figures N400Cu.ps, Kr400Li.ps, Kr400C.ps, Kr400CH2.ps, Kr400Al.ps, Kr400Cu.ps, Kr400Pb.ps, Xe400Li.ps, Xe400C.ps, Xe400CH2.ps, Xe400Al.ps, Xe400Cu.ps, Xe400Pb.ps, N400CCu.pdf, Kr400LiCCH2Al.pdf, Kr400CuPb.pdf, Xe400LiCCH2Al.pdf, and Xe400CuPb.pdf.

In our current calculations, we assume that the Li target consists of only ^{7}Li ions; C, of only ^{12}C; polyethylene consists of only CH_2; Al, of only ^{27}Al; Cu, of only ^{64}Cu; and Xe, of only ^{132}Xe. We calculate with MCNP6 these spectra using the GENXS option in parallel, with MPI. The main MCNP6 input files for reactions induced by N, Kr, and Xe are: **N400C_n**, **N400Cu_n**, **Kr400Li_n**, **Kr400C_n**, **Kr400CH2_n**, **Kr400Al_n**, **Kr400Cu_n**, **Kr400Pb_n**, **Xe400Li_n**, **Xe400C_n**, **Xe400CH2_n**, **Xe400Al_n**, **Xe400Cu_n**, and **Xe400Pb_n**, respectively. (The first letters in these names indicate the beam-ion, followed by "400", the incident energy in MeV/nucleon, followed by letters showing the target-ion, with the last portion as "_n", indicating that we calculate neutron spectra for these reactions; we keep the same notations for all the output files, which have by the end the letters "mpi", indicating that the calculations were dome with MPI, and a final "o", showing that these are output MCNP6 files.) For the second input files required by the GENXS option we use the same file, **in-xe**, for all three reactions. Because we calculated all these test-problems with good statistics, of 10^7 inelastic simulated events, even with MPI, using 64 processors, on the **Moonlight** supercomputer at LANL, we could not complete all the calculations in a single run in the frame of the 10 hours allocated for our interactive work. Therefore, the problems for Kr+Cu, Xe+Li, Xe+Cu, and Xe+Pb have been ran is several steps, using the "continue" option of MCNP6. In all these cases, we used a two-line auxiliary input file named, **inp_1e7**, to continue our MCNP6 calculations, as described in Sec. 2. All input files for these test-problems are presented in subdirectory /VALIDATION_LAQGSM/Inputs/. Below, we show explicitly only **N400C_n**, as **in-xe** was presented in the previous section, # 6.2, and the two-line input file needed for the "continue" run of MCNP6 was shown in Sec. 5.4. (Users of MCNP6 should change the **par** parameter on the **sdef** input card to specify another projectile, and the **m1** card, in order to chose another target nucleus; let us repeat here again that all input files for this test-problem are presented explicitly in subdirectory /VALIDATION_LAQGSM/Inputs/.)

N400C_n:

```
MCNP6 test: p-spectra from 400 MeV/A N14 + C12 by LAQGSM03.03
  1  1  1.0   -1 2 -3
  2  0        -4 (1:-2:3)
  3  0         4

c -------------------------------------------------------------
  1  cz  4.0
  2  pz  -1.0
  3  pz  1.0
  4  so  50.0

c -------------------------------------------------------------
```

```
dbcn 28j 1
  m1 06012  1.0
  sdef erg=5600 par=07014 dir=1 pos=0 0 0 vec 0 0 1
  imp:n 1 1 0
  imp:h 1 1 0
  phys:n 53008
  phys:h 53000
  phys:/ 53008
  phys:* 53008
  phys:z 53008
  phys:k 53008
  phys:? 53008
  phys:q 53008
  phys:g 53008
  phys:d 53008
  phys:t 53008
  phys:s 53008
  phys:a 53008
  phys:# 53008
  mode  n h / * z k ? q g d t s a #
LCA  2 1 5j -1 1j 1 66   $ use LAQGSM, nevtype = 66: LCA(11)=66 !!!
lcb  0 0 0 0 0 0
lea  2j 0
  tropt genxs in-xe  nreact on  nescat off
c ------------------------------------------------------------
  print 40 110 95
  nps 10000000
c  nps 700000
c  prdmp 2j -1
```

Neutron double-differential spectra calculated by MCNP6 using LAQGSM03.03 with the GENXS option at 80, 60, and 40 ($\pm$2.5) degrees are tabulated in units of [b/sr/MeV] in the 2nd, 4th, and 6th pairs of columns of the first part of the "neutron production cross section" tables (with the neutron energy tabulated in MeV in the 1st column) of the MCNP6 output files N400C_n.mpi.o, N400Cu_n.mpi.o, Kr400Li_n.mpi.o, Kr400C_n.mpi.o, Kr400CH2_n.mpi.o, Kr400Al_n.mpi.o, Kr400Cu_n.mpi.o, Kr400Pb_n.mpi.10.o (the final output file from the "continue" run; the initial output file for this reaction was Kr400Pb_n.mpi.o), Xe400Li_n.mpi.10.o (the final output file from the "continue" run; the initial output file for this reaction was Xe400Li_n.mpi.o), Xe400C_n.mpi.o, Xe400CH2_n.mpi.o, Xe400Al_n.mpi.o, Xe400Cu_n.mpi.10.o (the final output file from the "continue" run; the initial output file for this reaction was Xe400Cu_n.mpi.o), and Xe400Pb_n.mpi.10.o (the final output file from the "continue" run; the initial output file for this reaction was Xe400Pb_n.mpi.o), for reactions induced by N, Kr, and Xe, respectively.

Similar spectra at 30, 20, 10, and 5 ($\pm$2.5) degrees are tabulated in units of [b/sr/MeV] in the 1st, 3rd, 5th, and 6th pairs of columns of the second part of the same "neutron production cross section" tables (with the neutron energy tabulated in MeV in the 1st column)

of the same MCNP6 output files. All output files are presented in subdirectory */VALIDATION_LAQGSM/Templates/LINUX/.

For convenience of plotting these spectra with xmgrace, the MCNP6 neutron spectra at 5, 10, 20, 30, 40, 60, and 80 degrees are copied from the MCNP6 output files into separate files. We present in subdirectory /VALIDATION_LAQGSM/Experimental_data/400NKrXe+LiCCH2AlCuPb/ explicitly such files only for N+C, they are: 5.genxs.dat, 10.genxs.dat, 20.genxs.dat, 30.genxs.dat, 40.genxs.dat, 60.genxs.dat, and 80.genxs.dat. We do not show there explicitly such files for other reactions: They are included in the templates for the xmgrace figures, N400Cu.fig, Kr400Li.fig, Kr400C.fig, Kr400CH2.fig, Kr400Al.fig, Kr400Cu.fig, Kr400Pb.fig, Xe400Li.fig, Xe400C.fig, Xe400CH2.fig, Xe400Al.fig, Xe400Cu.fig, and Xe400Pb.fig.

Besides the MCNP6 results, we show there for comparison also calculations by LAQGSM03.03 used as a stand alone code. Neutron double-differential spectra at 5, 10, 20, 30, 40, 60, and 80 (±2.5) degrees by LAQGSM03.03 used as a stand alone code for N+C are presented there in the files 5.laq.dat, 10.laq.dat, 20.laq.dat, 30.laq.dat, 40.laq.dat, 60.laq.dat, and 80.laq.dat. We do not show there explicitly such files for other reactions: They are all included in the template for the xmgrace figures listed above.

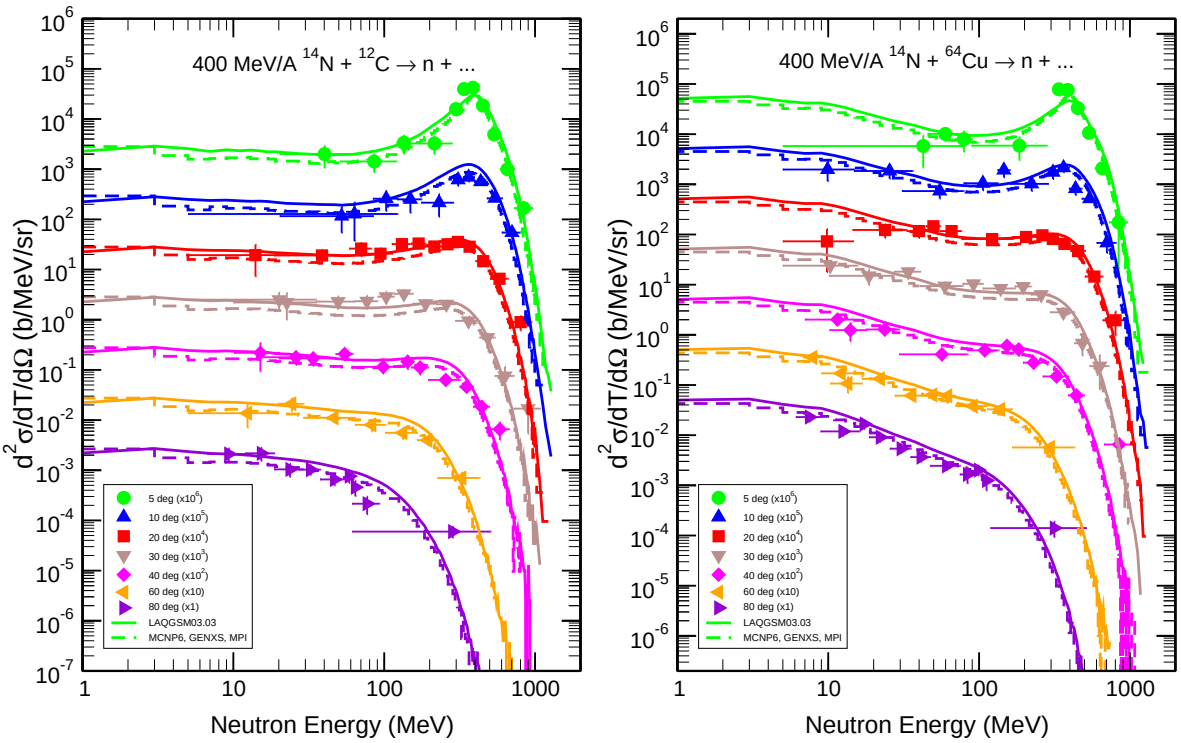

Figure 29: The same as in Fig. 28, but for interactions of 400 MeV/nucleon ^{14}N with ^{12}C and ^{64}Cu.

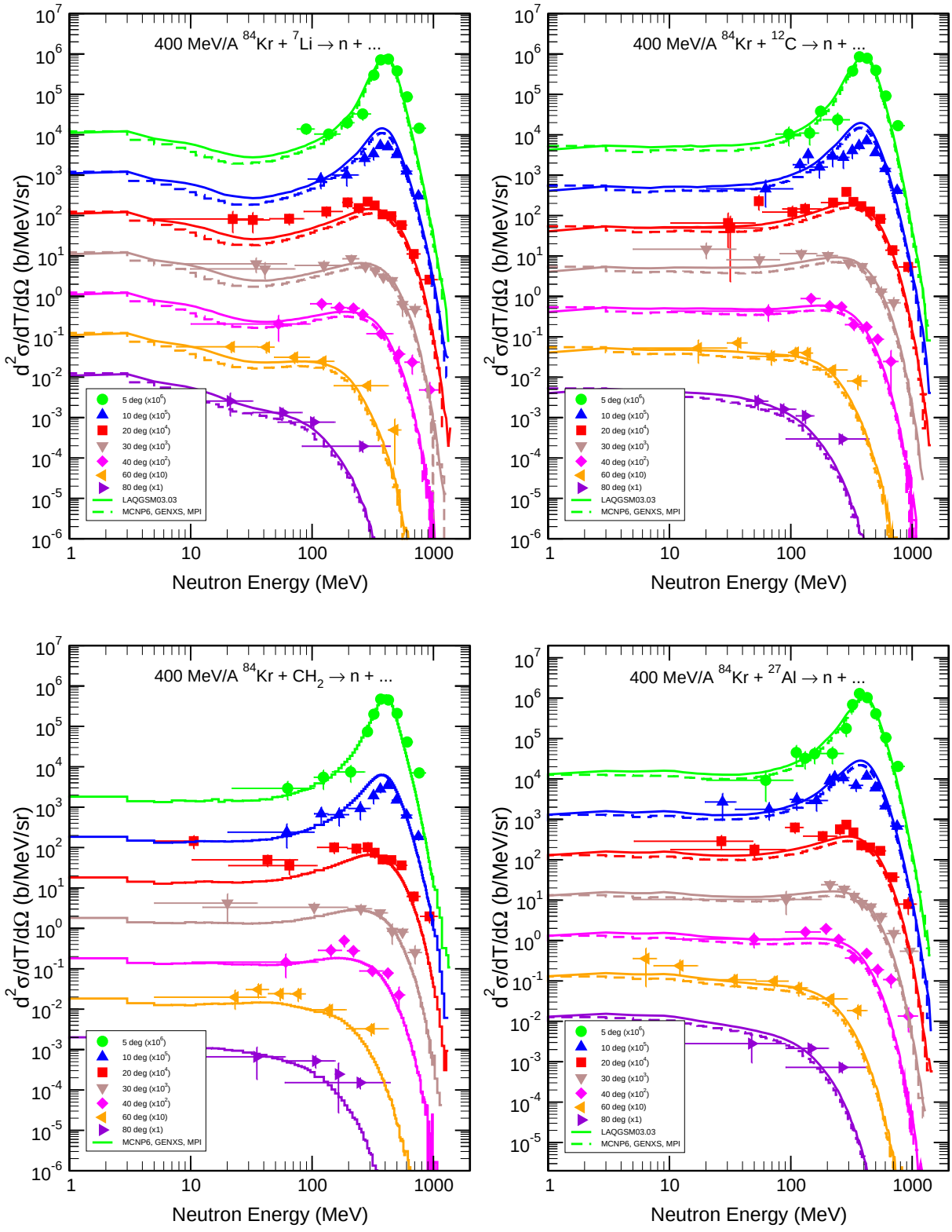

Figure 30: The same as in Fig. 28, but for interactions of 400 MeV/nucleon ^{84}Kr with ^{7}Li, ^{12}C, polyethylene (CH$_2$), and ^{27}Al. Note that LAQGSM03.03 used as a stand alone code does not allow us to calculate reactions on targets composed of several different isotopes in a single run; therefore, for CH$_2$, we show here only results by MCNP6, which allows us to simulate interactions with targets of arbitrary compositions.

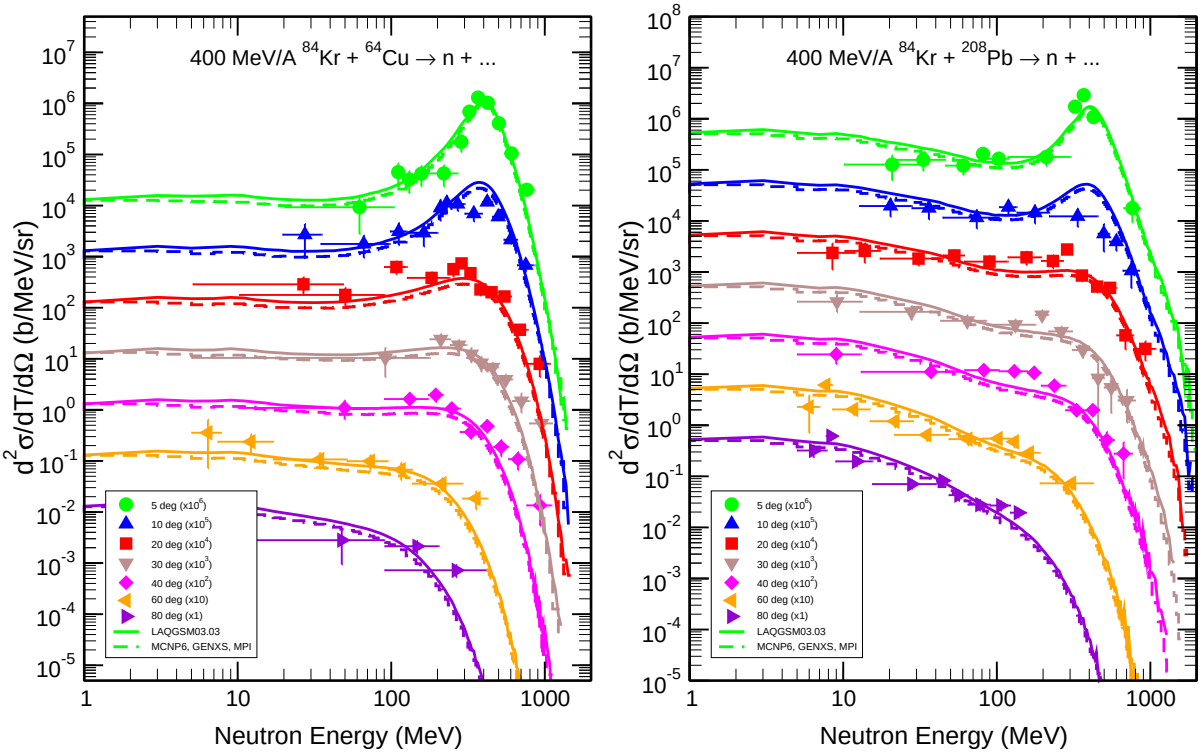

Figure 31: The same as in Fig. 30, but for interactions of ^{84}Kr with ^{64}Cu and ^{208}Pb.

The file N400C.fig is a template for plotting the neutron spectra at seven angles from the N+C reaction; templates for such spectra for all other reactions studied here are listed above. The Postscript files produced by xmgrace are: N400C.ps, N400Cu.ps, Kr400Li.ps, Kr400C.ps, Kr400CH2.ps, Kr400Al.ps, Kr400Cu.ps, Kr400Pb.ps, Xe400Li.ps, Xe400C.ps, Xe400CH2.ps, Xe400Al.ps, Xe400Cu.ps, and Xe400Pb.ps, respectively. For convenience of comparison, they are merged in several figures with the LaTeX files N400CCu.tex, Kr400LiCCH2Al.tex, Kr400CuPb.tex, Xe400LiCCH2Al.tex, and Xe400CuPb.tex. The final pdf files from LaTeX are: N400CCu.pdf, Kr400LiCCH2Al.pdf, Kr400CuPb.pdf, Xe400LiCCH2Al.pdf, and Xe400CuPb.pdf, presented in that subdirectory and shown here in Figs. 29 to 32.

From Figs. 29–33, we can see that the production version 1 of MCNP6 [6] using LAQGSM03.03 describes well the measured neutron spectra from these reactions, just as we had in Fig. 28 of the previous sub-section.

We see that the MCNP6 results using LAQGSM03.03 calculated with the GENXS option [63] agree well with similar results obtained by LAQGSM03.03 used as a stand alone code, but are a little lower (absolute normalization). This is OK and is just as expected, because, as already explained above in Sec. 4.1, in the "Beta 3" version of MCNP6 [5], Dr. Richard E. Prael changed the absolute normalization of the nucleus-nucleus reactions calculated with the GENXS option [63], to match the approximation adopted by MCNPX [8]: It agrees quite well with the total reaction cross sections for nucleus-nucleus reactions predicted by LAQGSM03.03 [16] used as a stand alone code, but it is a little lower.

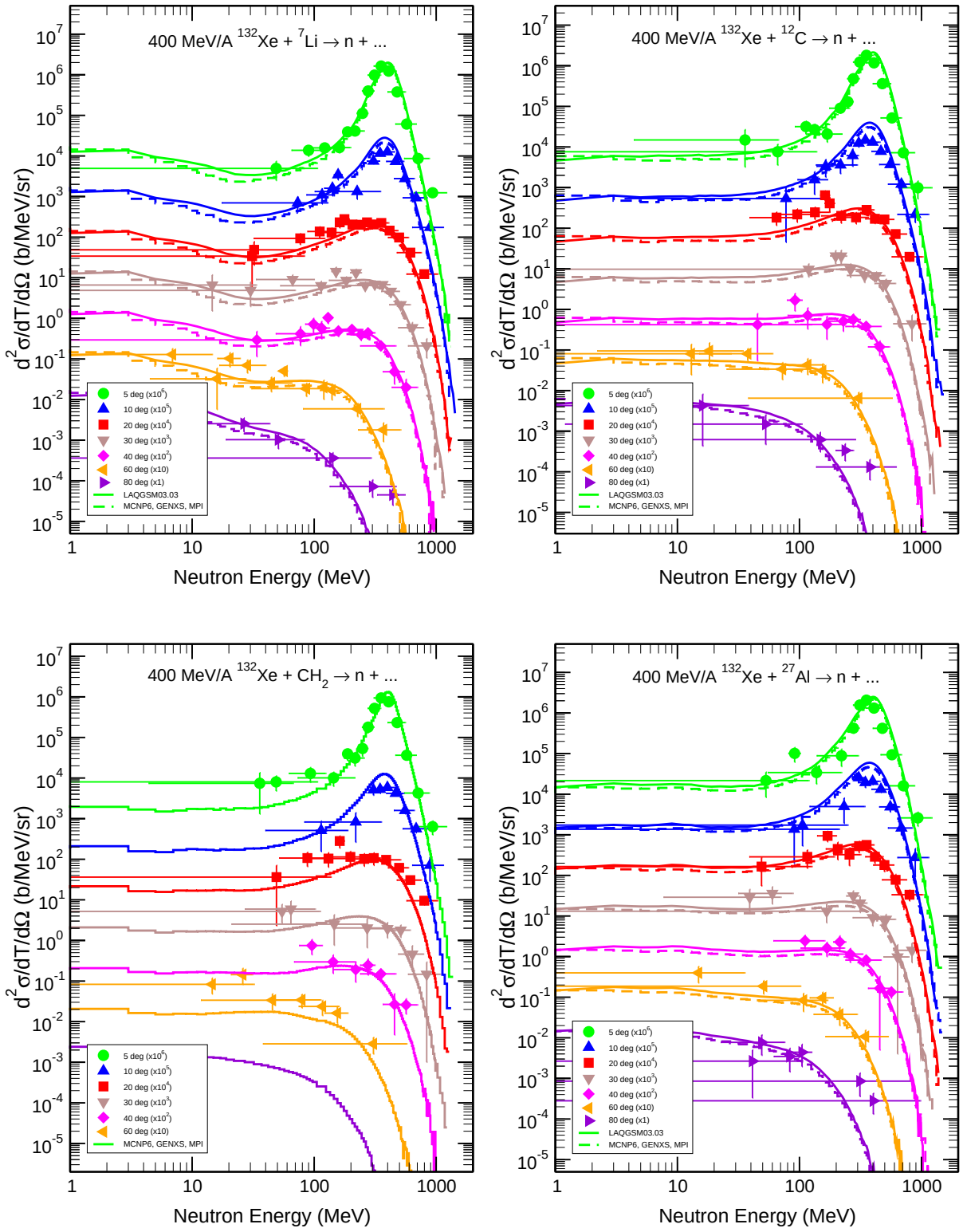

Figure 32: The same as in Fig. 30, but for interactions of ^{132}Xe with ^{7}Li, ^{12}C, polyethylene (CH_2), and ^{27}Al.

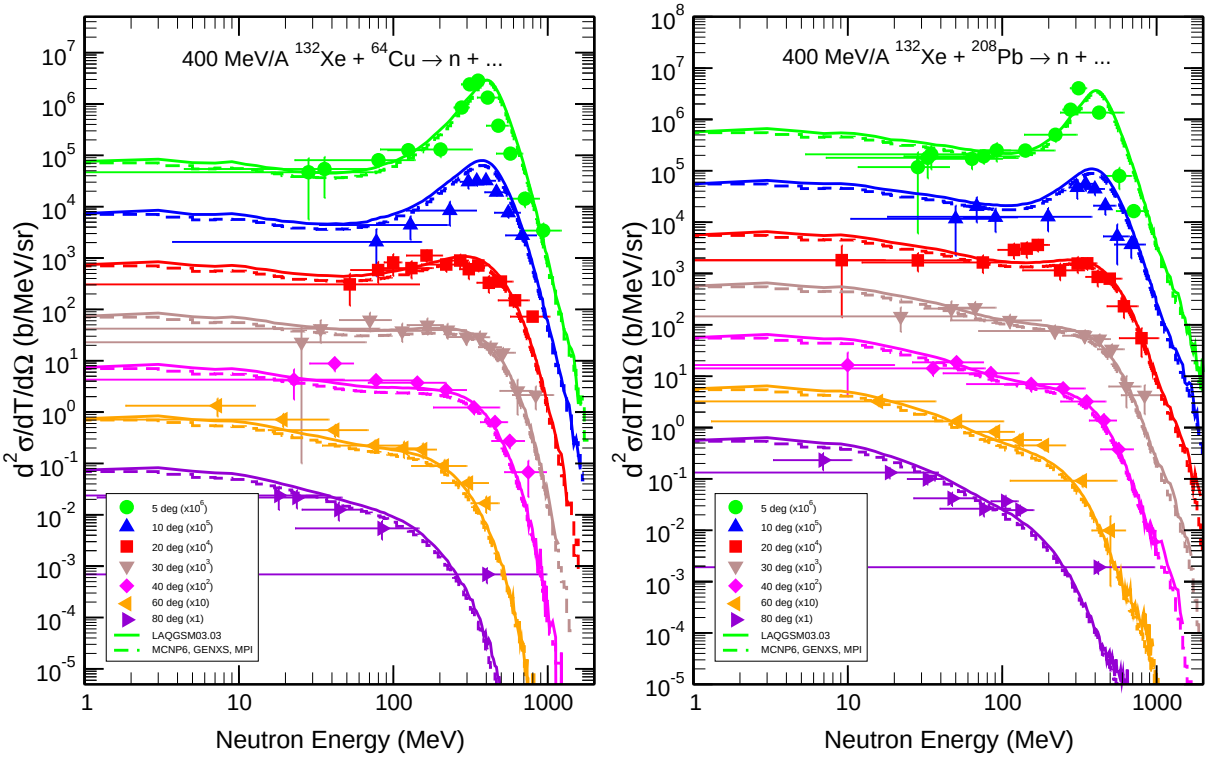

Figure 33: The same as in Fig. 32, but for interactions of ^{132}Xe with ^{64}Cu and ^{208}Pb.

Let us mention that similar good results for such spectra were obtained [90] very recently at Fermi National Accelerator Laboratory (FNAL) by Gudima, Mokhov, and Striganov with the MARS15 transport code using several versions of LAQGSM, different from our LAQGSM03.03 [16]. Our current good results together with similar results from Ref. [90] make questionable the quite poor results by a version of LAQGSM used in a version of MCNPX and much worse results by MARS15 using a version of LAQGSM published in Ref. [89]. We can assume together with the authors of Ref. [90] that either some errors were present in the input files used in the calculations performed in Ref. [89], or the compilation of MARS15 was done on their machine with some problems, or some other problems were involved in obtaining the questionable results presented in Ref. [89]. On August 20, 2013, we have urged the authors of Ref. [89] to resolve this issue and somehow revise and re-distribute their Report to its readers/users.

6.4. 500 MeV/A ^{56}Fe + Li, CH_2, and Al

This MCNP6 problem is to test the applicability of MCNP6 using the LAQGSM03.03 event generator to describe neutron spectra from thin Li, polyethylene (CH_2), and Al targets bombarded with 500 MeV/nucleon ^{56}Fe. Accurate prediction of such data is important for medical applications, space missions, and design and operation of rare isotope research facilities.

A direct "trigger" for this test-problem was the recent "Final Report on Benchmarking Heavy Ion Transport Codes FLUKA, HETC-HEDS, MARS15, MCNPX, and PHITS, DE-FG02-08ER41548, 2013" by R. M. Ronningen et al. [89] where not so good results by an old version MCNPX using an old version of LAQGSM were shown and much more worse results by a version of MARS15 using a version of LAQGSM were published: We need to check how

the production version of MCNP6 using the latest version of our LAQGSM03.03 describes such reactions.

The experimental data for this problem were measured at the Heavy Ion Medical Accelerator in the Chiba (HIMAC) facility of the National Institute of Radiological Science (NIRS), Japan and are published as figures in the paper [87]. They are provided in a tabulated form on the CD-ROM accompanying the book by Takahashi Nakamura and Lawrence Heilbronn [88]; part of these data are also available already in EXFOR.

Experimental neutron spectra from Li at 20, 30, 40, 60, and 80 degrees are presented here in the files Fe500Li.20.e.dat, Fe500Li.30.e.dat, Fe500Li.40.e.dat, Fe500Li.60.e.dat, and Fe500Li.80.e.dat, respectively. We do not present here explicitly similar experimental data for the CH_2 and Al targets: They are included in the xmgrace templates of the figures for CH_2 and Al, Fe500CH2.fig and Fe500Al.fig, can by found in the cited above literature, and are shown in our figures Fe500CH2.ps, Fe500Al.ps and Fe500LiCH2Al.pdf.

In our current calculations, we assume that the Li target consists of only ^{7}Li ions, polyethylene consists of only CH_2, and Al, of only ^{27}Al. We calculate with MCNP6 these spectra using the GENXS option in parallel, with MPI. The main MCNP6 input files for Li, CH_2, and Al targets are **Fe500Li_n**, **Fe500CH2_n**, and **Fe500Al_n**, respectively. For the second input file required by the GENXS option we use the same file, **in-xe**, for all three reactions. All input files are presented in subdirectory /VALIDATION_LAQGSM/Inputs/. Below, we show explicitly only **Fe500Li_n**, as **in-xe** was presented in sub-section # 6.2. (Users of MCNP6 should change the **m1** card, in order to chose CH_2 or Al as a target nucleus; let us remind here again that all input files for this test-problem are presented explicitly in subdirectory /VALIDATION_LAQGSM/Inputs/.)

Fe500Li_n:

```
MCNP6 test: p-spectra from 500 MeV/A Fe56 + Li7 by LAQGSM03.03
  1  1  1.0   -1 2 -3
  2  0        -4 (1:-2:3)
  3  0         4

c -------------------------------------------------------------
  1  cz  4.0
  2  pz  -1.0
  3  pz  1.0
  4  so  50.0

c -------------------------------------------------------------
dbcn 28j 1
  m1 03007  1.0
  sdef erg=28000 par=26056 dir=1 pos=0 0 0 vec 0 0 1
  imp:n 1 1 0
  imp:h 1 1 0
  phys:n 53008
  phys:h 53000
  phys:/ 53008
  phys:* 53008
```

```
  phys:z 53008
  phys:k 53008
  phys:? 53008
  phys:q 53008
  phys:g 53008
  phys:d 53008
  phys:t 53008
  phys:s 53008
  phys:a 53008
  phys:# 53008
  mode  n h / * z k ? q g d t s a #
LCA  2 1 5j -1 1j 1 66   $ use LAQGSM, nevtype = 66: LCA(11)=66 !!!
lcb  0 0 0 0 0 0
lea  2j 0
  tropt genxs in-xe  nreact on  nescat off
c ---------------------------------------------------------------
  print 40 110 95
  nps 10000000
c  nps 700000
c  prdmp 2j -1
```

Though for reactions induced by ^{56}Fe, for Li and Al targets, neutron spectra have been published only at 20, 30, 40, 60, and 80 degrees, and for CH_2, only at 20, 40, 60, and 80 degrees, we calculated with MCNP6 and with LAQGSM03.03 used as a stand alone code neutron spectra at 7 angles from all these targets, namely at 5, 10, 20, 30, 40, 60, and 80 degrees, to be able to compare with similar spectra calculated for other reactions, discussed in the previous two sub-sections.

Neutron double-differential spectra calculated by MCNP6 using LAQGSM03.03 with the GENXS option at 80, 60, and 40 ($\pm$2.5) degrees are tabulated in units of [b/sr/MeV] in the 2nd, 4th, and 6th pairs of columns of the first part of the "neutron production cross section" table (with the neutron energy tabulated in MeV in the 1st column) of the MCNP6 output files Fe500Li_n.mpi.o, Fe500CH2_n.mpi.o, and Fe500Al_n.mpi.o, for Li, CH_2, and Al, respectively. Similar spectra at 30, 20, 10, and 5 ($\pm$2.5) degrees are tabulated in units of [b/sr/MeV] in the 1st, 3rd, 5th, and 6th pairs of columns of the second part of the same "neutron production cross section" table (with the neutron energy tabulated in MeV in the 1st column) of the MCNP6 output files Fe500Li_n.mpi.o, Fe500CH2_n.mpi.o, and Fe500Al_n.mpi.o for Li, CH_2, and Al, respectively. All output files are presented in subdirectory */VALIDATION_LAQGSM/Templates/LINUX/. For convenience of plotting these spectra with xmgrace, the MCNP6 neutron spectra at 5, 10, 20, 30, 40, 60, and 80 degrees are copied from the MCNP6 output files in separate files. We present explicitly in subdirectory */VALIDATION_LAQGSM/Experimental_data/500Fe+LiCH2Al/ such files only for Li, they are: 5.genxs.dat, 10.genxs.dat, 20.genxs.dat, 30.genxs.dat, 40.genxs.dat, 60.genxs.dat, and 80.genxs.dat. We do not show there explicitly such files for CH_2 and Al: They are included in the template for the xmgrace figures, Fe500CH2.fig and Fe500Al.fig.

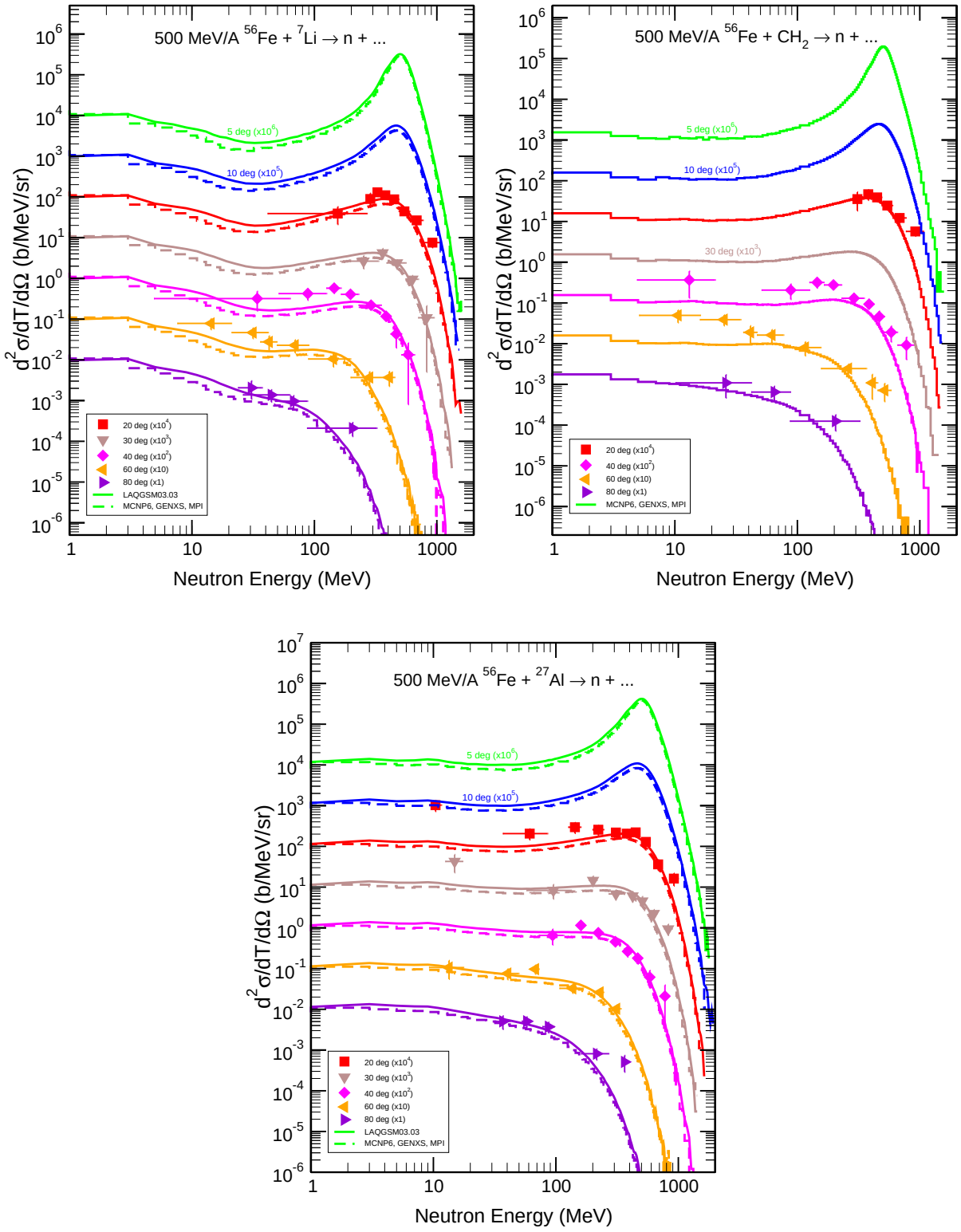

Figure 34: The same as in Fig. 30, but for interactions of 500 MeV/nucleon ^{56}Fe with ^{7}Li, polyethylene (CH_2), and ^{27}Al.

Besides the MCNP6 results, we show there for comparison also calculations by LAQGSM03.03 used as a stand alone code. Neutron double-differential spectra at 5, 10, 20, 30, 40, 60, and 80 ($\pm$2.5) degrees by LAQGSM03.03 used as a stand alone code for Li are presented there in the files 5.laq.dat, 10.laq.dat, 20.laq.dat, 30.laq.dat, 40.laq.dat, 60.laq.dat, and 80.laq.dat. We do not show there explicitly such files for CH2 and Al: They are included in the templates for the xmgrace figures, Fe500CH2.fig and Fe500Al.fig.

The files Fe500Li.fig, Fe500CH2.fig, and Fe500Al.fig are templates for plotting the Li, CH_2, and Al and spectra with xmgrace at all seven angles. The Postscript files produced by xmgrace, Fe500Li.ps, Fe500CH2.ps, and Fe500Al.ps, are merged in a single figure with the LaTeX file Fe500LiCH2Al.tex. The final pdf file from LaTeX with spectra for Li, CH_2, and Al targets is Fe500LiCH2Al.pdf, presented in the same subdirectory, and also shown here in Fig. 34.

From Figs. 34, we can see that the production version 1 of MCNP6 [6] using LAQGSM03.03 describes well the measured neutron spectra from these reactions, just as we had in Figs. 28–33 of the two previous sub-sections for other reactions.

We see that the results by MCNP6 using LAQGSM03.03 calculated with the GENXS option [63] agree well with similar results obtained by LAQGSM03.03 used as a stand alone code, but are a little lower (absolute normalization). This is OK and is just as expected, because, as already explained above in Sec. 4.1, in the "Beta 3" version of MCNP6 [5], Dr. Richard E. Prael changed the absolute normalization of the nucleus-nucleus reactions calculated with the GENXS option [63], to match the approximation adopted by MCNPX [8]: It agrees quite well with the total reaction cross sections for nucleus-nucleus reactions predicted by LAQGSM03.03 [16] used as a stand alone code, but it is a little lower.

Let us mention that similar good results for such spectra were obtained [90] very recently at Fermi National Accelerator Laboratory (FNAL) by Gudima, Mokhov, and Striganov with the MARS15 transport code using several versions of LAQGSM, different from our LAQGSM03.03 [16]. Our current good results together with similar results from Ref. [90] make questionable the quite poor results by a version of LAQGSM used in a version of MCNPX and much worse results by MARS15 using a version of LAQGSM published in Ref. [89]. We can assume together with the authors of Ref. [90] that either some errors were present in the input files used in the calculations performed in Ref. [89], or the compilation of MARS15 was done on their machine with some problems, or some other problems were involved in obtaining the questionable results presented in Ref. [89]. On August 20, 2013, we have urged the authors of Ref. [89] to resolve this issue and somehow revise and re-distribute their Report to its readers/users.

6.5. 600 MeV/A ^{28}Si + C, Cu, and Pb

This MCNP6 problem is to test the applicability of MCNP6 using the LAQGSM03.03 event generator to describe neutron spectra from thin C, Cu, and Pb targets bombarded with 600 MeV/nucleon ^{28}Si. Accurate prediction of such data is important for medical applications, space missions, and design and operation of rare isotope research facilities.

A direct "trigger" for this test-problem was the recent "Final Report on Benchmarking Heavy Ion Transport Codes FLUKA, HETC-HEDS, MARS15, MCNPX, and PHITS, DE-FG02-08ER41548, 2013" by R. M. Ronningen et al. [89] where not so good results by an old version MCNPX using an old version of LAQGSM were shown and much more worse results by a version of MARS15 using a version of LAQGSM were published: We need to check how the production version of MCNP6 using the latest version of our LAQGSM03.03 describes such

reactions.

The experimental data for this problem were measured at the Heavy Ion Medical Accelerator in the Chiba (HIMAC) facility of the National Institute of Radiological Science (NIRS), Japan and are published as figures in the paper [87]. They are provided in a tabulated form on the CD-ROM accompanying the book by Takahashi Nakamura and Lawrence Heilbronn [88]; part of these data are also available already in EXFOR.

Experimental neutron spectra from C at 5, 10, 20, 30, 40, 60, and 80 degrees are presented in subdirectory */VALIDATION_LAQGSM/Experimental_data/600Si+CCuPb/ in the files Si600C.exp.5.dat, Si600C.exp.10.dat, Si600C.exp.20.dat, Si600C.exp.30.dat, Si600C.exp.40.dat, Si600C.exp.60.dat, and Si600C.exp.80.dat, respectively. We do not present there explicitly similar experimental data for the Cu and Pb targets: They are included in the xmgrace templates of the figures for Cu and Pb, Si600Cu_MPI.fig and Si600Pb.fig, can by found in the cited above literature, and are shown in our figures Si600Cu_MPI.ps, Si600Pb.ps, and Si600CCuPb.pdf.

In our current calculations, we assume that the C target consists of only ^{12}C ions, Cu consists of only ^{64}Cu, and Pb, of only ^{208}Pb. We calculate with MCNP6 neutron spectra from C and Pb using the GENXS option with MPI, as described in Sec. 2. In the case of Cu, we perform a different study here: As we have already in the LAQGSM test-problem # 1 this reaction calculated with the "noact = -2" option in a sequential mode (see Ref. [15]), we calculate here this reaction also with the "noact = -2" option, but with MPI. Then, we simply compare the old results obtained in a sequential run with the current MPI results, but both using the "noact = -2" option.

The main MCNP6 input files for C, Cu, and Pb targets are **Si600C_n**, **Si600CuREP**, and **Si600Pb_n**, respectively. For the second input file required by the GENXS option we use the same file, **in-xe**, for both C and Pb target; the "noact = -2" option used for Cu does not require a second input file. All input files are presented in subdirectory /VALIDATION_LAQGSM/Inputs/. Below, we show explicitly only **Si600C_n**, as **in-xe** was presented in sub-section # 6.2, and the input file for Cu, using the "noact = -2" option, was shown and discussed in detail in Seq. 3.1 of Ref. [15]. (Users of MCNP6 should change the **m1** card, in order to chose Pb as a target nucleus; let us remind here again that all input files for this test-problem are presented explicitly in subdirectory /VALIDATION_LAQGSM/Inputs/.)

Fe500Li_n:

```
MCNP6 test: p-spectra from 600 MeV/A Si28 + C12 by LAQGSM03.03
  1  1  1.0   -1 2 -3
  2  0        -4 (1:-2:3)
  3  0         4

c -------------------------------------------------------------
  1  cz  4.0
  2  pz  -1.0
  3  pz  1.0
  4  so  50.0

c -------------------------------------------------------------
dbcn 28j 1
  m1 06012  1.0
```

```
  sdef erg=16800 par=14028 dir=1 pos=0 0 0 vec 0 0 1
  imp:n 1 1 0
  imp:h 1 1 0
  phys:n 53008
  phys:h 53000
  phys:/ 53008
  phys:* 53008
  phys:z 53008
  phys:k 53008
  phys:? 53008
  phys:q 53008
  phys:g 53008
  phys:d 53008
  phys:t 53008
  phys:s 53008
  phys:a 53008
  phys:# 53008
  mode  n h / * z k ? q g d t s a #
LCA  2 1 5j -1 1j 1 66   $ use LAQGSM, nevtype = 66: LCA(11)=66 !!!
lcb  0 0 0 0 0 0
lea  2j 0
  tropt genxs in-xe  nreact on  nescat off
c ------------------------------------------------------------------
  print 40 110 95
  nps 10000000
c  nps 700000
c  prdmp 2j -1
```

Neutron double-differential spectra calculated by MCNP6 using LAQGSM03.03 with the GENXS option at 80, 60, and 40 (±2.5) degrees are tabulated in units of [b/sr/MeV] in the 2nd, 4th, and 6th pairs of columns of the first part of the "neutron production cross section" table (with the neutron energy tabulated in MeV in the 1st column) of the MCNP6 output files Si600C_n.mpi.o and Si600Pb_n.mpi.o, for C and Pb, respectively. Similar spectra at 30, 20, 10, and 5 (±2.5) degrees are tabulated in units of [b/sr/MeV] in the 1st, 3rd, 5th, and 6th pairs of columns of the second part of the same "neutron production cross section" table (with the neutron energy tabulated in MeV in the 1st column) of the MCNP6 output files Si600C_n.mpi.o and Si600Pb_n.mpi.o, for C and Pb, respectively. The format of the MCNP6 output file for Cu, obtained with the "noact = -2" option, Si600CuREP.mpi.o, is completely different from the output files for C and Pb obtained with the GENXS option. A detailed description of the output file for Cu, for the "noact = -2" option, is presented in test-problem # 1 (see pp. 10–15 of Ref. [15]). All output files are presented in subdirectory */VALIDATION_LAQGSM/Templates/LINUX/. For convenience of plotting these spectra with xmgrace, the MCNP6 neutron spectra at 5, 10, 20, 30, 40, 60, and 80 degrees are copied from the MCNP6 output files into separate files. We present in subdirectory */VALIDATION_LAQGSM/Experimental_data/600Si+CCuPb/ explicitly such files only for C; they are: 5.genxs.dat, 10.genxs.dat, 20.genxs.dat, 30.genxs.dat, 40.genxs.dat, 60.genxs.dat, and 80.genxs.dat. We do not show there explicitly such files for Cu and Pb: They are included

in the templates for the xmgrace figures, Si600Cu_MPI.fig and Si600Pb.fig.

Besides the MCNP6 results, we show in the same subdirectory, for comparison, also calculations by LAQGSM03.03 used as a stand alone code. Neutron double-differential spectra at 5, 10, 20, 30, 40, 60, and 80 ($\pm$2.5) degrees by LAQGSM03.03 used as a stand alone code for C are presented there in the files 5.laq.dat, 10.laq.dat, 20.laq.dat, 30.laq.dat, 40.laq.dat, 60.laq.dat, and 80.laq.dat. We do not show there explicitly such files for Cu and Pb: They are included in the templates for the xmgrace figures, Si600Cu_MPI.fig and Si600Pb.fig.

The files Si600C.fig, Si600Cu_MPI.fig, and Si600Pb.fig are templates for plotting the C, Cu, and Pb spectra with xmgrace at all seven angles. The Postscript files produced by xmgrace, Si600C.ps, Si600Cu_MPI.ps, and Si600Pb.ps, are merged in a single figure with the LaTeX file Si600CCuPb.tex. The final pdf file from LaTeX with spectra for C, Cu, and Pb targets is Si600CCuPb.pdf, presented in the same subdirectory, and also shown below in Fig. 35.

From Figs. 35, we can see that the production version 1 of MCNP6 [6] using LAQGSM03.03 describes well the measured neutron spectra from these reactions, just as we had in Figs. 28–34 of the three previous sub-sections for other reactions.

We see that the results by MCNP6 using LAQGSM03.03 calculated with the GENXS option [63] agree well with similar results obtained by LAQGSM03.03 used as a stand alone code, but are a little lower (absolute normalization). This is OK and is just as expected, because, as already explained above in Sec. 4.1, in the "Beta 3" version of MCNP6 [5], Dr. Richard E. Prael changed the absolute normalization of the nucleus-nucleus reactions calculated with the GENXS option [63], to match the approximation adopted by MCNPX [8]: It agrees quite well with the total reaction cross sections for nucleus-nucleus reactions predicted by LAQGSM03.03 [16] used as a stand alone code, but it is a little lower.

Let us mention that similar good results for such spectra were obtained [90] very recently at Fermi National Accelerator Laboratory (FNAL) by Gudima, Mokhov, and Striganov with the MARS15 transport code using several versions of LAQGSM, different from our LAQGSM03.03 [16]. Our current good results together with similar results from Ref. [90] make questionable the quite poor results by a version of LAQGSM used in a version of MCNPX and much worse results by MARS15 using a version of LAQGSM published in Ref. [89]. We can assume together with the authors of Ref. [90] that either some errors were present in the input files used in the calculations performed in Ref. [89], or the compilation of MARS15 was done on their machine with some problems, or some other problems were involved in obtaining the questionable results presented in Ref. [89]. On August 20, 2013, we have urged the authors of Ref. [89] to resolve this issue and somehow revise and re-distribute their Report to its readers/users.

7. Conclusion

MCNP6, the latest and most advanced LANL Monte Carlo transport code representing a recent merger of MCNP5 and MCNPX, but containing also many new features not addressed by its precursors, has been validated and verified against a variety of intermediate and high-energy experimental data, against calculations by several other models and codes, and was also tested on many problems at lower energies, below 150 MeV, where it uses data libraries instead of event-generators. In the present primer, we performed all our calculations in parallel, with MPI, and compared our results with similar calculations done in a sequential mode.

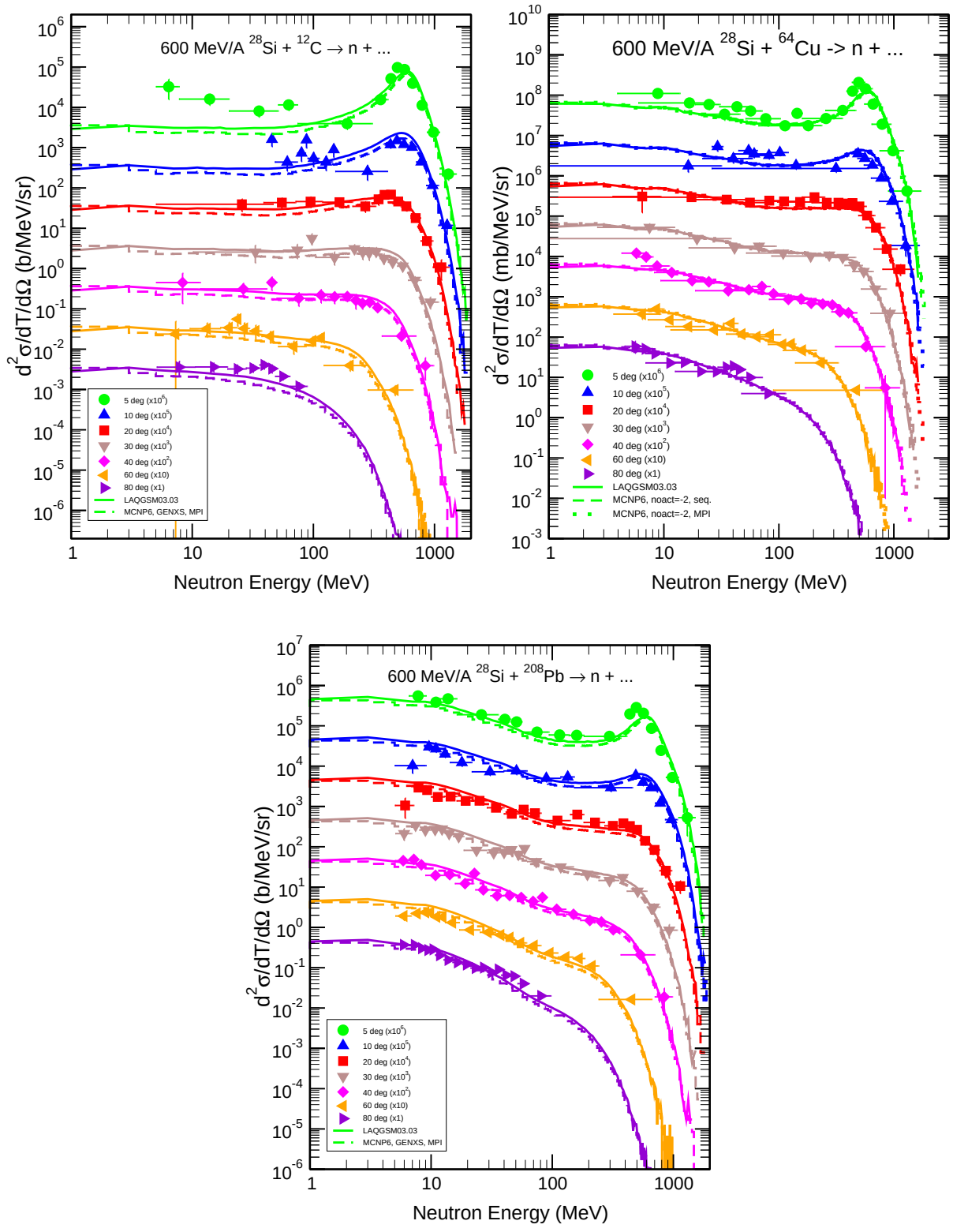

Figure 35: The same as in Fig. 30, but for interactions of 600 MeV/nucleon ^{28}Si with ^{12}C, ^{64}Cu, and ^{208}Pb.

In the beginning, we recalculated with MPI 18 problems testing the MCNP6 CEM, Bertini, INCL+ABLA, and ISABEL event-generators, calculated initially in a sequential mode and discussed in detail in our MCNP6 CEM Testing Primer [13]. After that, we recalculated with MPI all the 18 test problems from our second MCNP6 Testing Primer [15], also calculated initially in a sequential mode and intended mostly to V&V MCNP6 with the Los Alamos version of the Quark-Gluon String Model (LAQGSM) event-generator LAQGSM03.03, used currently in MCNP6 as the main "working horse" to simulate ultra-relativistic reactions and all the interactions of two heavy-ions. Then, in our current MCNP6 MPI Testing Primer, we added many new test-problems, both at lower energies, to use data libraries, and at energies above 150 MeV, to V&V all the MCNP6 event-generators with different versions of MCNP6, from Beta 1 [3] up to the latest, production version [6].

Our study shows that all the MCNP6 results calculated in a sequential mode practically coincide with similar results obtained in parallel, with MPI, with only some tiny differences observed in the last digits of some calculated values, which are lower than the statistical uncertainties of our Monte Carlo simulations, and lower than the error of the available experimental data.

During our V&V work with MPI, we have detected about a dozen little "bugs" in MCNP6 or some problems in some event-generators that showed up while simulating our test-problems with MPI. All of them have been fixed, so that MCNP6 does not crash on our test-problems and does not provide unphysical results. We continue our work to solve some known physical problems, to improve the predictive power of MCNP6.

From the results presented here as well as in our two previous MCNP6 Testing Primers [13, 15], we can conclude that MCNP6 is a reliable and useful Monte Carlo transport code for different applications involving reactions induced by almost all types of elementary particles and heavy-ions, in a very broad range of incident energies. We hope that the current primer will help future MCNP6 users construct their own input files and better understand the final MCNP6 results for applications using models at intermediate and high energies, as well as at lower energies, using data libraries.

Acknowledgments

I am grateful to my LANL colleagues, Jeff Bull, Grady Hughes, and Dick Prael for useful discussions, help, and/or for correcting some of the MCNP6/X bugs I have detected during my current V&V work.

I thank Drs. Vladimir Belyakov-Bodin and Anna Petrovna Krutekova for sending me their publications or/and files with numerical values of their experimental data I used in my present V&V work.

I thank Drs. Stanislav Simakov and Naohiko Otsuka for useful discussions and help on my study on monoenergetic neutron production from a ^{7}Li target bombarded with intermediate-energy protons.

I am grateful to Madison Theresa Sellers for kindly providing to me both numerical values of her experimental delayed neutron emission data from ^{235}U, ^{233}U, and ^{239}Pu and the MCNP6 input files she used to simulate her measurements. It is a pleasure to acknowledge Madison's supervisor at LANL, Dr. John T. (Tim) Goorley, for support and help in my numerous interactions with Madison, and for several useful discussions on this subject.

I thank Dr. Laurie S. Waters for kindly providing me her MCNPX input files for the delayed-neutron production from HEU problem, used here in the test-problem # 5.4 after a minor edition.

Last but not least, I thank Dr. Roger L. Martz for a very careful reading of the manuscript and many useful suggestions on its improvement. However, the author assumes responsibility for any remaining errors.

This work was carried out under the auspices of the National Nuclear Security Administration of the U.S. Department of Energy at Los Alamos National Laboratory under Contract No. DE-AC52-06NA25396.

References

[1] Tim Goorley, "Eolus L2: MCNP MCNPX merger (U)," LANL Report LA-UR-09-06034, Los Alamos (2009); H. Grady Hughes, John S. Hendricks, Forrest B. Brown, Gregg W. McKinney, Jeffrey S. Bull, Michael R. James, John T. Goorley, Michael L. Fensin, Thomas E. Booth, Laurie S. Waters, Robert A. Forster, Stepan G. Mashnik, Richard E. Prael, Joseph W. Durkee, Avneet Sood, Roger L. Martz, Anthony J. Zukaitis, Denise B. Pelowitz, Russell C. Johns, Jeremy E. Sweezy, "Recent Developments in MCNP and MCNPX," LA-UR-08-01065, Los Alamos (2008), Proc. workshop on Uncertainty Assessment in Computational Dosimetry Bologna, Italy, October 8-10, 2007; G. Gualdrini and P. Ferrari, (editors), (ISBN 978-3-9805741-9-8), 2008.

[2] T. Goorley, M. James, T. Booth, F. Brown, J. Bull, L. J. Cox, J. Durkee, J. Elson, M. Fensin, R. A. Forster, J. Hendricks, H. G. Hughes, R. Johns, B. Kiedrowski, R. Martz, S. Mashnik, G. McKinney, D. Pelowitz, R. Prael, J. Sweezy, L. Waters, T. Wilcox, T. Zukaitis, "MCNP6 initial release notes," LANL Report LA-UR-11-01765, Los Alamos (2011); "Initial MCNP6 Release Overview," LANL Report LA-UR-11-01766; "Initial MCNP6 Release Notes," LANL Report LA-UR-11-02352, Los Alamos (2011).

[3] T. Goorley, M. James, T. Booth, F. Brown, J. Bull, L. J. Cox, J. Durkee, J. Elson, M. Fensin, R. A. Forster, J. Hendricks, H. G. Hughes, R. Johns, B. Kiedrowski, R. Martz, S. Mashnik, G. McKinney, D. Pelowitz, R. Prael, J. Sweezy, L. Waters, T. Wilcox, T. Zukaitis, "Initial MCNP6 Release Overview. MCNP6 version 0.1," LA-UR-11-05198, Nuclear Technology, vol. 180, No. 3, Dec. 2012, pp. 298-315.

[4] T. Goorley, M. James, T. Booth, F. Brown, J. Bull, L.J. Cox, J. Durkee, J. Elson, M. Fensin, R.A. Forster, J. Hendricks, H.G. Hughes, R. Johns, B. Kiedrowski, R. Martz, S. Mashnik, G. McKinney, D. Pelowitz, R. Prael, J. Sweezy, L. Waters, T. Wilcox, T. Zukaitis, "Initial MCNP6 Release Overview. MCNP6 Beta 2," LA-UR-11-07082, Los Alamos (2011); "MCNP6 Beta 2 Known Issues," LA-UR-11-07081, Los Alamos (2011).

[5] T. Goorley, M. James, T. Booth, F. Brown, J. Bull, L.J. Cox, J. Durkee, J. Elson, M. Fensin, R.A. Forster, J. Hendricks, H.G. Hughes, R. Johns, B. Kiedrowski, R. Martz, S. Mashnik, G. McKinney, D. Pelowitz, R. Prael, J. Sweezy, L. Waters, T. Wilcox, T. Zukaitis, "Initial MCNP6 Release Overview – MCNP6 Beta 3," LA-UR-12-26631, Los Alamos (2012); "MCNP6 Beta 3 Known Issues," LA-UR-12-26627, Los Alamos (2012).

[6] T. Goorley, M. James, T. Booth, F. Brown, J. Bull, L.J. Cox, J. Durkee, J. Elson, M. Fensin, R.A. Forster, J. Hendricks, H.G. Hughes, R. Johns, B. Kiedrowski, R. Martz, S. Mashnik, G. McKinney, D. Pelowitz, R. Prael, J. Sweezy, L. Waters, T. Wilcox, T. Zukaitis, "Initial MCNP6 Release Overview – MCNP6 Version 1.0," LA-UR-13-22934; DOI: 10.2172/1086758; www.osti.gov/servlets/purl/1086758/; "MCNP6 Production Release," LA-UR-13-23708, Los Alamos (2013).

[7] X-5 Monte Carlo Team, "MCNP — A General Monte Carlo N-Particle Transport Code, Version 5, Volume I: Overview and Theory" LANL Report LA-UR-03-1987; Volume II: "User's Guide," LANL Report LA-CP-03-0245; Volume III: "Developer's Guide," LANL Report LA-CP-03-0284.

[8] H. G. Hughes, R. E. Prael, and R. C. Little, "MCNPX — The LAHET/MCNP Code Merger," LANL Report LA-UR-97-4891, Los Alamos (1997); L. S. Waters, Ed., "MCNPX User's Manual, Version 2.3.0," LANL Report LA-UR-02-2607 (April, 2002); more recent references and many useful details on MCNPX may be found at the Web page http://mcnpx.lanl.gov/.

[9] Radiation Safety Information Computational Center Newsletter No. 579, August 2013, https://rsicc.ornl.gov/RSICCNewsletters.aspx.

[10] Stepan G. Mashnik and Arnold J. Sierk, "CEM03.03 User Manual," LANL Report LA-UR-12-01364, Los Alamos (2012), http://mcnp.lanl.gov/.

[11] S. G. Mashnik, M. I. Baznat, K. K. Gudima, A. J. Sierk, and R. E. Prael, "Extension of the CEM2k and LAQGSM Codes to Describe Photo-Nuclear Reactions," LANL Report LA-UR-05-2013, Los Alamos (2005), E-print: nucl-th/0503061; J. Nucl. Rad. Sci. **6**, No. 2., pp. A1-A19 (2005), http://www.radiochem.org/j-online.html.

[12] S. G. Mashnik, K. K. Gudima, R. E. Prael, A. J. Sierk, M. I. Baznat, and N. V. Mokhov, "CEM03.03 and LAQGSM03.03 Event Generators for the MCNP6, MCNPX, and MARS15 Transport Codes," Invited lectures presented at the Joint ICTP-IAEA Advanced Workshop on Model Codes for Spallation Reactions, February 4–8, 2008, ICTP, Trieste, Italy, IAEA Report INDC(NDS)-0530, Distr. SC, Vienna, Austria, August 2008, p. 51; LANL Report LA-UR-08-2931, Los Alamos (2008); E-print: arXiv:0805.0751.

[13] Stepan G. Mashnik, "Validation and Verification of MCNP6 against High-Energy Experimental Data and Calculations by other Codes. I. The CEM Testing Primer," LANL Report LA-UR-11-05129, Los Alamos (2011).

[14] Stepan G. Mashnik, "Validation and Verification of MCNP6 Against Intermediate and High-Energy Experimental Data and Results by Other Codes," Eur. Phys. J. Plus (2011) **126**: 49.

[15] Stepan G. Mashnik, "Validation and Verification of MCNP6 against High-Energy Experimental Data and Calculations by other Codes. II. The LAQGSM Testing Primer," LANL Report LA-UR-11-05627, Los Alamos (2011).

[16] S. G. Mashnik, K. K. Gudima, N. V. Mokhov, and R. E. Prael, "LAQGSM03.03 Upgrade and Its Validation," Research Note X-3-RN(U)07-15, August 27, 2007; LANL Report LA-UR-07-6198; E-print: arXiv:0709.173.

[17] Konstantin K. Gudima, Stepan G. Mashnik, and Arnold J. Sierk, "User Manual for the code LAQGSM," LANL Report LA-UR-01-6804, Los Alamos (2011), http://mcnp.lanl.gov.

[18] H. W. Bertini, "Low-Energy Intranuclear Cascade Calculation," Phys. Rev. **131** (1963) 1801–1871; "Intranuclear Cascade Calculation of the Secondary Nucleon Spectra from Nucleon-Nucleus Interactions in the Energy Range 340 to 2900 MeV and Comparison with Experiment", Phys. Rev. **188** (1969) 1711–1730.

[19] R. E. Prael and M. Bozoian, "Adaptation of the Multistage Preequilibrium Model for the Monte Carlo Method," LANL Report LA-UR-88-3238, Los Alamos (September 1988).

[20] L. Dresner, *EVAP – A Fortran Program for Calculation the Evaporation of Various Particles from Excited Compound Nuclei*, Oak Ridge National Laboratory Report ORNL-TM-196, 1962; Miraim P. Guthrie *EVAP-2 and EVAP-3: Modifications of a Code to Calculate Particle Evaporation from Excited Compound Nuclei*, Oak Ridge National Laboratory Report ORNL-4379, 1969 March, 36 pp.; M. P. Guthrie, *EVAP-4: Another Modification of a Code to Calculate Particle Evaporation from Excited Compound Nuclei*, Oak Ridge National Laboratory Report ORNL-TM-3119, 1970; P. Cloth, D. Filges, G. Sterzenbach, T. W. Armstrong, and B.L. Colborn, *The KFA-Version of the High-Energy Transport Code HETC and the Generalized Evaluation Code SIMPEL*, Kernforschungsanlage Jülich Report Jül-Spez-196, 1983.

[21] F. Atchison, "Spallation and Fission in Heavy Metal Nuclei under Medium Energy Proton Bombardment," in Proc. Meeting on Targets for Neutron Beam Spallation Source, Julich, June 11–12, 1979, pp. 17–46, G. S. Bauer, Ed., Jul-Conf-34, Kernforschungsanlage Julich GmbH, Germany (1980); "A Treatment of Fission for HETC," in *Intermediate Energy Nuclear Data: Models and Codes*, pp. 199–218 in: Proc. of a Specialists's Meeting, May 30–June 1, 1994, Issy-Les-Moulineaux, France, OECD, Paris, France (1994).

[22] J. Cugnon, C. Volant, and S. Vuillier, "Improved Intranuclear Cascade Model for Nucleon-Nucleus Interactions,"Nucl. Phys. **A620** (1997) 475–509; A. Boudard, J. Cugnon, S. Leray, and C. Volant, "Intranuclear Cascade Model for a Comprehensive Description of Spallation Reaction Data," Phys. Rev. C **66** (2002) 044615.

[23] A. R. Junghans, M. de Jong, H.-G. Clerc, A. V. Ignatyuk, G. A. Kudyaev, and K.-H. Schmidt, "Projectile-Fragment Yields as a Probe for the Collective Enhancement in the Nuclear Level Density," Nucl. Phys. A **629** (1998) 635–655; J.-J. Gaimard, and K.-H. Schmidt, "A reexamination of the abrasion-ablation model for the description of the nuclear fragmentation reaction," Nucl. Phys. A **531** (1991) 709–745.

[24] Y. Yariv and Z. Frankel, "Intranuclear Cascade Calculation of High-Energy Heavy-Ion Interactions," Phys. Rev. C **20** (1979) 2227–2243; Y. Yariv and Z. Frankel, "Inclusive Cascade Calculation of High Energy Heavy Ion Collisions: Effect of Interactions between Cascade Particles," Phys. Rev. C **24** (1981) 488–494; Y. Yariv, "ISABEL — INC Model for High-Energy Hadron-Nucleus Reactions," Proc. Joint ICTP-IAEA Advanced Workshop on Model Codes for Spallation Reactions, ICTP Trieste, Italy, 4-8 February 2008, INDC(NDS)-0530 Distr. SC, IAEA, Vienna, August 2008, pp. 15–28.

[25] M. B. Chadwick, P. Obložinský, M. Herman, N. M. Greene, R. D. McKnight, D. L. Smith, P. G. Young, R. E. MacFarlane, G. M. Hale, S. C. Frankle, A. C. Kahler, T. Kawano, R. C. Little, D. G. Madland, P. Moller, R. D. Mosteller, P. R. Page, P. Talou, H. Trellue, M. C. White, W. B. Wilson, R. Arcilla, C. L. Dunford, S. F. Mughabghab2 B. Pritychenko, D. Rochman, A. A. Sonzogni, C. R. Lubitz, T. H. Trumbull, J. P. Weinman, D. A. Brown, D. E. Cullen, D. P. Heinrichs, D. P. McNabb, H. Derrien, M. E. Dunn, N. M. Larson, L. C. Leal, A. D. Carlson, R. C. Block, J. B. Briggs, E. T. Cheng, H. C. Huria, M. L. Zerkle, K. S. Kozier, A. Courcelle, V. Pronyaev, and S. C. van der Marck, "ENDF/B-VII.0: Next Generation Evaluated Nuclear Data Library for Nuclear Science and Technology," Nuclear Data Sheets **107** (2006) 2931–3060.

[26] W. B. Wilson, T. R. England, R. E. MacFarlane, D. W. Muir, and P. G. Young, "The Status of Nuclear Data for Transmutation Calculations," LANL Report LA-UR-95-3431, Los Alamos (1995).

[27] "MCNP6^{TM} User's Manual, Version 1.0," LANL Report LA-CP-13-00634, Denise B. Pelowitz, editor, 2013.

[28] J. Taieb, K.-H. Schmidt, L. Tissan-Got, P. Armstrong, J. Benlliure, M. Bernas, A. Boudard, E. Casarejos, S. Czajkowski, T. Enqvist, R. Legrain, S. Leray, B. Mustapha, M. Pravikoff, F. Rejmund, C. Stéphan, C. Volant, and W. Wlazlo, "Evaporation Residues Produced in the Spallation Reaction ^{238}U + p at 1 A GeV," Nucl. Phys. **A724** (2003) 413–430.

[29] M. Bernas, P. Armbruster, J. Benlliure, A. Boudard, E. Casarejos, T. Enqvist, A. Kelic, R. Legraind, S. Leray, J. Pereira, F. Rejmund, M.-V. Ricciardi, K.-H. Schmidt, C. Stephan, J. Taieb, L. Tassan-Got, and C. Volant, "Very heavy fission fragments produced in the spallation reaction ^{238}U +p at 1A GeV," Nucl. Phys. **A765** (2006) 197–210.

[30] M. Bernas, P. Armstrong, J. Benlliure, A. Boudard, E. Casarejos, S. Czajkowski, T. Enqvist, R. Legrain, S. Leray, B. Mustapha, P. Napolitani, J. Pereira, F. Rejmund, M.-V. Ricciardi, K.-H. Schmidt, C. Stéphan, J. Taieb, L. Tissan-Got, and C. Volant, "Fission-Residues Produced in the Spallation Reaction ^{238}U +p at 1 A GeV," Nucl. Phys. **A725** (2003) 213–253.

[31] M. V. Ricciardi, P. Armbruster, J. Benlliure, M. Bernas, A. Boudard, S. Czajkowski, T. Enqvist, A. Kelić, S. Leray, R. Legrain, B. Mustapha, J. Pereira, F. Rejmund, K.-H. Schmidt, C. Stéphan, L. Tassan-Got, C. Volant, and O. Yordanov, "Light nuclides produced in the proton-induced spallation of ^{238}U at 1 GeV," Phys. Rev. C **73** (2006) 014607.

[32] I. Dostrovsky, R. Davis, Jr., A. M. Poskanzer, and P. L. Reeder, "Cross Sections for the Production of Li^9, C^{16}, and N^{17} in Irradiations with GeV-Energy Protons," Phys. Rev. **139** (1965) B1513–B1524.

[33] Th. Aoust and J. Cugnon, "Effects of Isospin and Energy Dependences of the Nuclear Mean Field in Spallation Reactions," Eur. Phys. J. A **21** (2004) 79–85; A. Boudard, J. Cugnon, S. Leray, and C. Volant, "A New Model for Production of Fast Light Clusters in Spallation Reactions," Nucl. Phys. **A740** (2004) 195–210; Th. Aoust and J. Cugnon, "Pion Physics in the Liège Intranuclear Cascade Model," Phys. Rev. C **74** (2006) 064607; Thierry Aoust and Joseph Cugnon, "Production of Z+1 and A+1 isotopes in proton-induced reactions on ^{A}Z nuclei, " Nucl. Phys. **A828** (2009) 52–71; Thierry Aoust, *Improvements of the Liege Intranuclear model for study of spallation targets for hybrid systems*, PhD thesis, University of Liege, 2007 (in French).

[34] Aleksandra Kelic, M. Valentina Ricciardi, Karl-Heinz Schmidt, "ABLA07 - towards a complete description of the decay channels of a nuclear system from spontaneous fission to multifragmentation," E-print: arXiv:0906.4193, June 23, 2009; Proc. Joint ICTP-IAEA Advanced Workshop on Model Codes for Spallation Reactions, ICTP Trieste, Italy, 4-8 February 2008, INDC(NDS)-0530 Distr. SC, IAEA, Vienna, August 2008, pp. 181–221.

[35] J.-C. David, A. Boudard, J. Cugnon, A. Kelic-Heil, S. Leray, D. Mancusi, M.V. Ricciardi, "INCL4.5 and Abla07 - Improved versions of the intranuclear cascade (INCL4) and deexcitation (Abla) models," Proc. SATIF 10, 2-4 June 2010, CERN, Geneve,

Report of Institute de Recherche sur les Lois Fondamentales de l'Univers Irfu-10-123 http://irfu.cea.fr/Documentation/Publications/consultation_new.php?domaine=Physique%20Nucl%E9aire&annee=2010.

[36] Denise B. Pelowitz, editor, *MCNPX^{TM} User's Manual, Version 2.6.0*, LA-CP-07-1473, Los Alamos, April 2008.

[37] *Benchmark of Spallation Models* organized at the International Atomic Energy Agency during 2008-2009 by Detlef Filges, Sylvie Leray, Jean-Christophe David, Gunter Mank, Yair Yariv, Alberto Mengoni, Alexander Stanculescu, Mayeen Khandaker, and Naohiko Otsuka, IAEA Vienna, Austria, http://nds121.iaea.org/alberto/mediawiki-1.6.10/index.php/Main_Page.

[38] M. Hagiwara, T. Sanami, Y. Iwamoto, N. Matsuda, Y. Sakamoto, Y. Nakane, H. Nakashima, K. Masumoto, Y. Uwamino, and H. Kaneko, "Spectrum Measurement of Neutrons and Gamma-rays from Thick $H_2^{18}O$ Target Bombarded with 18 MeV Protons", Proc. International Conference on Nuclear Data for Science and Technology, April 26-30, 2010, Jeju Island, Korea, J. Korean Phys. Soc., Vol. 59, No. 2, August 2011, pp. 2035-2038.

[39] R. E. Prael and H. Lichtenstein, *User guide to LCS: The LAHET Code System*, LANL Report LA-UR-89-3014, Los Alamos (1989); http://www-xdiv.lanl.gov/XTM/lcs/lahet-doc.html.

[40] A. Guertin, N. Marie, S. Auduc, V. Blideanu, Th. Delbar, P. Eudes, Y. Foucher, F. Haddad, T. Kirchner, Ch. Le Brun, C. Lebrun, F. R. Lecolley, J.F. Lecolley, X. Ledoux, F. Lefèbvres, T. Lefort, M. Louvel, A. Ninane, Y. Patin, Ph. Pras, G. Rivière, and C. Varignon, "Neutron and light-charged-particle productions in proton-induced reactions on ^{208}Pb at 62.9 MeV," Eur. Phys. J. A **23** (2005) 49–60.

[41] Yury E. Titarenko, Oleg V. Shvedov, Vyacheslav F. Batyaev, Eugeny I. Karpikhin, Valery M. Zhivun, Aleksander B. Koldobsky, Ruslan D. Mulambetov, Andrey N. Sosnin, Yuri N. Shubin, Anatoly V. Ignatyuk, Vladimir P. Lunev, Stepan G. Mashnik, Richard E. Prael, Tony A. Gabriel, and Marshall Blann "Experimental and theoretical study of the yields of radionuclides produced in 232-Th thin targets irradiated by 100 and 800 MeV protons," Proc. 3rd Int. Conf. on Accelerator Driven Transmutation Technologies and Applications (ADTTA'99), Praha, 7–11 June 1999, Czech Republic, Paper No. P-C24 on the ADTTA'99 Web page http://www.fjfi.cvut.cz/con_adtt99/ and on the CD-ROM with the Proceedings; numerical values of the measured data are available in the EXFOR database, Entry No. 00997.

[42] John Weidner, Meiring Nortier, Hong Bach, Mike Fassbender, George Goff, Wayne Taylor, Frank Valdez, Laura Wolfsberg, Mike Cisneros, Don Dry, Mike Gallegos, Russ Gritzo, Leo Bitteker, Aaron Couture, John Ullmann, John Weidner, and Steve Wender, preliminary LANL data presented in a 2010 LANL Chemistry Division talk entitled **"Accelerator-Based Production of the Therapy Isotope Ac-225"**; final LANL data have been published recently in: Jonathan W. Engle, Stepan G. Mashnik, John W. Weidner, Laura E. Wolfsberg, Michael E. Fassbender, Kevin Jackman, Aaron Couture, Leo J. Bitteker, John L. Ullmann, Mark S. Gulley, Chandra Pillai, Kevin D. John, Eva R. Birnbaum, and Francois M. Nortier, "Cross Sections from Proton Irradiation of Thorium at 800 MeV," LA-UR-13-23754 arXiv:1305.6638v1, Phys. Rev. C **88** (2013) 014604. .

[43] S. G. Mashnik, M. B. Chadwick, P. G. Young, R. E. MacFarlane, and L. S. Waters, "^{7}Li(p,n) Nuclear Data Library for Incident Proton Energies to 150 MeV," Los Alamos National Laboratory Report LA-UR-00-1067, Los Alamos (2000); http://mcnp.lanl.gov/.

[44] Alexander Prokofiev, Mark Chadwick, Stepan Mashnik, Nils Olsson, and Laurie Waters, "Development and Validation of the ^{7}Li(p,n) Nuclear Data Library and Its Application in Monitoring of Intermediate Energy Neutrons," LANL Report LA-UR-01-5631, Los Alamos (2001); E-print: nucl-th/0208076; Proc. ND2001, vol. 1; J. Nucl. Sci. Technol., **Supplement 2**, pp. 112-115, 2002.

[45] N. Otsuka and S.P. Simakov, "Compilation of Light-Ion Induced Neutron Spectra for Applications," IAEA Memo **CP-D/700 (Rev.2)**, Vienna, Austria, 29 February 2012.

[46] S. P. Simakov, U. Fischer, Pavel Bém, V. Burjan, M. Götz, M. Honusek, V. Kroha, J. Novak and E. Šimečková, "Analysis of the Dosimetry Cross Sections Measurements up to 35 MeV with a ^{7}Li(p,xn) Quasi-monoenergetic Neutron Source," J. Korean Phys. Society, Vol. 59, No. 2, August 2011, pp. 1856–1859.

[47] Stepan G. Mashnik and Jeffrey S. Bull, "MCNP6 Simulation of Quasi-Monoenergetic 7Li(p,n) Neutron Sources below 150 MeV," LANL Report LA-UR-13-20432, arXiv:1303.4321, proc. ND2013, to be published in Nuclear Data Sheets, 2014.

[48] Yoshitomo Uwaminoa, Titik Suharti Soewarsono, Hiroshi Sugita, Yoshitomo Uno, Takashi Nakamura, Tokushi Shibata, Mineo Imamura, Sei-ichi Shibata, "High-energy p-Li neutron field for activation experiment," Nucl. Instrum. Methods Phys. Res. A **389** (1997) 463–473.

[49] H. Grady Hughes, "Summary on DBCN Options in MCNP6," LANL Report LA-UR-13-23395, Los Alamos (May 9, 2013); http://mcnp.lanl.gov/.

[50] M. Lagarde-Simonoff and G. N. Simonoff, "Cross sections and recoil properties of ^{83,84,86}Rb formed by 0.6-21 GeV ^{1}H reactions with targets of Y to U," Phys. Rev. C **20** (1979) 1498–1516.

[51] J. W. Engle, S. G. Mashnik, H. Bach, A. Couture, K. Jackman, R. Gritzo, B. D. Ballard, M. Fassbender, D. M. Smith, L. J. Bitteker, J. L. Ullmann, M. Gulley, C. Pillai, K. D. John, E. R. Birnbaum, and F. M. Nortier, "Cross Sections from 800 MeV Proton Irradiation of Terbium," Nucl. Phys. **A893** (2012) 87–100.

[52] G. Andersson, M. Areskoug, H.-Å. Gustafsson, G. Hyltn, B. Schrøder, and E. Hagebø, "Binary fission in Tb and Ag by 600 MeV protons," Phys. Lett. **B 64** (1976) 421–423.

[53] L. A. Vaishnene, L. N. Andronenko, G. G. Kovshevny, A. A. Kotov, and G. E. Solyakin, "Fission cross sections of medium-weight and heavy nuclei induced by 1 GeV protons," Z. Phys. **A 302** (1981) 143–148.

[54] R. B. Firestone, *Table of Isotopes*, vols. 1 and 2, John Willey & Sons, Inc., New York, 1996.

[55] I. L. Azhgirey, V. I. Belyakov-Bodin, I. I. Degtyarev, N. P. Smirnov, S. G. Mashnik, "CTOF Measurements and Monte Carlo Analyses of Neutron Spectra for the Backward Direction from a Copper Target Irradiated with 800, 1000, and 1200 MeV Protons," LA-UR-12-26241; arXiv:1211.3047, submitted Atomic Energy.

[56] Stepan G. Mashnik, Arnold J. Sierk, and Richard E. Prael, "MCNP6 Fission Cross Section Calculations at Intermediate and High Energies, LANL Report LA-UR-12-00228, Los Alamos (2012); http://mcnp.lanl.gov/.

[57] A. V. Prokofiev, "Compilation and Systematics of Proton-Induced Fission Cross-Section Data," NIM **A463**, 557–575 (2001), and references therein; A. V. Prokofiev, S. G. Mashnik, and W. B. Wilson, "Systematics of Proton-Induced Fission Cross Sections for Intermediate Energy Applications," LANL Report LA-UR-02-5837, Los Alamos, 2002; E-print: nucl-th/0210071.

[58] L. Giot, J. A. Alcántara-Núñezb, J. Benlliure, D. Pérez-Loureiro, L. Audouin, A. Boudard, E. Casarejos, T. Enqvist, J. E. Ducret, B. Fernández-Domínguez, M. Fernández Ordóñez, F. Farget, A. Heinz, V. Henzl, D. Henzlova, A. Kelić-Heil, A. Lafriaskh, S. Leray, P. Napolitani, C. Paradela, J. Pereirab, M. V. Ricciardi, C. Stéphan, K.-H. Schmidt, C. Schmitt, L. Tassan-Got, C. Villagrasa, C. Volant, and O. Yordanov, "Isotopic production cross sections of the residual nuclei in spallation reactions induced by ^{136}Xe projectiles on proton at 500 A MeV," Nucl. Phys. **A899** (2013) 116–132.

[59] J. C. David, A. Boudard, J. Cugnon, S. Ghali, S. Leray, D. Mancusi, and L. Zanini, "Modeling astatine production in liquid lead-bismuth spallation targets," Eur. Phys. J. A **49** (2013) 29–41.

[60] J. P. Bondorf, A. S. Botvina, A. S. Iljinov, I. N. Mishustin, and K. Sneppen, "Statistical Multifragmentation of Nuclei," Phys. Rep. **257** (1995) 133–221.

[61] R. J. Charity, L. G. Sobotka, J. Cibor, K. Hagel, M. Murray, J. B. Natowitz, R. Wada, Y. El Masri, D. Fabris, G. Nebbia, G. Viesti, M. Cinausero, E. Fioretto, G. Prete, A. Wagner, and H. Xu, "Emission of Unstable Clusters from Yb Compound Nuclei," Phys. Rev. C **63** (2001) 024611; http://www.chemistry.wustl.edu/ rc/gemini/.

[62] Stepan G. Mashnik, "MCNP6 Study of Spallation Products from 500 MeV p + ^{136}Xe," LANL Report LA-UR-13-23189, Los Alamos (2013), Transactions of the American Nuclear Society, 2013 ANS Winter Meeting and Nuclear Expo, November 10–14, 2013, Washington, DC, USA.

[63] R. E. Prael, "Tally Edits for the MCNP6 GENXS Option," LANL Research Note X-5-RN(U) 04-41, Los Alamos (2004); LANL Report LA-UR-11-02146, Los Alamos (2011); http://mcnp.lanl.gov/.

[64] L. Sihver, K. Aleklett, W. Loveland, P. L. McGaughey, D. H. E. Gross, and H. R. Jaqaman, "Gold target fragmentation by 800 GeV protons," Nucl. Phys. **A543** (1992) 703–721.

[65] F. Rejmund, B. Mustapha, P. Armbruster, J. Benlliure, M. Bernas, A. Boudard, J. P. Dufour, T. Enqvist, R. Legrain, S. Leray, K.-H. Schmidt, C. Stephan, J. Taieb, L. Tassan-Got, and C. Volant, "Measurement of Isotopic Cross Sections of Spallation Residues in 800 A MeV 197-Au + p Collisions," Nucl. Phys. **A683** (2001) 540–565.

[66] J. Benlliure, P. Armbruster, M. Bernas, A. Boudard, J. P. Dufour, T. Enqvist, R. Legrain, S. Leray, B. Mustapha, F. Rejmund, K.-H. Schmidt, C. Stephan, L. Tassan-Got, and C. Volant, "Isotopic Production Cross Sections of Fission Residues in 197-Au-on-Proton Collisions at 800 A MeV," Nucl. Phys. **A683** (2001) 513–539.

[67] J. R. Cummings, W. R. Binns, T. L. Garrard, M. H. Israel, J. Klarmann, E. C. Stone, and C. J. Waddington, "Determination of the cross sections for the production of fragments from relativistic nucleus-nucleus interactions. I. Measurements," Phys. Rev. C **42** (1990) 2508.

[68] L. Y. Geer, J. Klarmann, B. S. Nilsen, C. J. Waddington, W. R. Binns, J. R. Cummings, and T. L. Garrard, "Charge-changing fragmentation of 10.6 GeV/nucleon ^{197}Au nuclei," Phys. Rev. C **52** (1995) 334.

[69] C. Scheidenberger, I. A. Pshenichnov, K. Sümmerer, A. Ventura, J. P. Bondorf, A. S. Botvina, I. N. Mishustin, D. Boutin, S. Datz, H. Geissel, P. Grafström, H. Knudsen, H. F. Krause, B. Lommel, S. P. Moller, G. Münzenberg, R. H. Schuch, E. Uggerhj, U. Uggerhj, C. R. Vane, Z. Z. Vilakazi, and H. Weick, "Charge-changing interactions of ultrarelativistic Pb nuclei," Phys. Rev. C **70** (2004) 014902.

[70] Mukhtar Ahmed Rana and Shahid Manzoor, "Examining the fragmentation of 158 A GeV lead ions on copper target: Charge-changing cross sections," Radiation Measurements **43** (2008) pp. 1383–1389.

[71] Michal Mocko, "Rare Isotope Production," PhD thesis, Michigan State University, 2006, http://groups.nscl.msu.edu/nscl_library/Thesis/index.htm.

[72] K. Summerer and B. Blank, "Modified empirical parameterization of fragmentation cross sections," Phys. Rev. C **61** (2000) 034607.

[73] J.-J. Gaimard and K.-H. Schmidt, "A reexamination of the abrasion-ablation model for the description of the nuclear fragmentation," Nucl. Phys. **A531** (1991) 709.

[74] Denis Lacroix, Aymeric Van Lauwe, and Dominique Durand, "Event generator for nuclear collisions at intermediate energies," Phys. Rev. C **69** (2004) 054604.

[75] Akira Ono, Hisashi Horiuchi, "Antisymmetrized molecular dynamics for heavy ion collisions," Prog. Part. Nucl. Phys. **53** (2004) 501.

[76] V. Föhr, A. Bacquias, E. Casarejos, T. Enqvist, A. R. Junghans, A. Kelić-Heil, T. Kurtukian, S. Lukić, D. Pérez-Loureiro, R. Pleskač, M. V. Ricciardi, K.-H. Schmidt, and J. Taïeb, "Experimental study of fragmentation products in the reactions ^{112}Sn+^{112}Sn and ^{124}Sn+^{124}Sn at 1A GeV," Phys. Rev. C **84**, 054605 (2011).

[77] Stepan G. Mashnik and Arnold J. Sierk, "MCNP6 Study of Fragmentation Products from ^{112}Sn+^{112}Sn and ^{124}Sn+^{124}Sn at 1 GeV/nucleon," LANL Report LA-UR-13-20555, Los Alamos (20130, arXiv:1303.4316, proc. 2013, New York, NY, USA, to be published in Nuclear Data Sheets, January, 2014.

[78] S. G. Mashnik, K. K. Gudima, M. I. Baznat, A. J. Sierk, R. E. Prael, and N. V. Mokhov, "CEM03.S1, CEM03.G1, LAQGSM03.S1, and LAQGSM03.G1 Versions of CEM03.01 and LAQGSM03.01 Event-Generators," Research Note X-3-RN(U)06-07, LANL Report LA-UR-06-1764, Los Alamos (2006), http://mcnp.lanl.gov/.

[79] S. G. Mashnik, K. K. Gudima, and M. I. Baznat, "Multifragmentation vs. Evaporation vs. Binary-Decay in Fragment Production," LANL Report LA-UR-06-1955, Los Alamos (2006); arXiv:nucl-th/0603046.

[80] Davide Mancusi, Alain Boudard, Joseph Cugnon, Jean-Christophe David, Thomas Gorbinet, and Sylvie Leray, "Elusiveness of evidence for multifragmentation in 1-GeV proton-nucleus reactions," Phys. Rev. C **84**, 064615 (2011).

[81] A. F. Barghouty, C. Brofferio, S. Capelli, M.Clemenza, O. Cremonesi, S.Cebrián, E. Fiorini, R. C. Haight, E. B. Norman, M. Pavan, E.Previtali, B. J. Quiter, M.Sisti, A. R. Smith, and S. A. Wender, "Measurements of proton-induced radionuclide production cross sections to evaluate cosmic-ray activation of tellurium," arXiv:1010.4066; 19 Oct 2010; Nucl. Instrum. Meth. B **295** (2013) 16–21.

[82] David Kenneth Smith "Recent Activities of the International Atomic Energy Agency to Combat Illicit Trafficing of Nuclear and Other Radioactive Material," International Workshop on Nuclear Forensics following on Nuclear Security Summit, Japan Atomic Energy Agency, Oct. 5–6, 2010, www.jaea.go.jp/04/np/activity/2010-10-05/2010-10-05-12.pdf.

[83] M. T. Sellers, D. G. Kelly, and E. C. Corcoran, "An automated delayed neutron counting system for mass determinations of special nuclear materials," J. Radioanal. Nucl. Chem. **291** (2012) 281–285.

[84] Madison Sellers, Tim Goorley, Emily Corcoran, and David Kelley, "MCNP6 Delayed Neutron Emission Validation with Experimental Measurements," LANL Report LA-UR-11-05868, Los Alamos, October 11, 2011; Madison T. Sellers, Emily C. Corcoran, David G. Kelley, and Tim Goorley, "A Preliminary Comparison of MCNP6 Delayed Neutron Emission from ^{235}U and Experimental Measurements," LANL Report LA-UR-12-00219, Los Alamos (2012), American Nuclear Society 2012 Summer Conference, June 24-28, 2012, Chicago, IL, Transactions of the American Nuclear Society, Vol. 106, No. 1, pp. 813-816, June 2012.

[85] Randy Spaulding, Chris L. Morris, Steven J. Greene, Jeffrey D. Bacon, Gregory H. Canvan, Kiwhan Chung, Jay S. Eloson, Gary E. Hogan, Mark F. Makela, Fessaha G. Mariam, Matthew M. Murray, Alexander Saunder, Zhehui Wang, Laurie S. Waters, and Fred J. Wysocki, "Measurement of Proton-Induced Delayed Neutron Cross-Sections," LANL Report LA-UR-10-00625, APS "April" Meeting 2010, February 12-16, 2010, Washington, DC, USA; Chris L. Morris, Kiwhan Chung, Steven Greene, Gary Hogan, Mark Makela, Fessaha Mariam, Edward C. Milner, Matthew Murray, Alexander Saunder, Randy Spaulding, Zhehui Wang, Laurie Waters, and Frederick Wysocki, "Active Interrogation Using Energetic Protons," LANL Report LA-UR-10-04680, Institute of Nuclear Materials Management 51th Annal Meeting, July 11-15, 2010, Baltimore, Maryland.

[86] B. M. Abramov, P.N. Alekseev, Yu. A. Borodin, S. A. Bulychjov, I. A. Dukhovskoy, A. I. Khanov, A. P. Krutenkova, V. V. Kulikov, M. A. Martemyanov, M. A. Matsyuk, and E. N. Turdakina, "Quark cluster contribution to cumulative proton emission in fragmentation of carbon ions," arXiv:1304.6220; Pis'ma v ZhETF **97** (2013) 509 [in Russian], JETP Lett. **97** (2013) 439 [in English]; numerical values of measured spectra were kindly provided to us by Dr. Anna Petrovna Krutenkova.

[87] L. Heilbronn, C. J. Zeitlin, Y. Iwata, T. Murakami, H. Iwase, T. Nakamura, T. Nunomiya, H. Sato, H. Yashima, R. M. Ronningen, and K. Ieki, "Secondary Neutron-Production Cross Sections from Heavy-Ion Interactions Between 230 and 600 MeV/Nucleon," Nucl. Sci. Eng. **157** (2007) 142–158.

[88] Takahashi Nakamura and Lawrence Heilbronn, *Handbook on Secondary Particle Production and Transport by High-Energy Heavy Ions (with CD-Rom)*," World Scientific, Singapore, 2006.

[89] Georg Bollen, Mikhail Kostin, Reginald M. Ronningen, Man Yee Betty Tsang, Roger Roberts, Amy Coronado, Kyle Bort, Igor Remec, Lawrence H. Heilbronn, Josh Marshall, Tony Gabriel, Koji Niita, and Yosuke Iwamoto, "Final Report on Benchmarking Heavy Ion Transport Codes FLUKA, HETC-HEDS MARS15, MCNPX, and PHITS," DE-FG02-08ER41548, http://www.osti.gov/bridge/purl.cover.jsp?purl=/1082753/.

[90] Konstantin Gudima, Nikolai Mokhov, and Sergei Striganov, "Regarding "Final Report on Benchmarking Heavy Ion Transport Codes FLUKA, HETC-HEDS MARS15, MCNPX, and PHITS, DE-FG02-08ER41548," Fermilab, Accelerator Physics Center, August 20, 2013.